Extracting Speed Signatures from Gait Data

SJT Murdoch

Bioengineering Unit
University of Strathclyde

This thesis is submitted in fulfilment of requirements for the degree of M.Sc.

August 2011

Declaration of Authenticity and Author's Rights

This thesis is the result of the author's original research. It has been composed by the author and has not been previously submitted for examination which has led to the award of a degree.

Susan J.T. Murdoch
August 2011

Acknowledgements

Thanks to my supervisor Dr. Heba Lakany for her guidance and support throughout this project.

Thanks to Dr. Ben Stansfield and Dr. Marietta van der Linden for access to the slow walking data set.

Thanks also to the staff of the Bioengineering Unit for the taught portion of the M.Sc. course.

Best wishes to my classmates and friends on the M.Sc. and first year doctoral course.

Finally, thanks go to my parents and to my fiancé Gordon for all your love and support throughout this year.

Abstract

In this study, an existing dataset of children walking with normal gait and progressively slower gait speed is used to investigate data analysis methods with the aim of developing a technique to identify signature patterns of different walking speeds. Such signature patterns could form the basis of an automated analysis method by separating out the effects of slower walking speed from the effects of pathology on patients' gait.

Normalised data is compared for different speeds and converted to the frequency domain using fast Fourier transform (FFT) to explore data signatures for different walking speeds. Kinematic and kinetic data in the sagittal, coronal and transverse planes, as well as ground reaction force data, are considered.

It is shown that the first 8 harmonics found by FFT transform into the frequency domain give enough information to reconstruct the original signal for each of the parameters considered. The amplitudes of these harmonics are plotted versus walking speed to elicit signature trends for different speeds. Trends seen across the whole subject group are also seen in a case study comparing the tallest and smallest subjects.

This study demonstrates that signature trends for different walking speeds can be seen in kinematic and kinetic gait data, and further analysis is suggested to quantify these signatures.

Contents

List of Figures

List of Tables

Chapter 1

Introduction

1.1 Gait Analysis

Human walking is a complex, cyclical activity. Changes of direction, acceleration, moment and power of lower limb segments are all combined with precise timing to maintain symmetry, balance and provide forward motion.

Analysis of human gait is of interest to a number of different fields of research, including rehabilitation engineering, sports science, biometrics and even civil engineering [1]. Gait data records various features of an individual person's walking pattern, which can include the locations and relative motion of different limb segments, and the forces, moments and powers involved in the motion.

Kinetic and kinematic gait data recorded is high in volume, interdependence and complexity, and there are a range of different techniques and approaches in existence for the analysis and modelling of such data [2, 3].

The main challenges with gait analysis, for whatever purpose it is carried out, come from this high volume and complexity, along with the inherent step to step and person to person variability of gait data obtained from even the simplest walking test. Reducing the volume and complexity of this data for clearer interpretation has been the subject of much research in recent years [4].

Here we consider gait data from a clinical point of view, where gait analysis is used in conjuction with physical examination and other techniques in the assessment and monitoring of individuals with various pathologies. In order for gait analysis to become a useful diagnostic tool in a clinical setting, there is a

need for an improved method of automated analysis, straightforward to apply and interpret, which could be performed in close to real time and give a clear indication of gait deviations. Various studies [5, 6, 7] are developing methods of automated analysis to provide clearer output information for clinicans. This would support the clinician in their interpretations, as well as providing a training tool for clinical trainees. It could also provide an improved visualisation of gait comparisons for patients or their carers to gain a better understanding of their condition.

1.2 This Study

1.2.1 Motivation

In this study, a previously recorded data set [8] of children walking with normal gait and progressively slower gait speed is used to develop a method of analysis for clinical gait data.

The initial study was carried out with the intention of providing more relevant data for comparison with clinical data from child patients with pathological conditions such as cerebral palsy.

Normative data, an average set of data derived from healthy individuals, is used for comparison with patients' recorded gait data to assist clinicians in determining the nature and severity of any gait deviations. This normative set of data is often unique to the clinical centre, or may be shared by a number of centres.

In order to give a true reflection of the effect of pathology on gait, it is important that the normative data set chosen for comparison is relevant to the patient. For example it seems unrealistic to use normative data gained from a set of healthy adult subjects walking at their own natural speed to compare to gait data from a child with significant pathologies affecting their walking speed.

1.2.2 Aim

The aim of this study is to develop a technique to identify signature patterns of different gait speeds.

The analysis methods described here use algorithms to extract signature details from the time and frequency domain gait data in order to identify variations within a single subject and among the group of subjects as walking speed, and so smoothness of movement, are decreased. It is intended that such signatures could potentially be used in an automated analysis method as a diagnostic tool by separating out the effects of slower walking speed from the effects of pathology on patients' gait. Such an automated system could provide fast, reliable analysis results to clinicians without the need for specialist data processing.

Chapter 2

Background

2.1 Gait Analysis as Diagnostic Assessment Tool

Gait analysis covers a range of purposes, including clinical diagnostics, as well as athletic performance monitoring and biometrics. This study considers gait analysis from a clinical point of view as a diagnostic assessment tool for the evaluation and monitoring of patients.

Gait analysis is an important clinical method of assessment [9, 10, 11] for a range of different pathological conditions affecting patients' mobility. Clinical gait recording produces a large volume of highly complex data, which often requires specialist skills to analyse and interpret. Recent improvements in the technology used to record gait data have not reduced the need for analytical techniques to interpret and quantify the underlying walking patterns [12, 13, 14] .

Chau [3, 2] carried out an extensive review of different techniques used in gait analysis in 2001. These techniques include a range of methods of data reduction as well as data mining techniques. Multivariate statistical methods such as principal component analysis and factor analysis allow for dimension reduction and discovering interactions between parameters, but interpretation can be subjective. Data mining techniques such as neural networks can be used to classify gait data but require training with relevant inputs.

Rather than the selection of any one technique as ideal for gait analysis, more recent techniques use different combinations of analytical methods to investigate and explain variations in gait.

2.2 Kinetic and Kinematic Data

While different recording techniques such as electromyography (EMG) and Doppler radar tracking are used in the study of gait, it is kinetic and kinematic data such as joint moments and angles, as well as ground reaction force measurements that are most commonly collected in clinical gait laboratories. This type of data can be observed in the time domain as plots of gait parameter waveforms with time or % gait cycle, and can also be converted to the frequency domain to investigate the frequency content of the waveforms.

2.2.1 Time Domain Analysis

Time domain studies of kinetic and kinematic data have been carried out for decades, and the typical clinical gait analysis report consists of a set of gait parameter time plots. Such analysis relies on the peak and trough parameter values, ranges of motion and timings of different phases of the gait cycle in order to compare with normative data sets [15].

2.2.2 Frequency Domain Analysis

Conversion of time domain signals into the frequency domain have allowed further analysis of gait data by investigating the frequency content of the original signal [16, 17, 18, 19, 20]. Such studies use the method of Fourier transforms, discussed later in Chapter 3. This decomposes a complex cyclical time signal into a set of component sinusoidal harmonic waveforms. The calculated coefficients represent the amplitude and the phase of these harmonics and a frequency amplitude spectrum can be produced to represent the signal.

Analysis in the frequency domain can reveal changes in the spectral content of signals which may not be detected in the time domain, due to certain pathological conditions. Normative frequency spectra can be used for comparisons.

Fourier transform based frequency spectra do not however give any information as to which point in the gait cycle is affected by different frequency harmonics. Other methods using wavelet transforms [21] to convert time data into the time-frequency domain are also used in gait analysis [22]. Wavelet transforms decompose a signal to give a set of eigenvalues for different wavelet components.

2.3 Gait Indices and Signatures

Gait indices are increasingly used as a method of describing gait by a single value or vector giving a measure of the deviation from normality. Schutte et al. [23] used a PCA based technique to reduce a given set of gait measurements to a single index. Other methods use principal component analysis (PCA) or different multivariate statistical techniques to reduce multidimensional data to a single index or set of indices [24, 25, 26, 27, 28, 29].

Such methods have the advantage of using a large number of gait features to produce a single valued index or set of indices representing the variation of the data set from normative. By quantifying this deviation from normal gait, the intention is to reduce the subjectivity of interpretation of gait data. However, the effectiveness depends on the combination of gait parameters selected to combine to form the indices, and also on the set of normative data used.

Once established, the gait index calculation can be automated. The clinician then does not require analytical expertise but can compare the index with ranges of values to categorise the severity of different pathologies.

2.3.1 Principal Component Analysis (PCA)

Principal component analysis is a method used to reduce the dimensionality of multivariate datasets, whether in time or frequency domains. PCA is an orthogonal transformation which takes multidimensional data and finds a smaller number of uncorrelated orthogonal components so that the first component represents the largest variation in the data, and so on for the others.

PCA is used in gait analysis for dimension reduction and classification [30, 31, 32], on its own or in combination with other analytical techniques.

2.3.2 Gait Signatures

Gait signatures of individuals are of interest in biometrics for recognition and identification [33]. In clinical diagnostics, signatures for specific gait deviations or pathologies are of more interest [34, 35]. Signatures differ from gait indices in that they aim to classify not only normal from non-normal gait, but to identify specific types of abnormal gait.

These methods involve sophisticated data mining using neural networks to extract different patterns of deviations from normal data [36, 35].

2.4 Walking Speed Studies

Pathological conditions which might lead to a patient undergoing gait analysis will often result in slower walking speed when compared to healthy individuals. For this reason it seems unrealistic for most normative data sets used for comparisons to use the healthy subjects' normal faster walking speed. Indeed the original study [8], which provided the data set used here, was an investigation of normative comparisons at clinically relevant walking speeds.

Normalised walking speed has been shown to affect gait parameters for both adults [37] and for children [38, 39, 40, 41]. This study looks at walking speeds within the clinically relevant range to investigate the existence of identifiable signatures for different speeds which could distinguish between the effects of speed and of pathology.

Chapter 3

Method

3.1 Data Set

The data set used for this study was previously recorded [8] at the Anderson Gait Laboratory in Edinburgh. The study was carried out to consider slow walking speed for healthy children to establish normative comparisons for young patients with pathologies such as cerebral palsy. This was intended to help differentiate the effects of slow walking speed on gait parameters from the effects of the pathology.

Walking trials were recorded for a total of 35 children without walking problems between the ages of 8 and 11 years. This age range of healthy subjects was chosen to mirror the typical age range of cerebral palsy patients attending the centre. The children were asked to walk initially at their own normal walking speed, then progressively slower in subsequent trials in order to simulate the slower gait associated with pathological conditions such as cerebral palsy.

A Vicon motion capture system was used along with a Kistler force plate, to collect spatiotemporal, kinematic joint angles, kinetic joint moments and powers, and ground reaction force data for each walking trial. Each subject carried out a number of trials, ranging from 12 to 35. Some of these trials recorded only partial data depending on foot placement on the force plates, the kinematic data for these trials is used but they are disregarded for kinetics and ground reaction.

The data set was anonymised before I gained access, with subjects identified by initials and only accompanied by such body parameter data as was needed for normalisation, including age as well as body height, mass and weight.

3.1.1 Trials Banded by Speed

In the original study, the trials were categorised into bands A to E by normalised walking speed, A slowest to E fastest. The trials in band E represent the self selected normal walking speed for most subjects, although some achieved a faster band F. Band F is not considered in the original paper as it is only achieved by some of the subjects. In this study however, all of the trials including the fastest band F are considered.

3.2 Pre-processing of Data

3.2.1 MATLab Software Package

Mathworks MATLab package was used for the majority of data manipulation and analysis in this study, using scripts and functions adapted or developed for this study. A selection of the scripts written as part of this study and developed for the treatment of the data are included in Appendix B.

3.2.2 Converting Data Files

The raw data files were received as *.gcd* files as saved by the Vicon recording software system. These files could be opened in a text viewer such as Notepad++ for inspection, but were unsuitable for opening or importing into MATLab. The first task therefore on accessing the data set was to read the *.gcd* files for each run into MATLab in a suitable format.

Data from each trial was stored in a single *.gcd* file containing all of the spatiotemporal, kinematic, kinetic and ground reaction force data, with each subject's trials collected in a single folder. The data was separated out into a matrix for each group of parameters. A MATLab script was developed to read the data from each *.gcd* file and insert it into the four matrices SpatioTemporal, Kinematics, Kinetics and GroundReaction. These four matrices could then be saved as a single *.mat* file associated with each original *.gcd* file. The MATLab function written for the conversion of data files from .gcd format to the required matrices stored in a *.mat* file can be seen in Appendix B.

The detail of parameters recorded and the structures of each of the matrices are shown in Appendix A.

The resulting Spatiotemporal matrix contains the single values of the parameters cadence, stride time, stride length, step length and speed, as well as the percentage of gait cycle for the landmarks opposite foot off, opposite foot contact, step time, single support, double support and foot off, for each of Left and Right sides. These features are descriptive of the gait cycle in distance and time.

The Kinematics, Kinetics and Ground Reaction Force matrices consist of columns of 51 data points for each measured parameter. The 51 data points correspond to time in 2% intervals throughout a single gait cycle. Kinematics contains the lower limb joint angles in the sagittal, coronal and transverse planes for each of Left and Right sides. Kinetics contains the moments and powers associated with the lower limb joints for whichever side foot was in contact with the force plate. The Ground Reaction Force matrix contains the forces applied in the antero-posterior, medio-lateral and vertical directions by the force plate on the contacting foot, as well as the x, y, z coordinates of the centre of pressure of the foot.

This conversion was carried out for each data file and the resulting *.mat* files saved in the folder for each subject.

3.2.3 Normalisation

In order to be able to compare and average over a number of subjects, the gait data had to be normalised [42, 43] to dimensionless quantities using each subject's body parameters. Once the data was saved in the required format for further processing within MATLab, a MATLab function was written to calculate the normalised values for each parameter. The normalisation function is included in Appendix B. The values of each subject's body height, body weight and body mass from the body parameters data measured during the trials were used with the following set of equations:

For Speed in $mm.s^{-1}$

$$Normalised\ Speed = \frac{Speed}{1000 \times BH \times \sqrt{\left(\frac{9.81}{BH}\right)}} \tag{3.1}$$

For Cadence in s^{-1}

$$Normalised\ Cadence = \frac{Cadence}{\sqrt{\left(\frac{9.81}{BH}\right)}} \tag{3.2}$$

For Time in s

$$Normalised\ Time = Time \times \sqrt{\left(\frac{9.81}{BH}\right)} \tag{3.3}$$

For Length in mm

$$Normalised\ Length = \frac{Length}{1000 \times BH} \tag{3.4}$$

For Moment in $Nm.kg^{-1}$

$$Normalised\ Moment = Moment \times \frac{BM}{BW \times BH} \tag{3.5}$$

For Power in $Nm.s^{-1}.kg^{-1}$

$$Normalised\ Power = Power \times \frac{BM}{\sqrt{\left(\frac{9.81}{BH}\right)} \times BW \times BH} \tag{3.6}$$

For Force in N

$$Normalised\ Force = \frac{Force}{BW} \tag{3.7}$$

BH = Body height in m, BM = Body mass in kg, and BW = Body weight in N

For the spatiotemporal timings of landmarks in % of cycle, and also for joint angles in °, no normalisation is necessary as these quantities are already defined as ratios.

The normalisation was carried out in this way for each data file and saved as separate files labelled *N.mat* within the subject folders.

3.3 Further Processing and Analysis

With the data files for each subject and each trial converted and normalised, further processing could now begin. For each parameter of interest, functions and scripts were written to pull the relevant data for a single trial or single subject, or across the entire data set into another MATLab matrix.

3.3.1 Speed Banding of Trials

Similarly to the original study, the trials were categorised by the average of left and right side normalised walking speeds, as drawn from the normalised SpatiotemporalN matrix, with the following criteria:

Band A	$NSpeed \leq 0.15$
Band B	$0.15 < NSpeed \leq 0.20$
Band C	$0.20 < NSpeed \leq 0.25$
Band D	$0.25 < NSpeed \leq 0.30$
Band E	$0.30 < NSpeed \leq 0.35$
Band F	$NSpeed > 0.35$

Within the script (shown in Appendix B) carrying out this categorisation, the file identifiers and the average speed for each trial were also saved for further use.

3.3.2 Time Domain Data

Considering data in the time domain, each parameter of interest, beginning with the kinematic joint angles, was drawn from the normalised trial data and collated into a new matrix. A sample section of script used to pull data for each parameter is shown in Appendix B.

The new matrix of data for each parameter was used to calculate an average curve for each speed band, with associated standard deviation, which could then be plotted versus % gait cycle. The overall range of motion for each trial was calculated and averaged for each speed band.

Observations of the overall shape of these time domain plots, as discussed in Chapter 4, along with the calculated ranges of motion, allowed comparison of the joint angles between the different speed bands.

This averaging by speed band procedure was carried out for the sagittal kinetics data, as well as for the ground reaction forces, and the results are discussed in Chapter 4.

A similar time domain analysis was carried out for the tallest and smallest individual subjects of the group, to investigate whether speed signatures applied equally to these individuals as to the average of the normative group. These results are shown in Chapter 5.

3.3.3 Analysis in the Frequency Domain

After gaining a general overview of the effect of speed on the gait data in the time domain, the next step was conversion into the frequency domain. It has been demonstrated that frequency domain studies of gait [16, 17, 18, 19, 20] can provide a more in-depth analysis of gait parameters, when compared to time domain analysis.

The Fourier transform technique is one of a range of methods of transformation of data from the time domain into the frequency domain by separating out the frequency content of the original signal. Fast Fourier transform is a method using more time efficient calculations to achieve a discrete Fourier transform. This technique decomposes any given time domain input signal into a spectrum of component sinusoidal waveforms. In the frequency domain, the Fourier transform produces two signals the real part given by the cosine wave amplitudes and the imaginary part given by the sine wave amplitudes. The frequency of the fundamental harmonic, of which the other harmonics are multiples, is found from the inverse of the period of the original signal.

The general equation for the Fourier series is

$$F(t) = a_0 + \sum_{n=1}^{N/2} \left[a_n \cdot \cos \frac{2\pi nt}{T} + b_n \cdot \sin \frac{2\pi nt}{T} \right] \tag{3.8}$$

Where the constant term a_0 is the mean value of the waveform over a cycle.

$$a_0 = \frac{1}{N} \sum_{N=0}^{N/2} F(t) \tag{3.9}$$

a_n and b_n are Fourier coefficients, calculated by

$$a_n = \frac{2}{N} \sum_{N=0}^{N/2} F(t) \cdot \cos\left(\frac{2\pi nt}{T}\right) \tag{3.10}$$

$$b_n = \frac{2}{N} \sum_{N=0}^{N/2} F(t) \cdot \sin\left(\frac{2\pi nt}{T}\right) \tag{3.11}$$

The MATLab function *fft* was used within the script shown in Appendix B to carry out this transform on each parameter time series for each speed band. The resulting components were displayed as a frequency spectrum by plotting the amplitude of each harmonic (the absolute value of the fft component, scaled by the length of the data set) versus the frequency of each harmonic.

From observation of these frequency spectra, it could be seen that the contribution of the first few harmonics dominated the others. In order to determine how many harmonics to consider in the analysis, the inverse Fourier transform, MATLab function *ifft* was used to reconstruct a signal from the first few harmonics and compare this with the original signal. From carrying this out on different parameters using different numbers of harmonics it was determined that the first 8 frequency components of each signal were sufficient to give an adequate reconstruction of the signal. This means that for this data set, instead of requiring all 51 time data points, or indeed all 33 frequency components, the signals can be represented by 8 frequency components, reducing the need for data storage and reducing the number of calculations required in any further analysis.

The amplitude of each harmonic was plotted versus normalised walking speed for each band, to determine whether any harmonics showed a signature trend with speed. These plots are shown and discussed in Chapter 4.

Chapter 4

All Subjects Comparisons with Walking Speed

Data from all subjects, categorised into speed bands as described in Chapter 3, was collated for each parameter of interest in turn. From these collated data sets, means and standard deviations were calculated for each speed band A to F, as well as the consideration of all trials across speed bands.

4.1 Time Domain

The data set was recorded in the time domain, with the 51 data points for each parameter representing 2% intervals from 0 to 100% of a complete gait cycle. This means that instead of absolute timings in seconds, the timings are already normalised by overall gait cycle time, allowing comparisons for different subjects and speeds.

Here we consider the time domain curves of different gait parameters and the effects of normalised walking speed category.

4.1.1 Spatiotemporal Landmarks

The measured spatiotemporal landmarks dividing up the gait cycle into phases include initial foot contact (IFC), taken as the start and finish of a gait cycle, opposite foot off (OFO), opposite foot contact (OFC) and foot off (FO). These landmarks were measured as % gait cycle for each trial carried out, and were

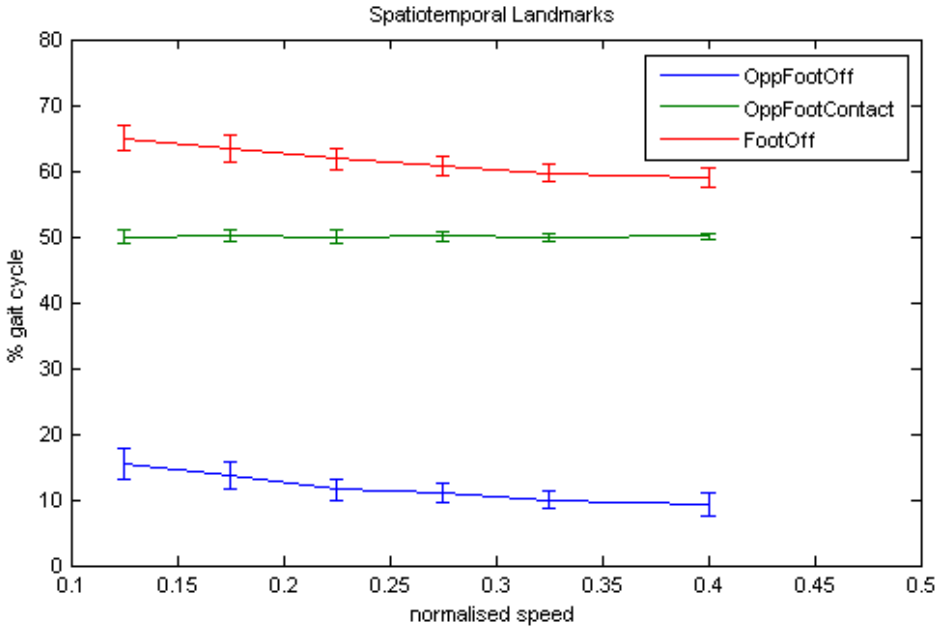

Figure 4.1: Spatiotemporal Landmarks versus Normalised Speed

collated for each speed band. Figure 4.1 shows an errorbar plot of % gait cycle for each landmark versus midpoint normalised walking speed for each band.

From this plot it can be seen that both opposite foot off and foot off are delayed for slower walking speeds with a difference of 6% gait cycle between fastest and slowest bands. The opposite foot contact however stays constant. This indicates that for slower walking speeds, the length of single stance is shorter on both sides, with lengthened double stance in between.

This effect can also be observed in time domain plots as a shift of features associated with these gait cycle landmarks.

4.1.2 Kinematics

The kinematics of gait, or study of relative motion, is observed here by measurement of the joint angles between neighbouring body segments of the lower limb during walking. Joint angles for the left and right hip, knee and ankle were recorded in the sagittal, coronal and transverse planes. By plotting these angles in the time domain versus % of one complete gait cycle it is possible to compare the curves produced by the different walking speed bands.

Sagittal Plane

The sagittal plane, or side-on view, is the plane in which the largest movements occur during forward locomotion. Here we consider the angles of hip and knee flexion, and ankle dorsi-plantarflexion.

Left and right hip flexion-extension angle, with flexion positive, is shown in Figure 4.2 plotted against % gait cycle for each speed band A to F. The mean range of this motion for both sides is shown in Table 4.1. From this, we can observe that the overall range of motion increases with speed from A slowest to F fastest, and also that both sides are symmetric in the increase.

Speed	Range in °			
	Left		Right	
	mean	std dev	mean	std dev
A	32.5	6.6	31.8	6.4
B	35.7	5.5	35.4	6.0
C	38.0	5.2	38.0	5.8
D	40.9	5.2	41.0	5.1
E	43.5	5.0	42.9	5.2
F	47.6	5.1	47.0	5.4

Table 4.1: Left and Right Hip Flexion Angle Range

Tables 4.2 and 4.3 show the range of motion respectively for knee flexion angle, flexion positive, and ankle dorsi-plantarflexion, dorsiflexion positive. The plots of angle versus % gait cycle can be found in Appendix C.

From Table 4.2 it can be seen that the knee flexion range also begins to increase with speed until band D, after which there is no significant further increase. This would seem to indicate that by speed band D, normalised speed 0.25-0.30, both knees are achieving close to maximum range of motion. From the plot of knee flexion angle versus % gait cycle in Appendix C, it can be seen that in addition to the overall range of motion increasing with speed, both the first peak during load acceptance of the stance phase and the second peak during swing phase also increase with speed.

From Table 4.3 it can be seen that the ankle dorsi-plantarflexion ranges for bands A and B are very close, band C is greater, and bands D,E and F are also very close and greater than A and B. This would indicate that there is some

tendency to a greater range of motion with increased speed, reaching a maximum by band D. The difference between the range of motion seen for slowest band A and fastest band F is far smaller than for hip or knee flexion. There is also greater variability in these values as seen from the standard deviations. From the plot versus % gait cycle in Appendix C, it can be seen that not only does the range of motion change with speed, but a shift towards plantarflexion is seen with increasing speed and the shape of the curve changes also. The fastest bands E and F show a broader, lower peak of dorsiflexion during stance phase and a larger peak of plantarflexion at push-off.

Speed	Range in °			
	Left		Right	
	mean	std dev	mean	std dev
A	44.0	8.5	44.2	8.4
B	48.2	6.9	47.2	7.1
C	50.3	6.4	50.6	5.8
D	53.4	5.5	53.0	5.8
E	53.1	6.1	53.8	5.5
F	54.9	5.4	54.0	4.5

Table 4.2: Left and Right Knee Flexion Angle Range

Speed	Range in °			
	Left		Right	
	mean	std dev	mean	std dev
A	21.4	4.9	22.1	6.1
B	22.4	5.5	22.4	6.2
C	23.4	5.5	24.0	6.4
D	25.8	5.7	25.5	6.2
E	25.3	5.9	26.5	5.6
F	25.6	6.3	26.4	5.9

Table 4.3: Left and Right Ankle Dorsi-Plantarflexion Angle Range

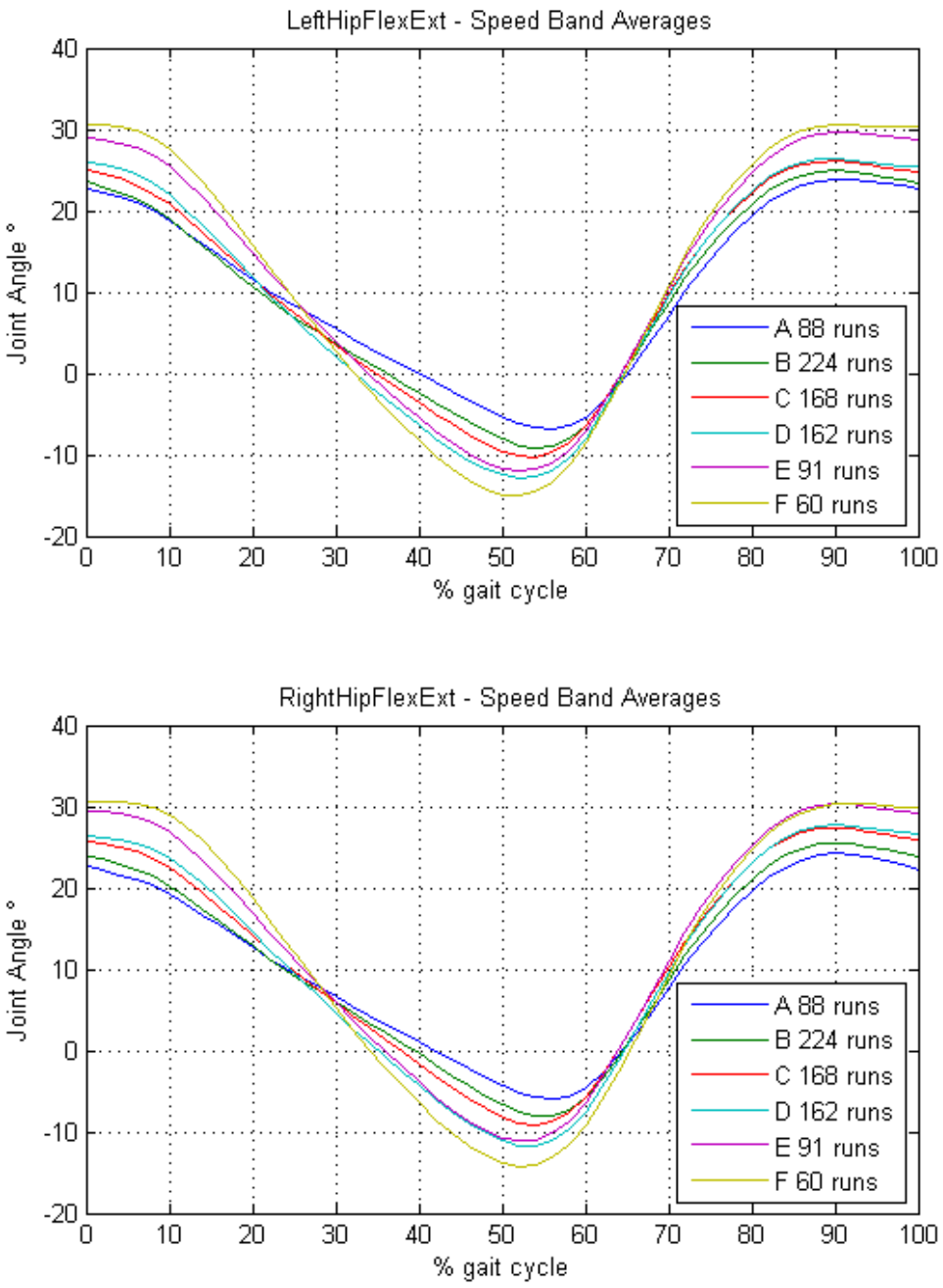

Figure 4.2: Left and Right Hip Flexion Angle

Coronal Plane

In the coronal or frontal plane during walking, the joint angles observed are the ab- or adduction (outward or inward tilting) of the hip, varus or valgus of the knee (bow-leg or knock-knee), and the inward or outward rotation of the ankle.

Plots of the coronal joint angles versus % gait cycle are shown in Appendix C. Tables 4.4, 4.5 and 4.6 show the ranges of motion of the hip, knee and ankle respectively.

The left and right side hip ab-adduction plots versus % gait cycle are shown in Appendix C, with adduction positive. From this and Table 4.4 it can be seen that the overall range of motion increases with speed and is symmetric for both sides. The shape of the curve also changes with speed, with the faster bands showing a higher peak of adduction in stance phase while the slower bands show a much lower double peak. This indicates that the slower walking speeds tend more to hip abduction.

Knee varus/valgus plot versus % gait cycle, with varus positive, is shown in Appendix C. From this and Table 4.5 it can be seen that there is some tendency for the overall range of motion to increase with speed, but that the fastest speed shows a slight reduction in range. It can also be seen that the first peak on load acceptance shows a greater reduction with slower speeds than the second peak in swing phase. This indicates that the lateral motion at the knee during stance phase shows the greatest variation with speed.

Foot rotation plot versus % gait cycle, with internal rotation positive, is shown in Appendix C. From this and Table 4.6 it can be seen that there is a small increase in overall range with speed and also that for slower speeds the tendency is more to internal rotation.

It is of interest to note that the variations in the coronal plane parameters are larger than those seen in the sagittal plane.

Speed	Range in °			
	Left		Right	
	mean	std dev	mean	std dev
A	7.7	3.0	8.5	2.9
B	9.0	3.2	9.7	3.6
C	9.6	3.3	10.3	3.2
D	10.3	3.1	11.1	3.1
E	11.4	3.4	12.2	3.7
F	13.7	3.2	13.9	3.5

Table 4.4: Left and Right Hip Ab-Ad-duction Angle Range

Speed	Range in °			
	Left		Right	
	mean	std dev	mean	std dev
A	10.1	3.3	11.8	4.6
B	11.5	4.5	13.3	5.0
C	12.6	4.1	14.2	4.7
D	13.1	4.4	14.5	5.3
E	13.6	4.5	15.4	6.1
F	11.8	4.5	14.3	6.0

Table 4.5: Left and Right Knee Valgus Varus Angle Range

Speed	Range in °			
	Left		Right	
	mean	std dev	mean	std dev
A	14.1	5.0	13.8	5.5
B	13.9	4.7	13.9	5.0
C	15.0	4.4	14.0	4.7
D	15.8	4.8	14.9	4.3
E	15.6	4.6	15.2	4.6
F	16.0	5.1	15.0	4.6

Table 4.6: Left and Right Foot Rotation Angle Range

Transverse Plane

The transverse or top-down plane shows the angles of rotation of the hip and knee and foot progression.

Plots of the transverse joint angles are shown in Appendix C and Tables 4.7, 4.8 and 4.9 show the overall ranges of motion of hip, knee and foot, with internal rotation positive for each.

From Table 4.7 it can be seen that there is a small increase in the range of hip rotation motion with speed, but the plots in Appendix C show that the fastest band F shows a different shape of curve from the other bands, which show similar curves with the slowest bands showing both attenuation of peaks and a shift downwards. This would indicate an increase in hip rotation through the slower speed bands, but a different pattern of motion at the fastest band F.

Table 4.8 shows an increase in overall knee rotation range of motion with speed, and the plot shown in Appendix C shows that the slower bands have smoother curves with more rounded peaks than the faster bands. While the first half of the gait cycle shows only a small change with speed, the second half of the cycle shows more marked differences, indicating that it is in the swing phase that the variation of knee rotation angle is most affected by walking speed.

Table 4.9 shows a general decrease in overall foot progression angle range of motion with increasing speed. The plot shown in Appendix C shows that there is a subtle smoothing of the curve, and shift towards negative values with slower speed bands. Again the greatest variation between speeds is seen in the second half of the gait cycle corresponding with swing phase.

Like the coronal plane, the transverse plane joint angles show both a smaller range of motion and larger variation than the sagittal plane. A greater tendency to asymmetry between the left and right sides is also seen in the coronal and transverse planes.

Speed	Range in °			
	Left		Right	
	mean	std dev	mean	std dev
A	14.1	4.1	12.6	4.0
B	14.6	4.1	13.2	3.8
C	14.7	4.7	13.4	4.1
D	15.1	4.3	13.9	4.5
E	15.2	4.5	14.5	5.2
F	15.3	4.4	14.4	4.8

Table 4.7: Left and Right Hip Rotation Angle Range

Speed	Range in °			
	Left		Right	
	mean	std dev	mean	std dev
A	14.8	4.7	14.6	4.6
B	14.5	4.9	14.9	4.4
C	15.2	4.8	15.6	4.7
D	16.1	4.4	46.7	5.1
E	16.1	4.7	17.0	4.8
F	18.7	6.1	19.0	5.1

Table 4.8: Left and Right Knee Rotation Angle Range

Speed	Range in °			
	Left		Right	
	mean	std dev	mean	std dev
A	16.3	6.4	15.0	6.1
B	15.5	7.0	14.9	6.0
C	15.3	5.6	14.8	5.8
D	14.4	4.6	13.6	5.0
E	14.4	4.6	12.9	5.0
F	14.9	5.5	13.8	6.3

Table 4.9: Left and Right Foot Progression Angle Range

4.1.3 Kinetics

The hip, knee and ankle joint moments and powers are considered only in the sagittal plane, as these represent the major motions in walking.

Sagittal Plane

The plots of hip flexion moment and power, knee flexion moment and power, and dorsi-plantarflexion moment and power are shown in Appendix C. From these plots it can be seen that for all three joints, both moment and power show an increase in the amplitude of positive and negative peaks with increasing speed. The slowest band A shows a smoothed, attenuated version of each curve. This would indicate as expected a greater output of force and energy during the faster walking speeds.

The fastest band F, however, shows a different shape in ankle dorsi-plantarflexion moment and power curves, while the other bands differ mainly in magnitude. This seems to indicate a different pattern of muscle behaviour at the fastest speed.

4.1.4 Ground Reaction Forces

For some but not all of the trials recorded, a single footstrike was recorded as the subject walked over the force plate. For these trials, the ground reaction force acting on the subject's contacting foot in the antero-posterior, medio-lateral and vertical directions is now considered.

Antero-Posterior Direction

The antero-posterior direction of ground reaction force, positive in direction of progression, is shown in Figure C.12 plotted against % gait cycle. From this plot, it can be seen that with increasing walking speed A-F, the magnitude of normalised force both in shock absorption and in push-off increases. The shape of the curve changes little apart from magnitude, showing smooth transition between landing and foot off.

Medio-Lateral Direction

The medio-lateral direction of ground reaction force, positive in medial direction, is shown in Figure C.13 plotted against % gait cycle. The fastest band F displays a much larger first negative peak of force than second peak, and this is larger than the other speed bands indicating a different pattern of lateral foot motion from the other speeds.

The remaining speed bands show very similar first negative peak magnitudes, while the second negative peak is seen to increase for the slower speeds. This seems to indicate a tendency towards a lateral rocking motion in late stance for slower walking speeds.

Vertical Direction

The vertical ground reaction force is shown in Figure C.14 plotted against % gait cycle. It can be seen that with increasing speed the first peak of force increases significantly, and the second peak also increases but to a lesser extent. The local minimum between these peaks however decreases with speed, so that the slowest band A shows a plateau shape rather than a double peak. This would indicate that the slower walking speeds show a flatter placement of the foot on the force plate rather than the typical rocking motion of the ankle.

4.2 Frequency Domain

Considering gait data in the frequency domain, the 51-point time domain data sets for each parameter were transformed into the frequency domain using fast Fourier transforms as discussed in Chapter 3. This gives the amplitude and phase angle of component sinusoidal curves which can be superimposed to give the resultant time signal. These are known as the fundamental (0Hz frequency component) and harmonics of the time domain signal.

By doing this, it is possible to use a smaller number of the most significant frequency components rather than the 51 original data points.

Firstly, by plotting the amplitude versus frequency of the harmonic components, it is possible to see which harmonics make a significant contribution to the signal. By performing an inverse fast Fourier transform on the first few harmonics, it is possible to reconstruct an approximation of the original signal. For all of the parameters considered here, an adequate approximation was obtained using the first 8 harmonics out of 33 calculated. This means that for analysis purposes, these 8 harmonics give enough information to represent the entire signal, reducing the amount of data required.

Further, plots were constructed of the amplitude of these first 8 harmonics versus walking speed to investigate any trends.

Plots of the other parameters considered can also be found in Appendix C

4.2.1 Kinematics

The hip, knee and ankle joint angle signals are considered here in the frequency domain.

Sagittal Plane

Left and right hip flexion angle frequency components are shown in Figure 4.3. These plots show that for the hip flexion, it is the first harmonic which has the greatest contribution to the time domain plot, and also that the amplitude of the first harmonic is most sensitive to walking speed.

Figure 4.4 shows the reconstructions of the left and right hip flexion angle time domain plots using the first 8 frequency components. Comparison with 4.2

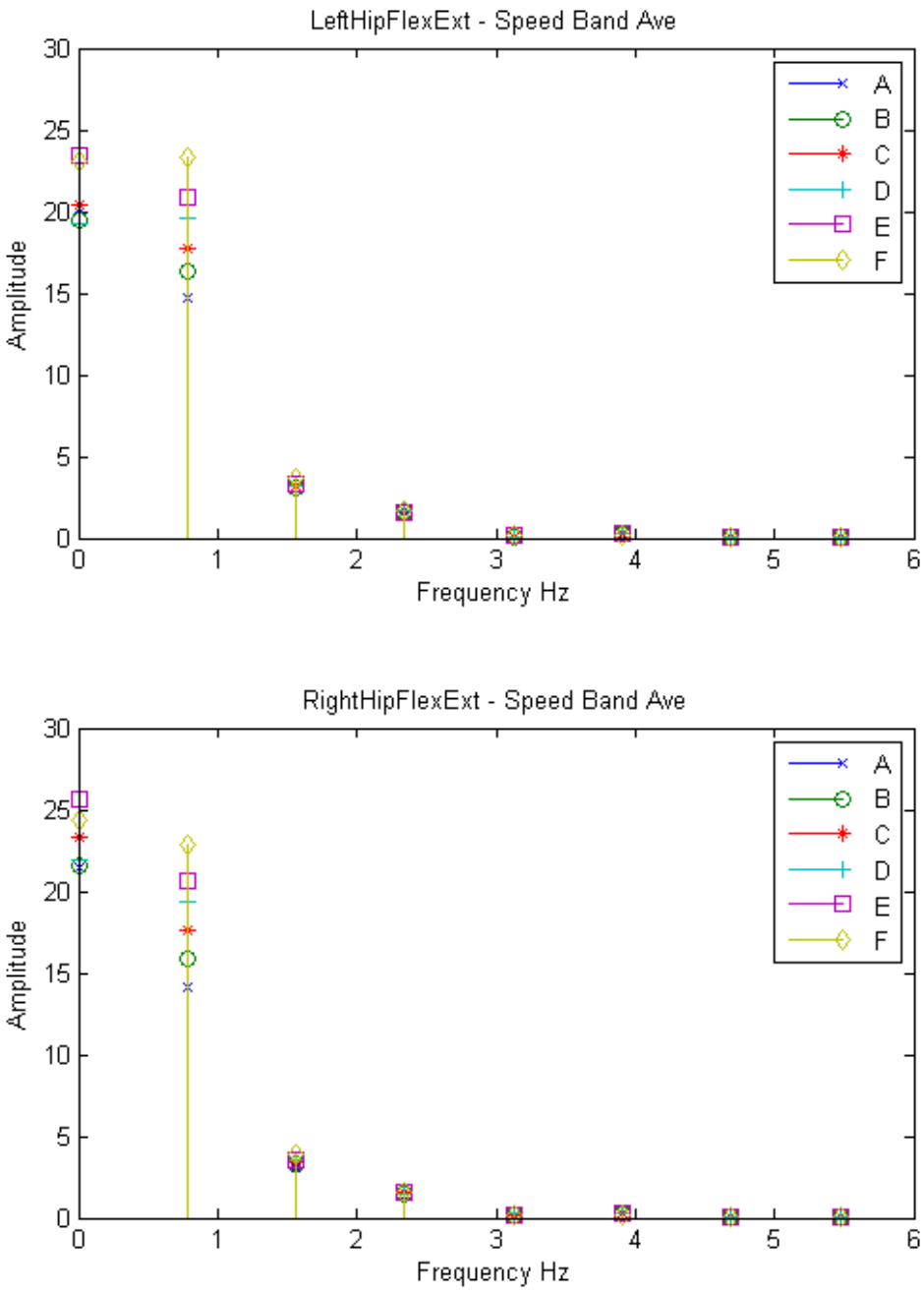

Figure 4.3: Left and Right Hip Flexion in Frequency Domain

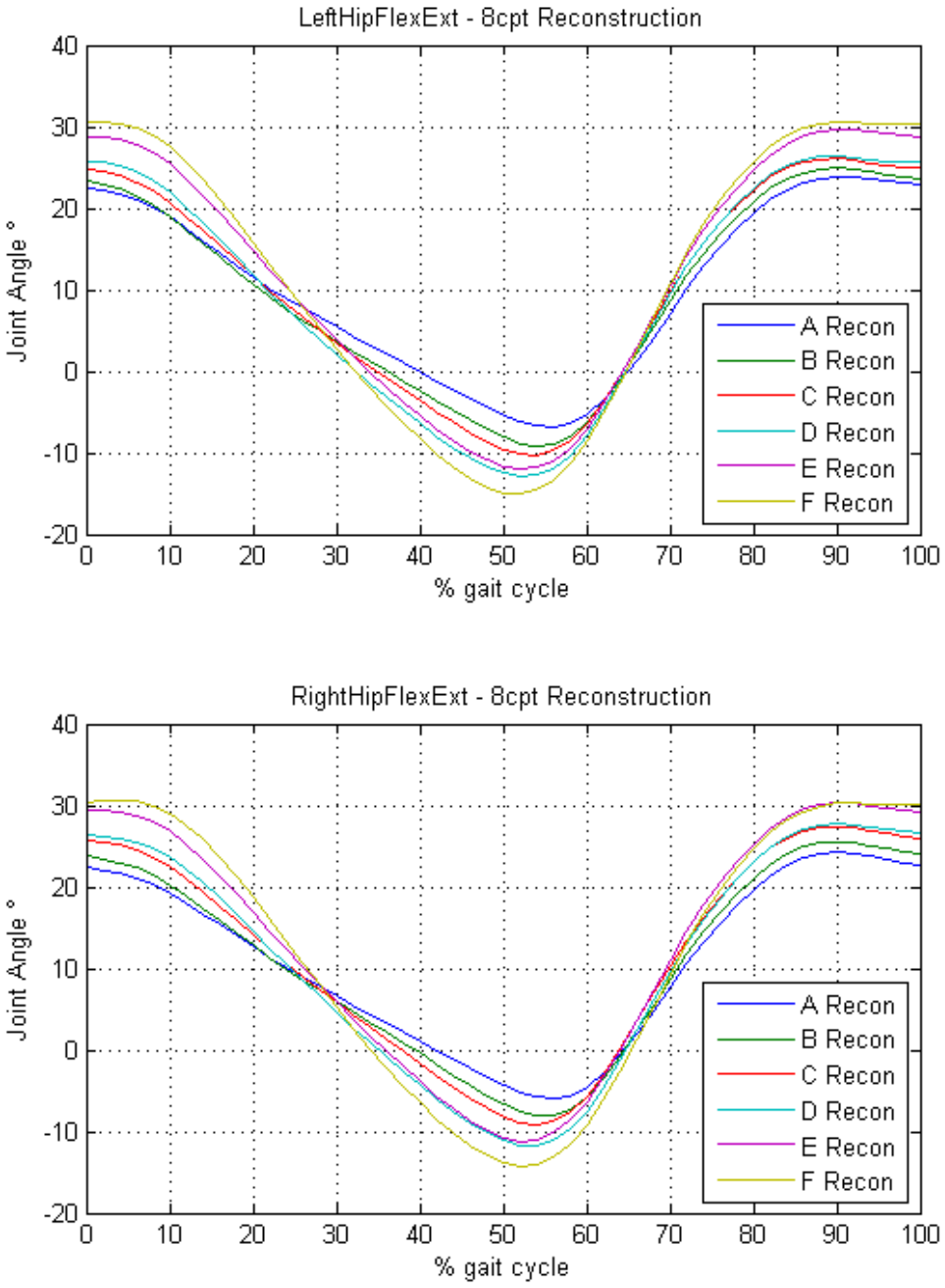

Figure 4.4: Left and Right Hip Flexion Angle Reconstruction from Eight Harmonics

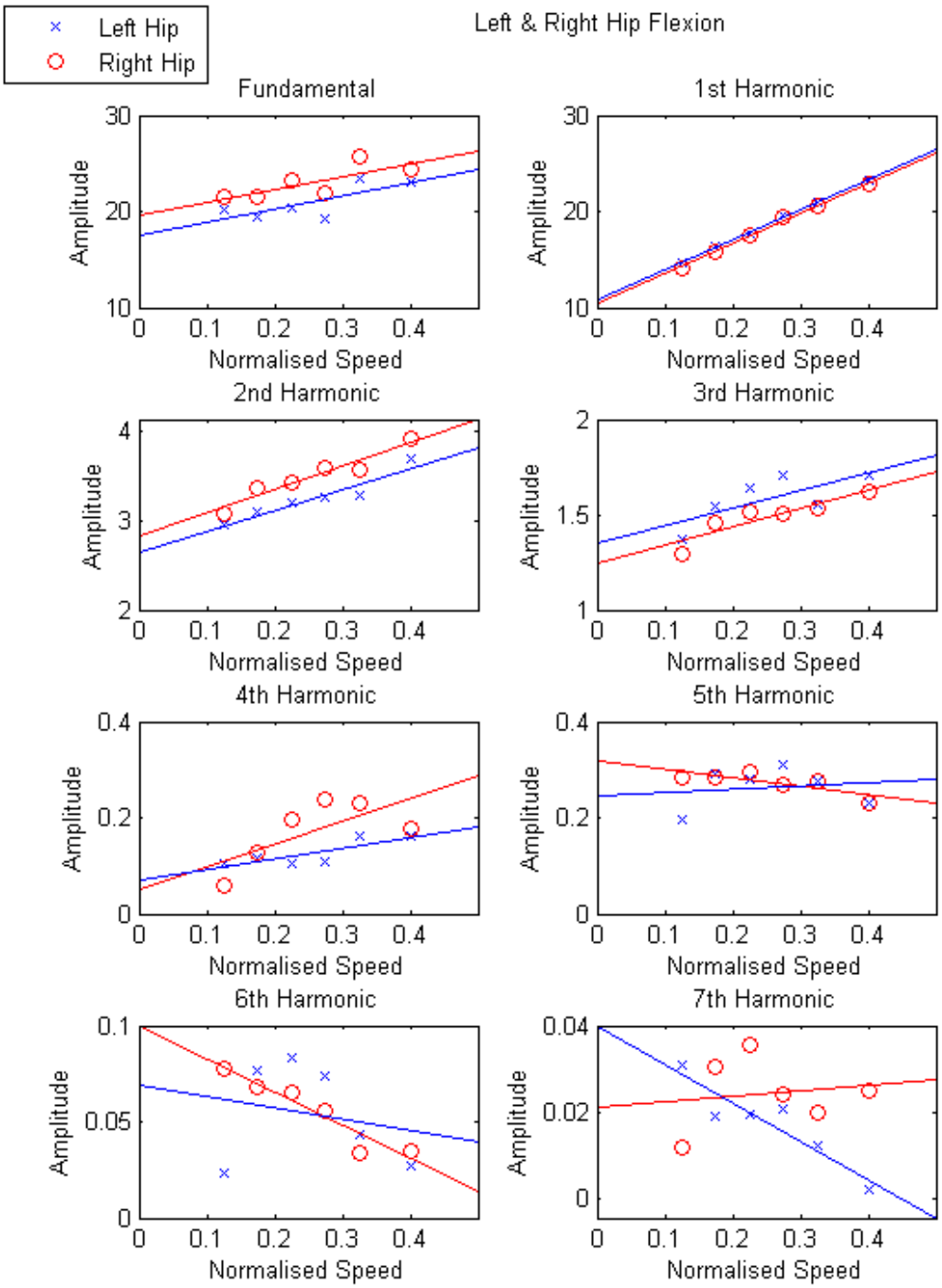

Figure 4.5: Left and Right Hip Flexion Harmonic Amplitudes versus Normalised Speed

shows that these are a good representation of the original signal. This allows us to consider only the first 8 frequency components for each parameter, and still retain an adequate level of detail.

Figure 4.5 shows the plots of amplitude of each harmonic versus walking speed, for the left and right hip flexion angles. These plots show that while other harmonics show some trend of increasing amplitude with walking speed, it is the first harmonic which clearly shows a linear relation between increasing speed and an increase in amplitude, and this relation is symmetric for left and right sides.

Similar plots for left and right knee flexion angle, shown in Appendix C, indicate that the fundamental as well as the first and second harmonics show a linear relation of increasing amplitude with increasing walking speed, with the second harmonic having the strongest correlation.

Plots for left and right dorsi-plantarflexion angle, shown in Appendix C, show that the more complex time domain curve has a greater frequency content than the hip or knee flexion, with more harmonics showing comparable amplitudes. The fundamental shows a decrease in amplitude with increasing speed, while the first three harmonics show an increase in amplitude. It is the third harmonic which shows the clearest linear correlation with speed.

Coronal Plane

Hip ab-adduction angle plots show that the first four frequency components have greatest contribution to the original signal. It is the first harmonic which has the greatest amplitude contribution, and also shows a clear linear relation between increasing walking speed and increasing amplitude.

Knee valgus varus angle plots show that the first four frequency components have the greatest contribution to the original signal, with amplitudes decreasing by harmonic number. While there does seem to be some trend towards increasing amplitude with increasing walking speed, it does not appear to be linear.

Foot rotation angle plots again show that the first four frequency components have the greatest contribution, but with some oscillation in amplitudes. The first and second harmonics show a linear trend of increasing amplitude with increasing walking speed.

Transverse Plane

Hip rotation angle plots show that the fundamental has the greatest contribution to the original signal, followed by the next three harmonics. The fundamental shows some increase of amplitude with increasing walking speed but this is not linear. The second harmonic also shows an increase in amplitude, while the first harmonic shows a trend of decrease in amplitude with increasing walking speed.

Knee rotation angle plots show that the first four frequency components have the greatest contribution to the original signal, with amplitudes decreasing by harmonic number. While the fundamental, first and third harmonics show some trend of increasing amplitude with increasing walking speed, it is the second harmonic which has a clear linear relation between increasing amplitude and walking speed.

Foot progression angle plots show that the fundamental has the greatest contribution to the original signal. While the fundamental shows some trend to decrease in amplitude with increasing walking speed, the magnitude is not symmetrical between left and right.

It can be seen that the clearest patterns between harmonic amplitude of joint angles and walking speed were seen in the sagittal plane.

4.2.2 Kinetics

Sagittal Plane

Hip flexion moment shows the greatest contribution to the original signal from the first harmonic, and this shows the clearest linear trend of increasing amplitude with increasing walking speed, followed by the third harmonic. Hip flexion power shows the first six harmonics contributing to the signal, with the second harmonic the greatest. The first six harmonics also show linear trends of increasing amplitude with increasing walking speed.

Knee flexion moment and power both show contributions from all eight harmonics considered to their complex signals. Moment shows the clearest linear relation between increasing amplitude and increasing walking speed for the second and third harmonics, while power shows clear trends for the first and third

harmonics increasing amplitude with increasing walking speed.

Ankle dorsi-plantarflexion moment shows decreasing amplitude with harmonic number, and a linear trend for increasing amplitude with increasing walking speed. Power shows contributions from all harmonics considered, with the fundamental having lowest amplitude. The remaining harmonics all show linear trends of increasing amplitude with increasing walking speed.

The powers show the clearest correlation between harmonic amplitude and walking speed.

4.2.3 Ground Reaction Forces

Antero-Posterior Direction

The antero-posterior ground reaction force plots show contributions to the signal from the first, second, third, fourth and sixth harmonics, with the first harmonic having the greatest amplitude. These harmonics all show a linear trend for increasing amplitude with increasing walking speed.

Medio-Lateral Direction

The medio-lateral ground reaction force plots show contributions to the signal from the fundamental, first, third and fourth harmonics. These harmonics show no clear trends in amplitude with increasing walking speed.

Vertical Direction

The vertical ground reaction force shows greatest contributions to the signal from the fundamental, first and third harmonics, with the fundamental having the greatest amplitude. The third harmonic shows a clear linear relation between amplitude and walking speed.

The antero-posterior direction of ground reaction force shows the greatest effect of walking speed on the harmonic amplitudes.

Chapter 5

Case Study - Tallest and Smallest Individual Subjects

Here we consider the case study of the tallest and smallest individual subjects of the group, to investigate whether the trends seen for the averages across the population apply to these individuals at the extremes of the subject population. The tallest subject at 1.55m and the smallest subject at 1.22m represent the height range of the group. They also had the longest and shortest leg lengths respectively.

5.1 Frequency Domain Analysis

For both subjects the sagittal kinematic, sagittal kinetic and ground reaction force parameters have been collated for each trial, along with the normalised walking speed. This data has been converted into the frequency domain as discussed in Chapter **??**. Plots of amplitude versus walking speed for the first eight harmonics have been constructed for both tallest and smallest subject as was discussed in Chapter 4.

Further plots for the parameters considered here can be found in Appendix D.

5.1.1 Sagittal Plane Kinematics

The sagittal joint angles data for the tallest and smallest subjects was treated as discussed in Chapter 4. The plots of hip flexion harmonic amplitude versus normalised walking speed, for tallest and smallest subjects both left and right side, are shown in Figure 5.1. From this it can be seen that the first harmonic shows a clear linear trend between increasing amplitude and increasing walking speed for both subjects and both sides. This corresponds well with what was seen for the entire subject group in Figure 4.5.

Plots of left and right side knee flexion harmonic amplitude versus normalised walking speed, for both tallest and smallest subjects, are shown in Appendix D. From this it can be seen that the fundamental as well as the first and second harmonics show linear trends of increasing amplitude with increasing speed for both subjects and both sides. This corresponds with what was seen across the subject group in Appendix C, and again the second harmonic shows the strongest correlation.

Plots of left and right dorsi-plantarflexion harmonic amplitude versus normalised walking speed, for both tallest and smallest subjects, are shown in Appendix D. From this no clear linear trends can be seen between harmonic amplitude and walking speed, and both subjects show greater variations than in hip or knee flexion. This differs from what was seen for the equivalent plots for the subject group in Appendix C, so it seems that any trends for ankle dorsi-plantarflexion only become apparent when averaged across the population.

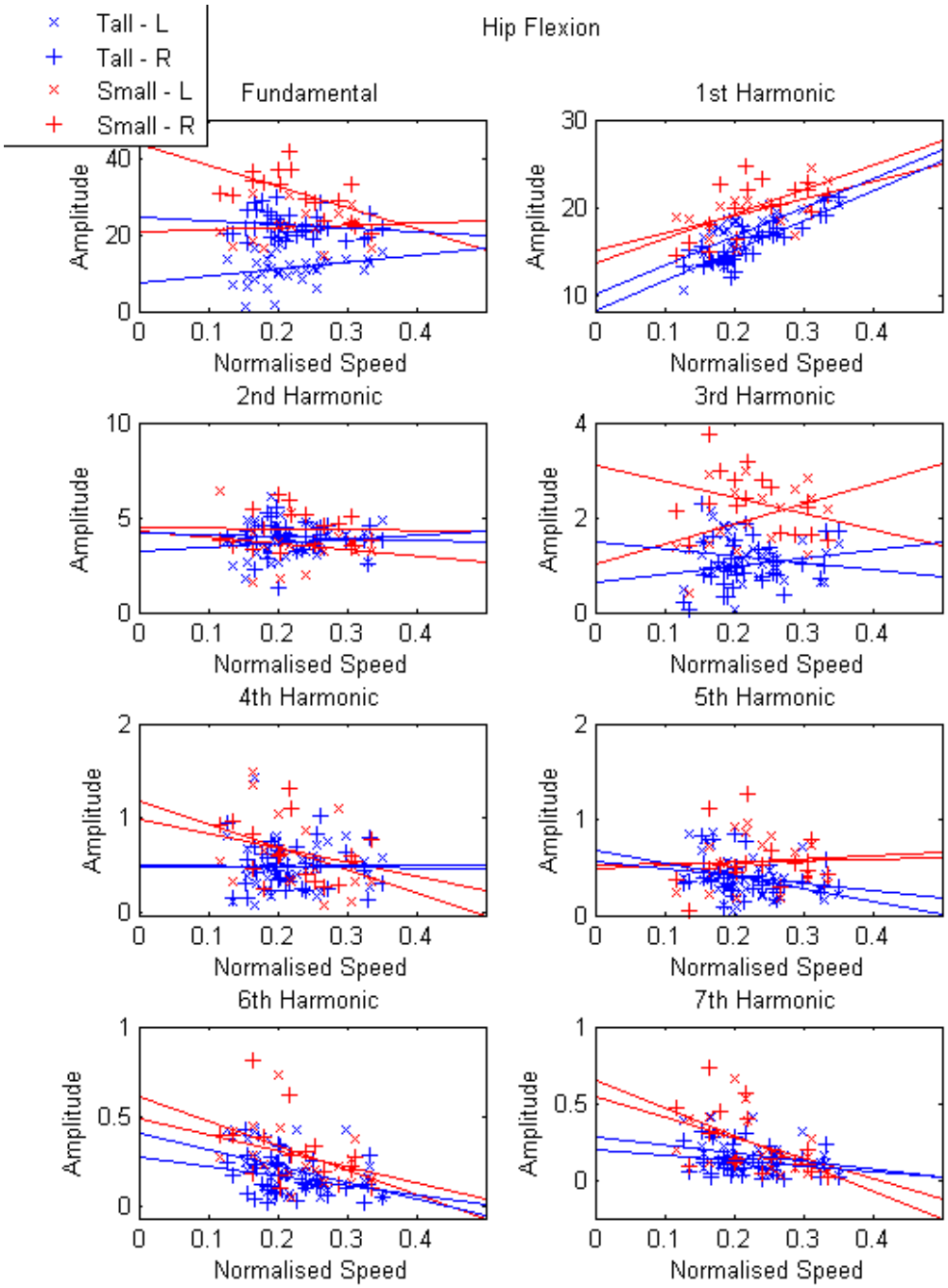

Figure 5.1: Tallest and Smallest Hip Flexion Harmonic Amplitudes versus Normalised Speed

5.1.2 Sagittal Plane Kinetics

Hip flexion moment plotted for the tallest and smallest subjects, as seen in Appendix D, shows a linear trend in the first harmonic increasing in amplitude with increasing walking speed. Hip flexion power shows a trend for the first, second and third harmonics to increase in amplitude with increasing speed, but the agreement between tallest and smallest is less clear. This corresponds with what was seen in the equivalent plots for all subjects seen in Appendix C.

Knee flexion moment plotted for the tallest and smallest subjects shows no clear trends in harmonic amplitude with increasing walking speed, and less agreement between tallest and smallest. Knee flexion power shows trends in the third and fifth harmonics increasing in amplitude with increasing speed, and better agreement between tallest and smallest.

Ankle dorsi-plantarflexion moment plotted for the tallest and smallest subjects shows no clear trends in harmonic amplitude with walking speed. Dorsi-plantarflexion power shows clear trends in the first and second harmonics to increasing amplitude with increasing speed, and agreement between the tallest and smallest subjects. This shows some agreement with the equivalent plots across all subjects seen in Appendix C, where all harmonics of power showed linear trends with speed.

5.1.3 Ground Reaction Force

Antero-Posterior Direction

The antero-posterior ground reaction force harmonic amplitude versus walking speed plots for tallest and smallest subjects, as seen in Appendix D, show a linear trend in the first, second and fourth harmonics to increase in amplitude with increasing speed. There is also reasonable agreement between the two subjects for these harmonics. This shows some correspondence with the plots in Appendix C for the subject group, but the trends are more apparent when averaged across all subjects.

Medio-Lateral Direction

The medio-lateral ground reaction force harmonic amplitude versus walking speed plots for tallest and smallest subjects show that the fundamental and first harmonics show some trend to decrease, and the second and fourth harmonics show a trend to increase with increasing speed. The equivalent plots for all subjects in Appendix C showed slight tendencies but no clear trends.

Vertical Direction

The vertical ground reaction force harmonic amplitude versus walking speed plots for tallest and smallest subjects show a linear trend in the third harmonic to increase in amplitude with increasing speed. This corresponds well to the equivalent plots for all subjects in Appendix C where it was the third harmonic which showed the clearest relation.

Overall, these frequency domain analyses of the tallest and smallest subjects have shown good agreement with the results seen for the averages across the subject group. Also, where clear trends were seen, they agreed well between the tallest and smallest individuals. This confirms that the findings for all subjects are representative of the entire group.

Chapter 6

Conclusions and Further Work

6.1 Summary

In this study, time and frequency domain analyses of a pre-existing data set have been carried out to investigate signatures of different normalised walking speeds.

The time domain analysis has shown that changes in the gait parameter waveforms occur at slower walking speeds. Ranges of motion of sagittal and coronal joint angles are smaller, with increased trial to trial variation in slower speeds. Shifting of opposite foot off point and foot off point mean that double support is maintained for a longer portion of the gait cycle in slower speeds. Sagittal joint moments and powers are lower in the slowest speeds, indicating less energy expenditure. The slowest speeds have attenuated ground reaction forces, with a tendency away from the double peak of vertical force towards a plateau. All of these features are characteristic of a more hesitant gait at slower speeds.

Frequency domain analysis has shown that particular harmonics of different gait parameters are affected more strongly by walking speed. Hip and knee joint angles show linear correlation between the first few harmonic amplitudes and walking speed. Joint powers and particularly the antero-posterior direction of ground reaction force show greater effects of walking speed on harmonic amplitudes.

6.2 Clinical Impact

This study considered the effects of walking speed on gait data gathered from a group of healthy children. We have seen that there are indeed significant variations between walking speed bands, evident across several gait parameters. These results emphasise the need for clinically relevant normative gait data and for better methods of quantifying the deviations from this.

It seems that some features of patients' gait which may be thought to be due to pathology, are driven at least in part by the walking speed achieved. A longer portion of the gait cycle spent in double stance with delayed foot-off, and smaller ranges of motion of sagittal joint angles at slower speeds are observed for healthy subjects. The reasons for walking speed are different, in that the healthy subjects changed their walking speed deliberately while patients' walking speed is driven by their pathology and compensation mechanisms, but the effects are linked. The normal subjects do retain a high degree of left-right symmetry while walking at slower speeds, while patients are likely to display more asymmetry, particularly in the case of hemiplegia.

6.3 Further Work

This study used a data set gathered from healthy children to investigate the extraction of signatures for different walking speeds among this group. Further analysis of this data set using more sophisticated methods such as PCA, might yield more detailed data signatures associated with the different walking speeds.

For example, a PCA technique based on that used by Schutte et al. [23] or Tingley [24] could carry out PCA analysis on the first eight frequency domain harmonics of the sagittal kinematic joint angles, sagittal kinetic moments and powers, and ground reaction forces to better quantify the contributions of the different gait parameters to the variations between different speeds. Instead of a single index determining normality, a speed index would be the goal of this next stage of analysis.

Another possible extension to this work would be to carry out the same analysis on walking speed data gathered from healthy adults. This would allow us to compare walking speeds among adults, as well as compare overall walking

patterns between juveniles and adults. Although mature gait is thought to be reached in early childhood [38], the effects of walking speed on adult gait may vary from those on children.

A similar exercise in data gathering could also be carried out for older adults, using healthy active older adults to provide normative data for comparison with elderly patients with a range of pathological conditions such as arthritis or post-stroke hemiplegia.

This study has demonstrated that signature trends for different walking speeds can be seen in kinematic and kinetic gait data. Further analysis of this or similar data sets in the frequency domain using orthogonal principal component analysis and data mining methods would enable these signatures to be better quantified in order to be of use in an automated analysis system.

Gait analysis makes an important contribution to the clinician's understanding of a patient's underlying mobility problems, and better differentiation between the effects of walking speed and the effects of a patient's pathology on gait should help this further.

Bibliography

[1] V. Racic, A. Pavic, and J. M. W. Brownjohn. Experimental identification and analytical modelling of human walking forces: Literature review. *JOURNAL OF SOUND AND VIBRATION*, 326(1-2):1–49, SEP 25 2009.

[2] T. Chau. A review of analytical techniques for gait data. part 2: neural network and wavelet methods. *Gait & Posture*, 13(2):102–120, 2001.

[3] T. Chau. A review of analytical techniques for gait data. part 1: fuzzy, statistical and fractal methods. *Gait & Posture*, 13(1):49–66, 2001.

[4] Roy B. Davis, Sylvia unpuu, Dennis Tyburski, and James R. Gage. A gait analysis data collection and reduction technique. *Human Movement Science*, 10(5):575 – 587, 1991.

[5] Sherif El-Sayed Hussein. Intelligent assessment for pathological gait analysis. In Y Chugui, YS Gao, KC Fan, R Taymanov, and K Sapozhnikova, editors, *MEASUREMENT TECHNOLOGY AND INTELLIGENT INSTRUMENTS IX*, volume 437 of *Key Engineering Materials*, pages 334–338, LAUBLSRUTISTR 24, CH-8717 STAFA-ZURICH, SWITZERLAND, 2010. TRANS TECH PUBLICATIONS LTD. 9th International Symposium on Measurement Technology and Intelligent Instruments, St Petersburg, RUSSIA, JUN 29-JUL 02, 2009.

[6] Kurt Manal and Steven J. Stanhope. A novel method for displaying gait and clinical movement analysis data. *Gait & Posture*, 20(2):222 – 226, 2004.

[7] S Wolf, T Loose, M Schablowski, L Doderlein, R Rupp, HJ Gerner, G Bretthauer, and R Mikut. Automated feature assessment in instrumented gait analysis. *GAIT & POSTURE*, 23(3):331–338, APR 2006.

[8] M.L. van der Linden, A.M. Kerr, M. E. Hazlewood, S. J. Hillman, and J.E. Robb. Kinematic and kinetic gait characteristics of normal children walking at a range of clinically relevant speeds. *JOURNAL OF PEDIATRIC ORTHOPAEDICS*, 22(6):800–806, NOV-DEC 2002.

[9] Jacquelin Perry. *Gait Analysis: Normal and Pathological Function.* Thorofare, NJ : SLACK, 1992.

[10] Michael Whittle. *Gait analysis : an introduction. 4th ed.* Edinburgh ; New York : Butterworth-Heinemann, 2007.

[11] Tishya A.L. Wren, George E. Gorton III, Sylvia unpuu, and Carole A. Tucker. Efficacy of clinical gait analysis: A systematic review. *Gait & Posture*, 34(2):149 – 153, 2011.

[12] D. H. Sutherland. The evolution of clinical gait analysis: Part ii kinematics. *Gait & Posture*, 16(2):159 – 179, 2002.

[13] D.H. Sutherland. The evolution of clinical gait analysis part iii - kinetics and energy assessment. *Gait & Posture*, 21(4):447 – 461, 2005.

[14] SR Simon. Quantification of human motion: gait analysis - benefits and limitations to its application to clinical problems. *JOURNAL OF BIOMECHANICS*, 37(12):1869–1880, DEC 2004.

[15] Oren Tirosh, Richard Baker, and Jenny McGinley. Gaitabase: Web-based repository system for gait analysis. *COMPUTERS IN BIOLOGY AND MEDICINE*, 40(2):201–207, FEB 2010.

[16] Erik K. Antonsson and Robert W. Mann. The frequency content of gait. *Journal of Biomechanics*, 18(1):39 – 47, 1985.

[17] Patrick E. Patterson and Lewis Brown. Biomechanical waveform analysis in the frequency domain. *Engineering in Medicine and Biology Magazine, IEEE*, 6(3):12 –16, 1987.

[18] Giannis Giakas and Vasilios Baltzopoulos. Time and frequency domain analysis of ground reaction forces during walking: an investigation of variability and symmetry. *Gait & Posture*, 5(3):189 – 197, 1997.

[19] N Stergiou, G Giakas, JE Byrne, and V Pomeroy. Frequency domain characteristics of ground reaction forces during walking of young and elderly females. *CLINICAL BIOMECHANICS*, 17(8):615–617, OCT 2002.

[20] R White, I Agouris, and E Fletcher. Harmonic analysis of force platform data in normal and cerebral palsy gait. *CLINICAL BIOMECHANICS*, 20(5):508–516, JUN 2005.

[21] Metin Akay. Wavelets in biomedical engineering. *Annals of Biomedical Engineering*, 23:531–542, 1995. 10.1007/BF02584453.

[22] M.N. Nyan, F.E.H. Tay, K.H.W. Seah, and Y.Y. Sitoh. Classification of gait patterns in the time-frequency domain. *Journal of Biomechanics*, 39(14):2647 – 2656, 2006.

[23] L. M. Schutte, U. Narayanan, J. L. Stout, P. Selber, J. R. Gage, and M. H. Schwartz. An index for quantifying deviations from normal gait. *Gait & Posture*, 11(1):25 – 31, 2000.

[24] Maureen Tingley, Carla Wilson, E. Biden, and W. R. Knight. An index to quantify normality of gait in young children. *Gait & Posture*, 16(2):149 – 158, 2002.

[25] Victoria L. Chester, Maureen Tingley, and Edmund N. Biden. An extended index to quantify normality of gait in children. *Gait & Posture*, 25(4):549 – 554, 2007.

[26] S. J. Hillman, M. E. Hazlewood, M. H. Schwartz, M. L. van der Linden, and J. E. Robb. Correlation of the edinburgh gait score with the gillette gait index, the gillette functional assessment questionnaire, and dimensionless speed. *Journal of Pediatric Orthopaedics*, 27(1):7–11, 2007.

[27] M. H. Schwartz and A. Rozumalski. The gait deviation index: A new comprehensive index of gait pathology. *Gait & Posture*, 28(3):351–357, 2008.

[28] Victoria Chester. Using waveform analyses to develop pediatric gait indices. *EXERCISE AND SPORT SCIENCES REVIEWS*, 37(4):211–217, OCT 2009.

[29] A. M. S. Muniz and J. Nadal. Application of principal component analysis in vertical ground reaction force to discriminate normal and abnormal gait. *GAIT & POSTURE*, 29(1):31–35, JAN 2009.

[30] Kevin J. Deluzio, Urs P. Wyss, Benny Zee, Patrick A. Costigan, and Charles Serbie. Principal component models of knee kinematics and kinetics: Normal vs. pathological gait patterns. *Human Movement Science*, 16(2-3):201 – 217, 1997. 3-D Analysis of Human Movement - II.

[31] Victoria L. Chester and Allan T. Wrigley. The identification of age-related differences in kinetic gait parameters using principal component analysis. *CLINICAL BIOMECHANICS*, 23(2):212–220, FEB 2008.

[32] Samantha M. Reid, Ryan B. Graham, and Patrick A. Costigan. Differentiation of young and older adult stair climbing gait using principal component analysis. *GAIT & POSTURE*, 31(2):197–203, FEB 2010.

[33] H. M. Lakany and G. M. Hayes. An algorithm for recognising walkers. *Audio- and Video-based Biometric Person Authentication*, 1206:111–118, 1997.

[34] H. M. Lakany. A generic kinematic pattern for human walking. *Neurocomputing*, 35:27–54, 2000.

[35] Heba Lakany. Extracting a diagnostic gait signature. *PATTERN RECOGNITION*, 41(5):1627–1637, MAY 2008.

[36] Gabor Barton, Adrian Lees, Paulo Lisboa, and Steve Attfield. Visualisation of gait data with kohonen self-organising neural maps. *GAIT & POSTURE*, 24(1):46–53, AUG 2006.

[37] C. Kirtley, M.W. Whittle, and R.J. Jefferson. Influence of walking speed on gait parameters. *Journal of Biomedical Engineering*, 7(4):282 – 288, 1985.

[38] BW Stansfield, SJ Hillman, ME Hazlewood, AA Lawson, AM Mann, IR Loudon, and JE Robb. Normalized speed, not age, characterizes ground reaction force patterns in 5-to 12-year-old children walking at self-selected speeds. *JOURNAL OF PEDIATRIC ORTHOPAEDICS*, 21(3):395–402, MAY-JUN 2001.

[39] M Diop, A Rahmani, A Belli, V Gautheron, A Geyssant, and J Cottalorda. Influence of speed variation and age on ground reaction forces and stride parameters of children's normal gait. *INTERNATIONAL JOURNAL OF SPORTS MEDICINE*, 26(8):682–687, OCT 2005.

[40] B.W. Stansfield, S.J. Hillman, M.E. Hazlewood, and J.E. Robb. Regression analysis of gait parameters with speed in normal children walking at self-selected speeds. *Gait & Posture*, 23(3):288 – 294, 2006.

[41] Noel Lythgo, Cameron Wilson, and Mary Galea. Basic gait and symmetry measures for primary school-aged children and young adults. ii: Walking at slow, free and fast speed. *Gait & Posture*, 33(1):29 – 35, 2011.

[42] At L. Hof. Scaling gait data to body size. *Gait & Posture*, 4(3):222 – 223, 1996.

[43] B. W. Stansfield, S. J. Hillman, M. E. Hazlewood, A. M. Lawson, A. M. Mann, I. R. Loudon, and J. E. Robb. Normalisation of gait data in children. *Gait & Posture*, 17(1):81 – 87, 2003.

Appendix A

Structure of Data Matrices

	column 1	column 2
row 1	LeftCadence	RightCadence
2	LeftStrideTime	RightStrideTime
3	LeftOppositeFootOff	RightOppositeFootOff
4	LeftOppositeFootContact	RightOppositeFootContact
5	LeftStepTime	RightStepTime
6	LeftSingleSupport	RightSingleSupport
7	LeftDoubleSupport	RightDoubleSupport
8	LeftFootOff	RightFootOff
9	LeftStrideLength	RightStrideLength
10	LeftStepLength	RightStepLength
11	LeftSpeed	RightSpeed

Table A.1: Spatiotemporal Matrix

	parameters
column 1	LeftPelvicTilt
2	LeftPelvicObliquity
3	LeftPelvicRotation
4	LeftHipFlexExt
5	LeftHipAbAdduct
6	LeftHipRotation
7	LeftKneeFlexExt
8	LeftKneeValgVar
9	LeftKneeRotation
10	LeftDorsiPlanFlex
11	LeftFootRotation
12	LeftFootProgression
13	RightPelvicTilt
14	RightPelvicObliquity
15	RightPelvicRotation
16	RightHipFlexExt
17	RightHipAbAdduct
18	RightHipRotation
19	RightKneeFlexExt
20	RightKneeAbAdduct
21	RightKneeRotation
22	RightDorsiPlanFlex
23	RightFootRotation
24	RightFootProgression

Table A.2: Kinematics Matrix

	parameters
column 1	HipFlexExtMoment
2	HipAbAdductMoment
3	HipRotationMoment
4	KneeFlexExtMoment
5	KneeValgVarMoment
6	KneeRotationMoment
7	DorsiPlanFlexMoment
8	FootAbAdductMoment
9	FootRotationMoment
10	HipPower
11	HipFlexExtPower
12	HipAbAdductPower
13	HipRotationPower
14	KneePower
15	KneeFlexExtPower
16	KneeValgVarPower
17	KneeRotationPower
18	AnklePower
19	DorsiPlanFlexPower
20	AnkleAbAdductPower
21	AnkleRotationPower

Table A.3: Kinetics Matrix

	parameters
column 1	AntPost Force
2	MedLat Force
3	Vertical Force
4	CoP X
5	CoP Y
6	CoP Z

Table A.4: Ground Reaction Matrix

Appendix B

Sample MATLab Scripts

Function to Convert .gcd Data Files

```
function [Spatiotemporal,Kinematics,Kinetics,GroundReaction]...
 = SMReaddata(Subject,item)
% SMReaddata reads from gait database .gcd files and saves it in matrices
% Spatiotemporal, Kinematics, Kinetics and GroundReaction
% Spatiotemporal matrix 11x2 right and left sides
% Kinematics matrix 51x24 right and left
% Kinetics matrix 51x27 right or left contacting foot
% GroundReaction matrix 51x6 right or left contacting foot
% Input Subject xx, item xxxxxx.gcd
% path to Gait data
path_to_data = sprintf('C:/Users/sjtm/Documents/project/SLOW_GCD/%s',Subject);
fid_name = sprintf( '%s/%s',path_to_data,item);
Fs = 25; % sampling rate
GaitCycle = Fs*2+1;
N=GaitCycle;
% Parameters
ST = 11; % spatiotemporal parameters
KM = 24; % Kinematics parameters R, L, Pelvic, Hip, Knee, Ankle
KN = 21; % Kinetics parameters Pwr, Mmnts
GR =  6; % Ground reaction forces and moments GRF, GRM
Sides = 2; % 1 Left and 2 Right
Left = 1;
Right = 2;
%size of Matrices
Spatiotemporal = zeros(ST,Sides);
Kinematics = zeros(N,KM);
Kinetics = zeros(N,KN);
```

```
GroundReaction = zeros(N,GR);
% Read SpatioTemporal Matrix
fid = fopen(fid_name,'r');
found = JumpTo(fid,'!LeftCadence');
if found == 1
    for s = 1:8,
        Ep = fscanf(fid,'%f\n', 1);
        Spatiotemporal(s,Left) = Ep;
        tline = fgetl(fid);
    end
end
fclose(fid);
fid = fopen(fid_name,'r');
found = JumpTo(fid,'!RightCadence');
if found == 1
    for s = 1:8,
        Ep = fscanf(fid,'%f\n', 1);
        Spatiotemporal(s,Right) = Ep;
        tline = fgetl(fid);
    end
end
fclose(fid);
% LHS stride, step, speed
fid = fopen(fid_name,'r');
found = JumpTo(fid,'!LeftStrideLength');
if found == 1
    for s = 9:ST,
        Ep = fscanf(fid,'%f\n', 1);
        Spatiotemporal(s,Left) = Ep;
        tline = fgetl(fid);
    end
end
fclose(fid);
% RHS stride, step, speed
fid = fopen(fid_name,'r');
found = JumpTo(fid,'!RightStrideLength');
if found == 1
    for s = 9:ST,
        Ep = fscanf(fid,'%f\n', 1);
        Spatiotemporal(s,Right) = Ep;
        tline = fgetl(fid);
    end
end
fclose(fid);
% Read Kinematics
```

```
% LHS body angles
fid = fopen(fid_name,'r');
found = JumpTo(fid,'!LeftPelvicTilt');
if found == 1
    for s = 1:KM/2,
        for i=1:N,
            Ep = fscanf(fid,'%f\n', 1);
            Kinematics(i,s) = Ep;
        end
        tline = fgetl(fid);
    end
end
fclose(fid);
%RHS body angles
fid = fopen(fid_name,'r');
found = JumpTo(fid,'!RightPelvicTilt');
if found == 1
    for s = (KM/2+1):KM,
        for i=1:N,
            Ep = fscanf(fid,'%f\n', 1);
            Kinematics(i,s) = Ep;
        end
        tline = fgetl(fid);
    end
end
fclose(fid);
% Read Kinetics
fid      = fopen(fid_name,'r');
found = JumpTo(fid,'!LeftHipFlexExtMoment');
if found == 1
    for s = 1:KN,
        for i=1:N,
            Ep = fscanf(fid,'%f\n', 1);
            Kinetics(i,s) = Ep;
        end
        tline = fgetl(fid);
    end
end
fclose(fid);
if found == 0
    fid      = fopen(fid_name,'r');
    found = JumpTo(fid,'!RightHipFlexExtMoment');
    if found == 1
        for s = 1:KN,
            for i=1:N,
```

```
                Ep = fscanf(fid,'%f\n', 1);
                Kinetics(i,s) = Ep;
            end
            tline = fgetl(fid);
        end
    end
    fclose(fid);
end
% Read GroundReaction
fid = fopen(fid_name,'r');
found = JumpTo(fid,'!LeftGroundReaction-3-2');
if found == 1
    for i=1:N,
        for j=1:6,
            Ep = fscanf(fid,'%f', 1);
            GroundReaction(i,j) = Ep;
        end
        tline = fgetl(fid);
    end
end
fclose(fid);
if found == 0
    fid = fopen(fid_name,'r');
    found = JumpTo(fid,'!RightGroundReaction-3-2');
    if found == 1
        for i=1:N,
            for j=1:6,
                Ep = fscanf(fid,'%f', 1);
                GroundReaction(i,j) = Ep;
            end
            tline = fgetl(fid);
        end
    end
    fclose(fid);
end
rootname = (item(1:length(item)-4));
datafile = sprintf( '%s/%s.mat',path_to_data,rootname);
save(fullfile(datafile),'Spatiotemporal','Kinematics','Kinetics',...
'GroundReaction')
end
```

Function Used to Normalise Data

```
function [SpatiotemporalN,KinematicsN,KineticsN,GroundReactionN]...
= NormaliseData( Subject, item )
% NormaliseData normalises gait data for body height, body weight, body mass
% Uses body parameters data for subject in file xxbodypar.mat
% Load in unnormalised gait data .mat file
path_to_data = sprintf('C:/Users/sjtm/Documents/project/SLOW_GCD/%s',Subject);
fid_name = sprintf( '%s/%s',path_to_data,item);
load(fid_name);
bodypar = sprintf('%s/%sbodypar.mat',path_to_data,Subject);
load(bodypar);
BH=bodypar(1,1);
BW=bodypar(1,2);
BM=bodypar(1,3);
SpatiotemporalN=Spatiotemporal;
KinematicsN=Kinematics;
KineticsN=Kinetics;
GroundReactionN=GroundReaction;
% Normalise Spatiotemporal Matrix
% cadence
SpatiotemporalN(1,1:2)=Spatiotemporal(1,1:2)*(1/sqrt(9.81/BH));
% stride time
SpatiotemporalN(2,1:2)=Spatiotemporal(2,1:2)*(sqrt(9.81/BH));
% stride,step length
SpatiotemporalN(9:10,1:2)=Spatiotemporal(9:10,1:2)*(1/(1000*BH));
% speed
SpatiotemporalN(11,1:2)=Spatiotemporal(11,1:2)*(1/(1000*BH*(sqrt(9.81/BH))));
% Kinematics Matrix contains angles - no need for normalisation
% Normalise Kinetics Matrix
% moments
KineticsN(:,1:9)=Kinetics(:,1:9)*(BM/(BW*BH));
% powers
KineticsN(:,10:21)=Kinetics(:,10:21)*(BM/(sqrt(9.81/BH)*(BW*BH)));
% Normalise GroundReaction Matrix
GroundReactionN(:,1:3)=GroundReaction(:,1:3)*(1/BW);
GroundReactionN(:,4:6)=GroundReaction(:,4:6)*(1/(1000*BH));
datafile = sprintf( '%s/%sN.mat',path_to_data,item);
save(fullfile(datafile),'SpatiotemporalN','KinematicsN','KineticsN',...
'GroundReactionN')
end
```

Function to Categorise Trials by Speed

```
function speeds(Subject)
% speeds(Subject) uses list.mat to find speeds for each trial
% categorises by speed band and saves lists and speeds
path = sprintf('C:/Users/sjtm/Documents/project/SLOW_GCD/%s',Subject);
list_id = sprintf( '%s/list',path);
load(list_id);
speeds=zeros(length(list),2);
AveSpeeds=zeros(length(list),1);
NList=cell(length(list),2);
AList=cell(1,1);
BList=cell(1,1);
CList=cell(1,1);
DList=cell(1,1);
EList=cell(1,1);
FList=cell(1,1);
a=1;
b=1;
c=1;
d=1;
e=1;
f=1;
for n=1:length(list)
    item=list{n,1};
    root=(item(1:length(item)-4));
    rootn=sprintf('%sN',root);
    nitem=sprintf('%s/%sN.mat',path,root);
    load(nitem)
    speeds(n,:)=SpatiotemporalN(11,:);
    AveSpeeds(n,1)=mean(speeds(n,:));
    NList{n,1}=sprintf('%sN',root);
    if AveSpeeds(n,1)<=0.15
        NList{n,2}='A';
        AList{a,1}=rootn;
        a=a+1;
    elseif AveSpeeds(n,1)<=0.20
        NList{n,2}='B';
        BList{b,1}=rootn;
        b=b+1;
    elseif AveSpeeds(n,1)<=0.25
        NList{n,2}='C';
        CList{c,1}=rootn;
        c=c+1;
```

```
    elseif AveSpeeds(n,1)<=0.3
        NList{n,2}='D';
        DList{d,1}=rootn;
        d=d+1;
    elseif AveSpeeds(n,1)<=0.35
        NList{n,2}='E';
        EList{e,1}=rootn;
        e=e+1;
    elseif AveSpeeds(n,1)>0.35
        NList{n,2}='F';
        FList{f,1}=rootn;
        f=f+1;
    end
end
datafile = sprintf( '%s/speedlist.mat',path);
save(fullfile(datafile),'NList','AveSpeeds','AList','BList','CList',...
'DList','EList','FList')
end
```

Script to Pull Parameter Data

```
%LeftHipFlexExt
% Gathers LeftHipFlexion data for all subjects by speed band
path = sprintf('C:/Users/sjtm/Documents/project/SLOW_GCD');
folderlist_id = sprintf( '%s/folderlist.mat',path);
% Read folderlist and loop through folders
load(folderlist_id)
ALHFE=cell(1,length(folderlist));
BLHFE=cell(1,length(folderlist));
CLHFE=cell(1,length(folderlist));
DLHFE=cell(1,length(folderlist));
ELHFE=cell(1,length(folderlist));
FLHFE=cell(1,length(folderlist));
for n=1:length(folderlist)
    Subject=folderlist{n,1};
    pathsubj = sprintf('C:/Users/sjtm/Documents/project/SLOW_GCD/%s',Subject);
    speeds=sprintf('%s/speedlist.mat',pathsubj);
    load(speeds)
    ALHFEM=zeros(51,length(AList));
    BLHFEM=zeros(51,length(BList));
    CLHFEM=zeros(51,length(CList));
    DLHFEM=zeros(51,length(DList));
    ELHFEM=zeros(51,length(EList));
    FLHFEM=zeros(51,length(FList));
% Band A
    for m=1:length(AList)
        item = AList{m,1};
        tf=isempty(item);
        if tf==0
        file=sprintf('%s/%s',pathsubj,item);
        load(file)
        ALHFEM(:,m)=KinematicsN(:,4);
        else
        end
    end
    ALHFE{1,n}=ALHFEM;
% Band B
    for m=1:length(BList)
        item = BList{m,1};
        tf=isempty(item);
        if tf==0
        file=sprintf('%s/%s',pathsubj,item);
        load(file)
```

```
        BLHFEM(:,m)=KinematicsN(:,4);
        else
        end
    end
    BLHFE{1,n}=BLHFEM;
% Band C
    for m=1:length(CList)
        item = CList{m,1};
        tf=isempty(item);
        if tf==0
        file=sprintf('%s/%s',pathsubj,item);
        load(file)
        CLHFEM(:,m)=KinematicsN(:,4);
        else
        end
    end
    CLHFE{1,n}=CLHFEM;
% Band D
    for m=1:length(DList)
        item = DList{m,1};
        tf=isempty(item);
        if tf==0
        file=sprintf('%s/%s',pathsubj,item);
        load(file)
        DLHFEM(:,m)=KinematicsN(:,4);
        else
        end
    end
    DLHFE{1,n}=DLHFEM;
% Band E
    for m=1:length(EList)
        item = EList{m,1};
        tf=isempty(item);
        if tf==0
        file=sprintf('%s/%s',pathsubj,item);
        load(file)
        ELHFEM(:,m)=KinematicsN(:,4);
        else
        end
    end
    ELHFE{1,n}=ELHFEM;
% Band F
    for m=1:length(FList)
        item = FList{m,1};
        tf=isempty(item);
```

```
        if tf==0
        file=sprintf('%s/%s',pathsubj,item);
        load(file)
        FLHFEM(:,m)=KinematicsN(:,4);
        else
        end
    end
    FLHFE{1,n}=FLHFEM;
end
ALHFEAll=cat(2,[ALHFE{1,:}]);
BLHFEAll=cat(2,[BLHFE{1,:}]);
CLHFEAll=cat(2,[CLHFE{1,:}]);
DLHFEAll=cat(2,[DLHFE{1,:}]);
ELHFEAll=cat(2,[ELHFE{1,:}]);
FLHFEAll=cat(2,[FLHFE{1,:}]);
% Clear empty columns from data
openvar('ALHFEAll')
for n=1:length(ALHFEAll(1,:))
    if n<=length(ALHFEAll(1,:))
        if ALHFEAll(1,n)==0
            ALHFEAll(:,n)=[];
        else
        end
    else
    end
end
openvar('BLHFEAll')
for n=1:length(BLHFEAll(1,:))
    if n<=length(BLHFEAll(1,:))
        if BLHFEAll(1,n)==0
            BLHFEAll(:,n)=[];
        else
        end
    else
    end
end
openvar('CLHFEAll')
for n=1:length(CLHFEAll(1,:))
    if n<=length(CLHFEAll(1,:))
        if CLHFEAll(1,n)==0
            CLHFEAll(:,n)=[];
        else
        end
    else
    end
```

```
end
openvar('DLHFEAll')
for n=1:length(DLHFEAll(1,:))
    if n<=length(DLHFEAll(1,:))
        if DLHFEAll(1,n)==0
            DLHFEAll(:,n)=[];
        else
        end
    else
    end
end
openvar('ELHFEAll')
for n=1:length(ELHFEAll(1,:))
    if n<=length(ELHFEAll(1,:))
        if ELHFEAll(1,n)==0
            ELHFEAll(:,n)=[];
        else
        end
    else
    end
end
openvar('FLHFEAll')
for n=1:length(FLHFEAll(1,:))
    if n<=length(FLHFEAll(1,:))
        if FLHFEAll(1,n)==0
            FLHFEAll(:,n)=[];
        else
        end
    else
    end
end
for n=1:length(FLHFEAll(1,:))
    if n<=length(FLHFEAll(1,:))
        if FLHFEAll(1,n)==0
            FLHFEAll(:,n)=[];
        else
        end
    else
    end
end
clearvars -except ALHFEAll BLHFEAll CLHFEAll DLHFEAll ELHFEAll FLHFEAll
save LeftHipFlexExt.mat
```

Script to Convert to Frequency Domain

```
% Calculates Frequency components from LeftHipFlexExt Speed band Averages
% also reconstructs signal with first 8 frequency components

path = sprintf('C:/Users/sjtm/Documents/project/SLOW_GCD');
LeftHipFlexExt = sprintf( '%s/LeftHipFlexExt.mat',path);
load(LeftHipFlexExt)

Fs = 50;                    % Sampling frequency
L = 51;                     % Length of signal

% frequency scale
NFFT = 2^nextpow2(L); % Next power of 2 from length of y
f = Fs/2*linspace(0,1,NFFT/2+1); % frequencies

for n=1:6
    y=LHFEAve(:,n);
    Y=fft(y);
    % Amplitude of frequency components
    LHFEAmpl(:,n)=2*abs(Y(1:NFFT/2+1))/L;
    % Band n Reconstruction 8 cpts
    LHFERecon(:,n) = 2*ifft(Y(1:8),L)-LHFEAmpl(1,n)/2;
end

save LeftHipFlexExt.mat f LHFEAmpl LHFERecon -append
```

Appendix C

All Subjects - Further Plots

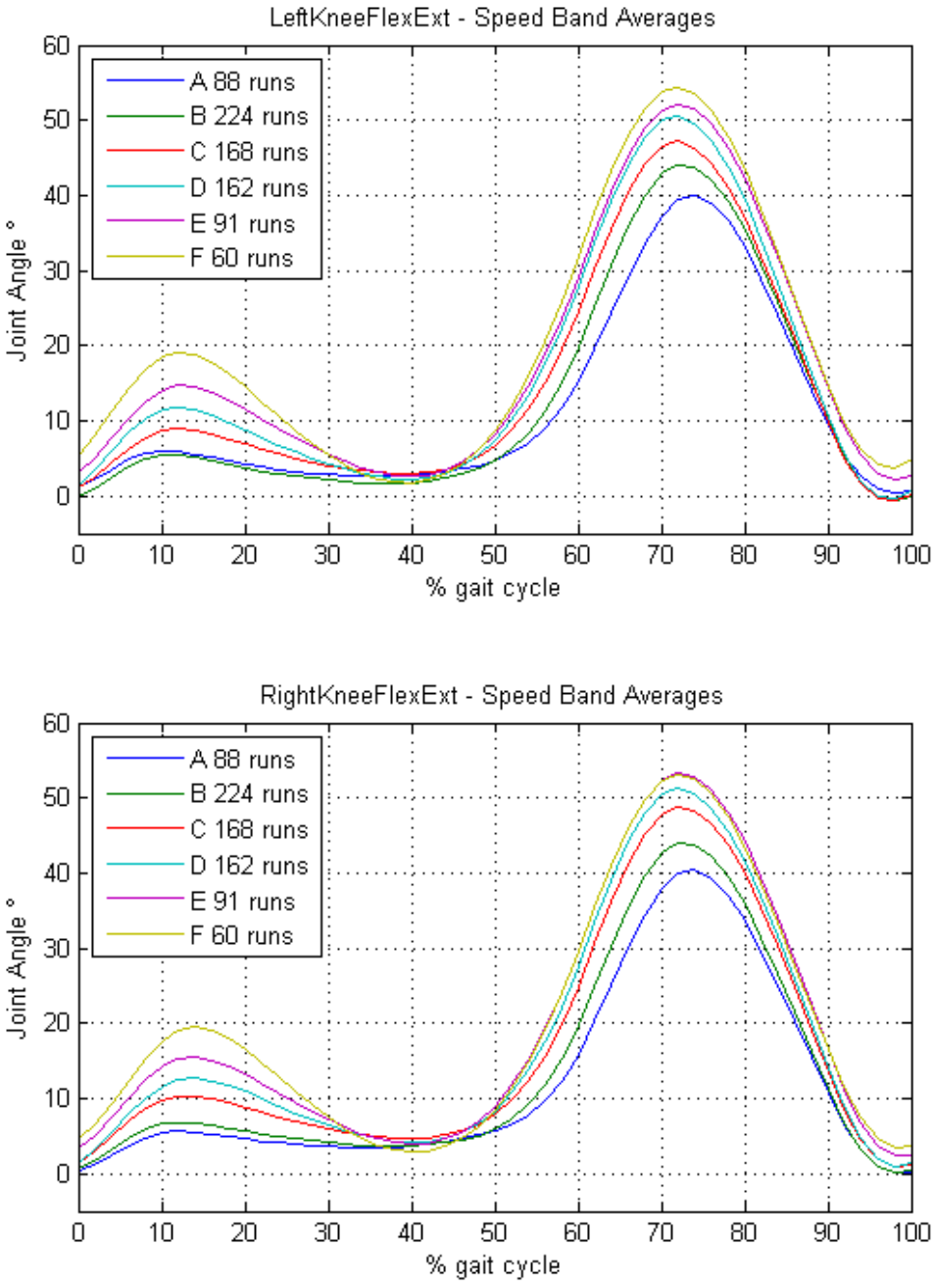

Figure C.1: Left and Right Knee Flexion Angle

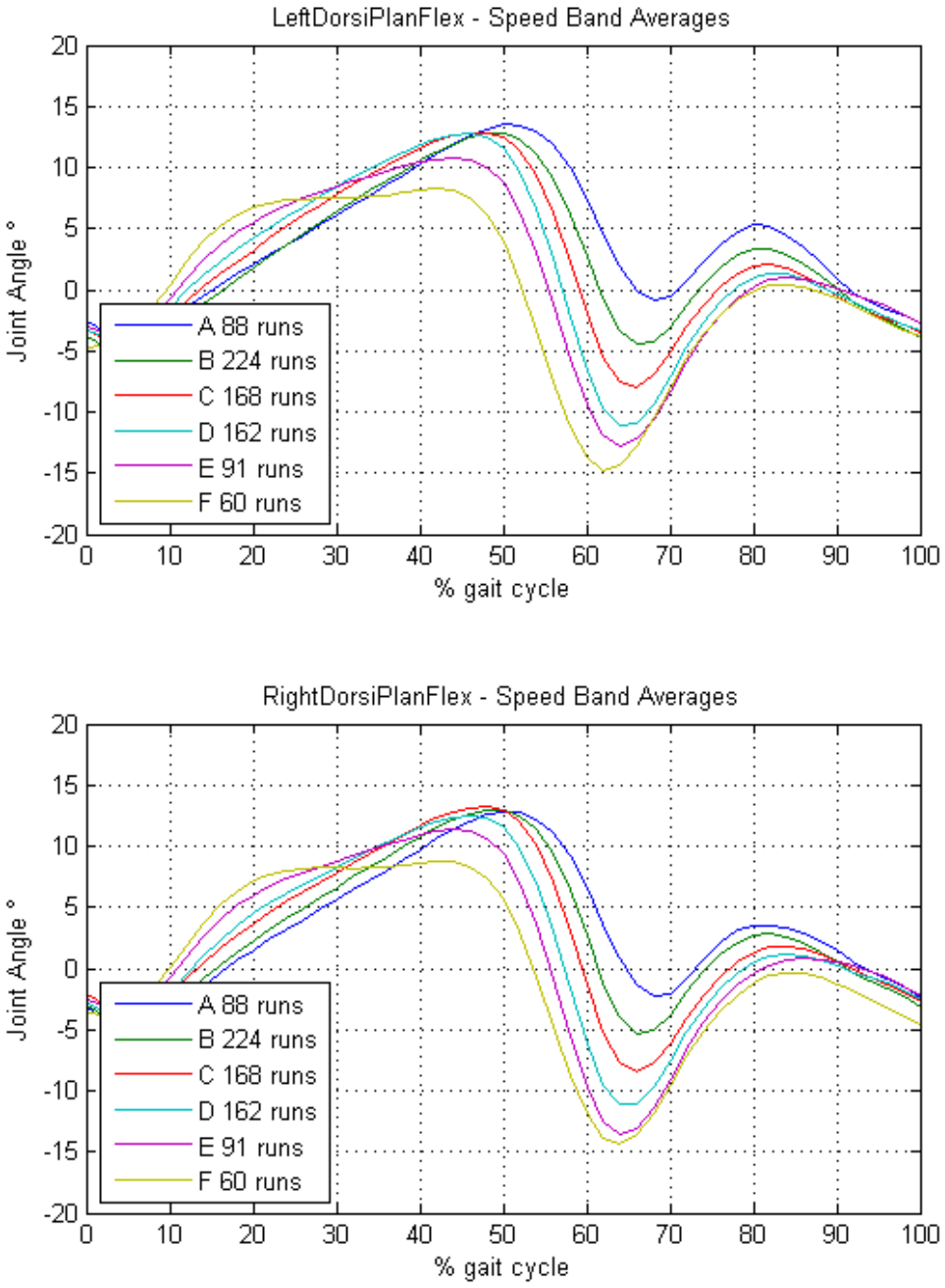

Figure C.2: Left and Right Dorsi-Plantarflexion Angle

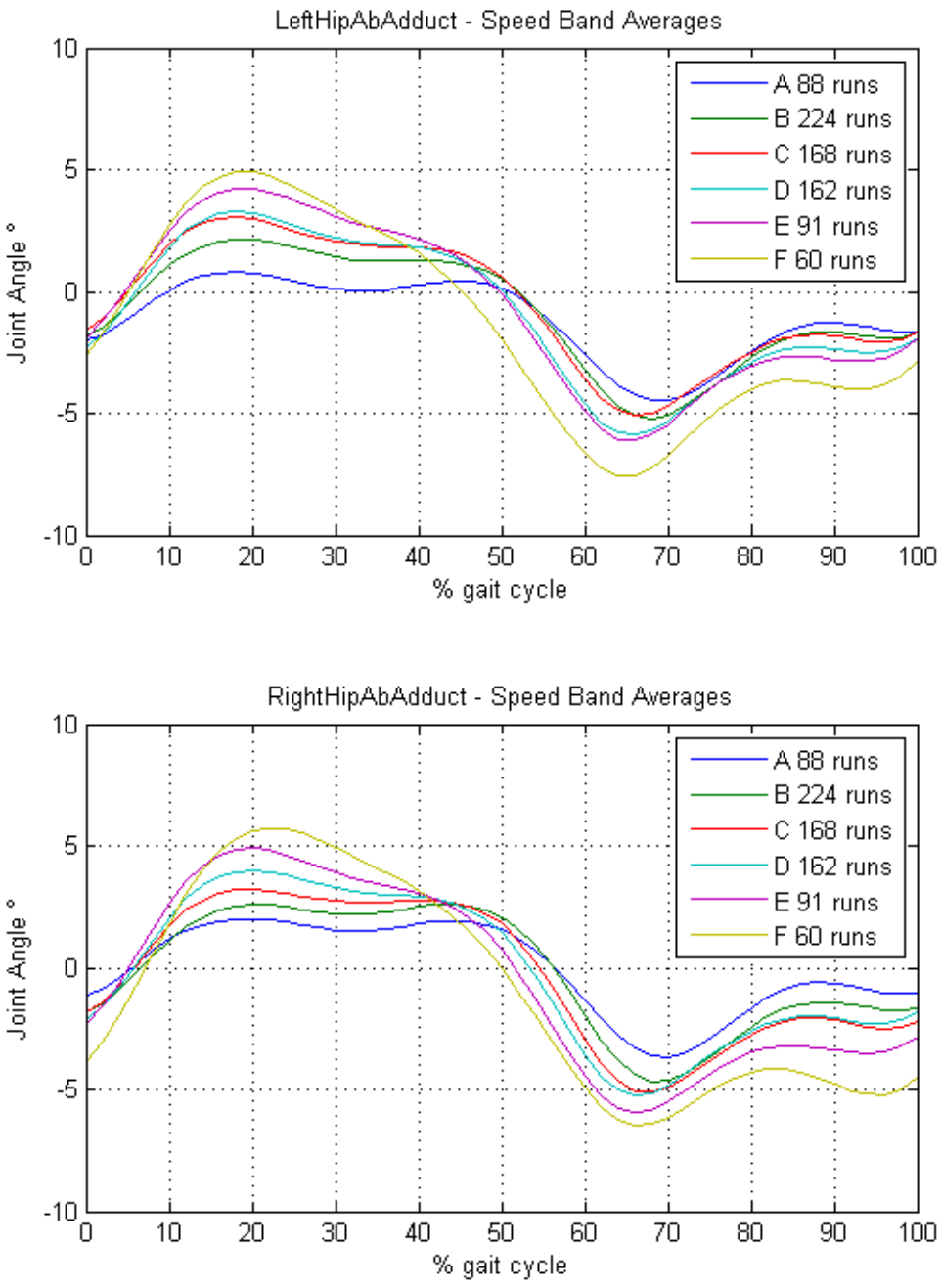

Figure C.3: Left and Right Hip Ab-Adduction Angle

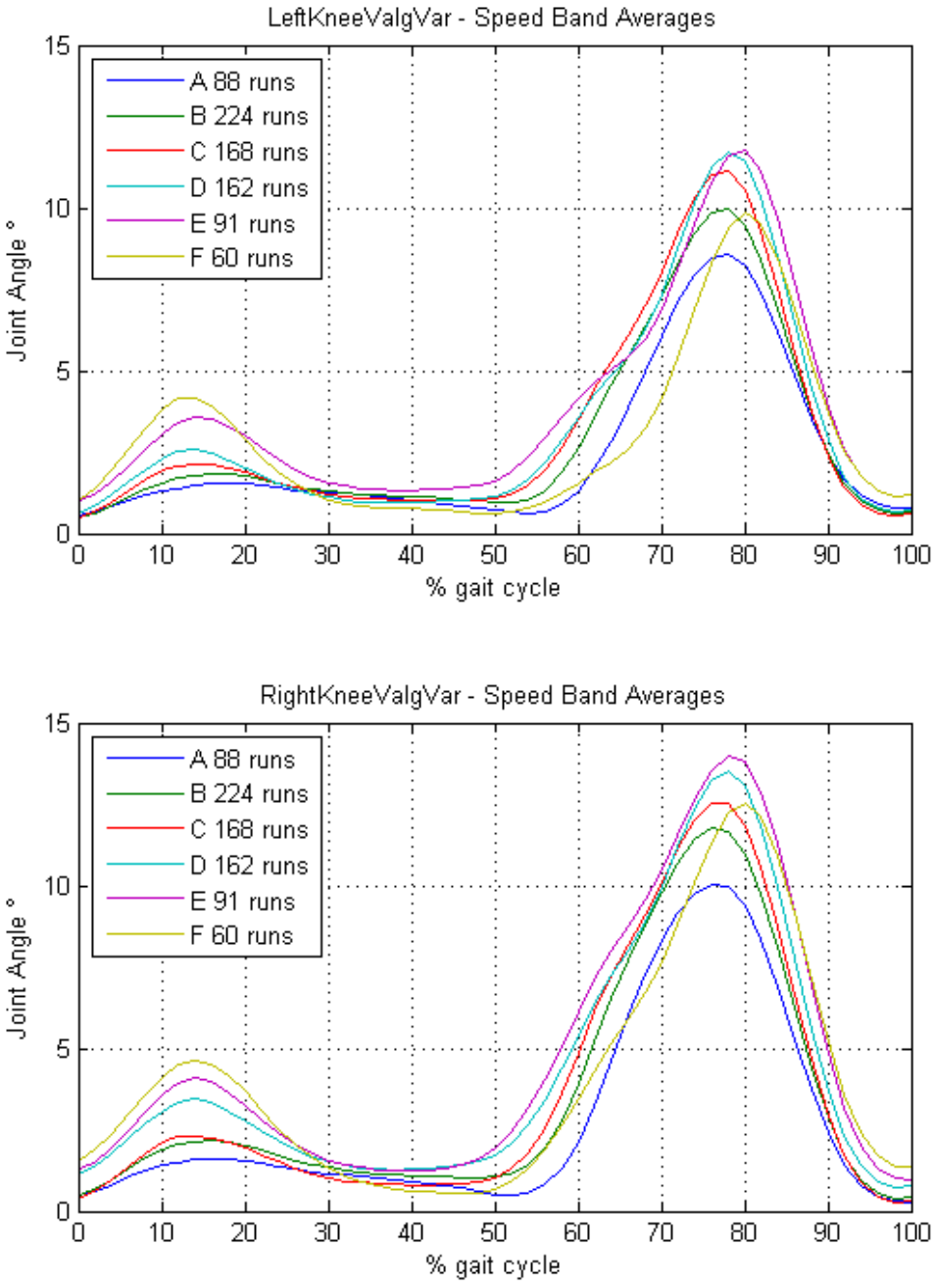

Figure C.4: Left and Right Knee Valgus Varus Angle

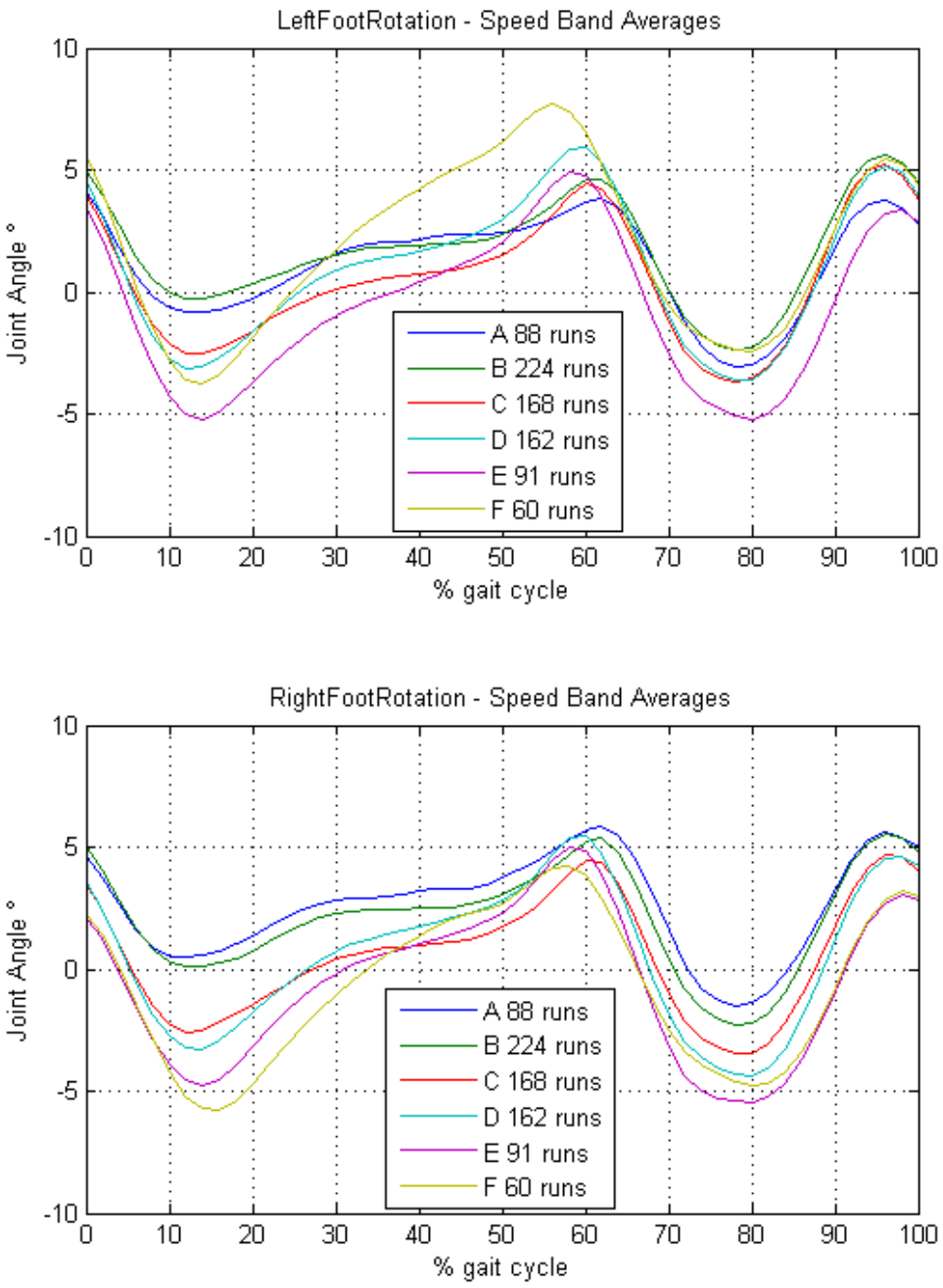

Figure C.5: Left and Right Foot Rotation Angle

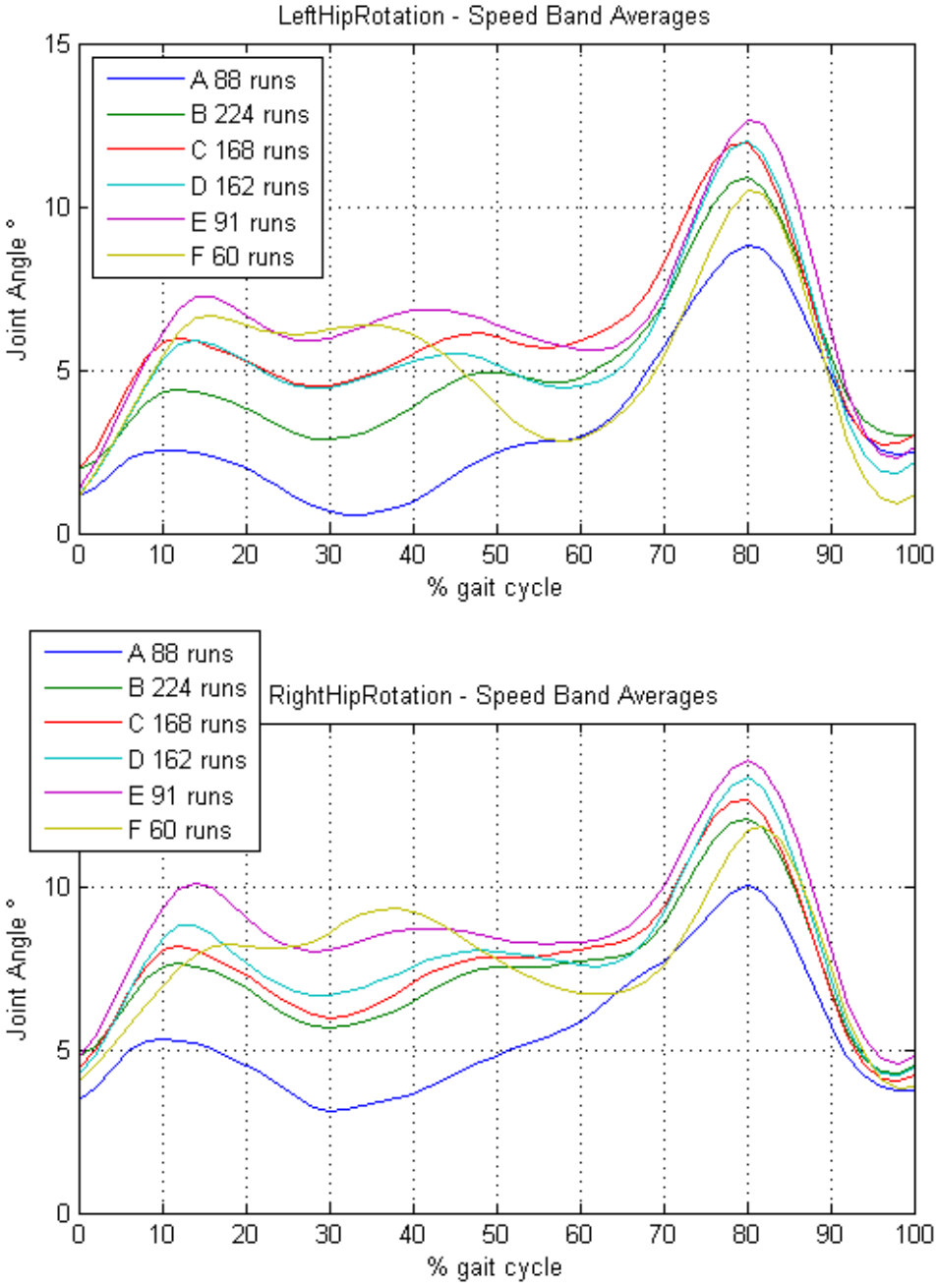

Figure C.6: Left and Right Hip Rotation Angle

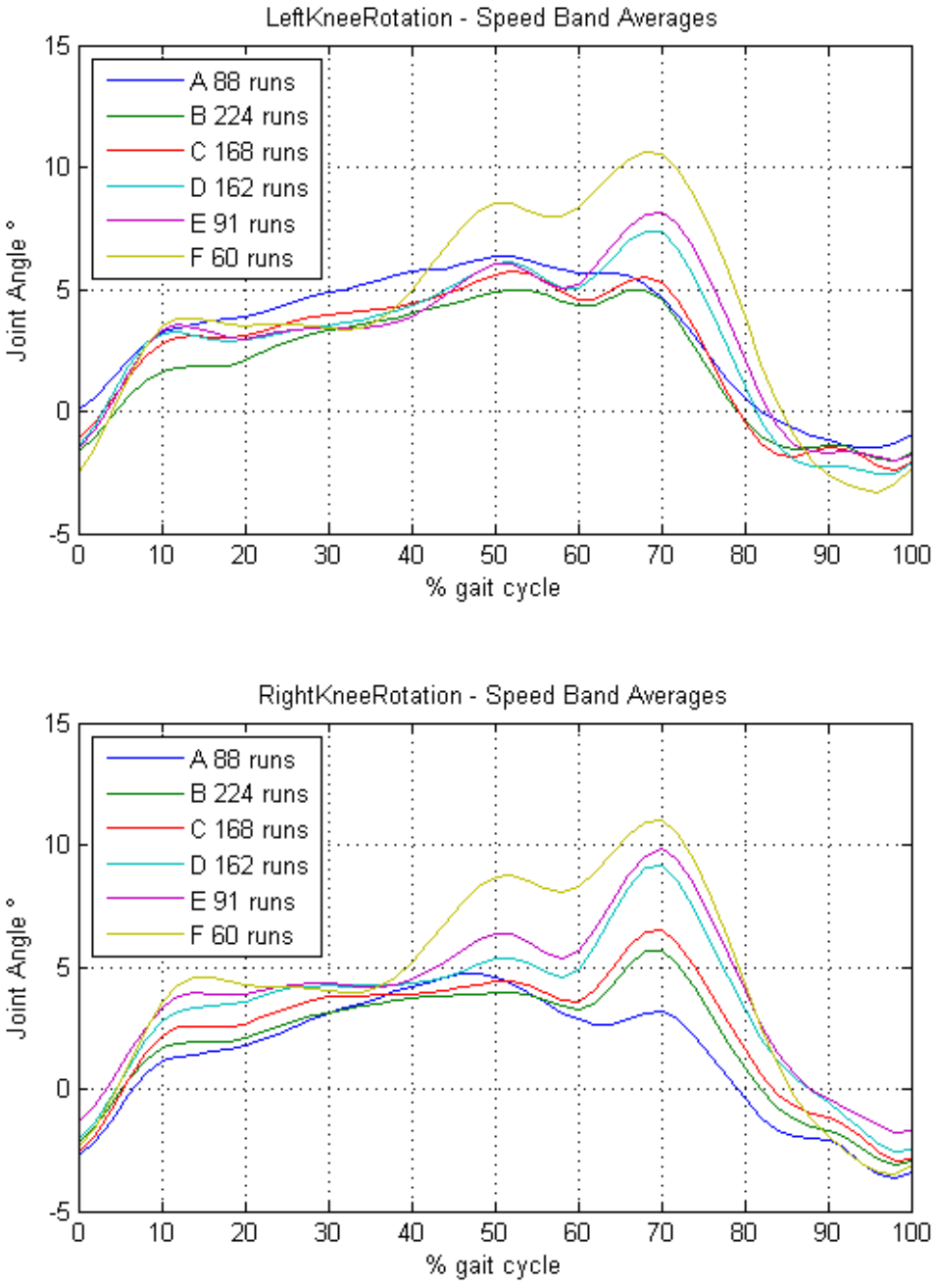

Figure C.7: Left and Right Knee Rotation Angle

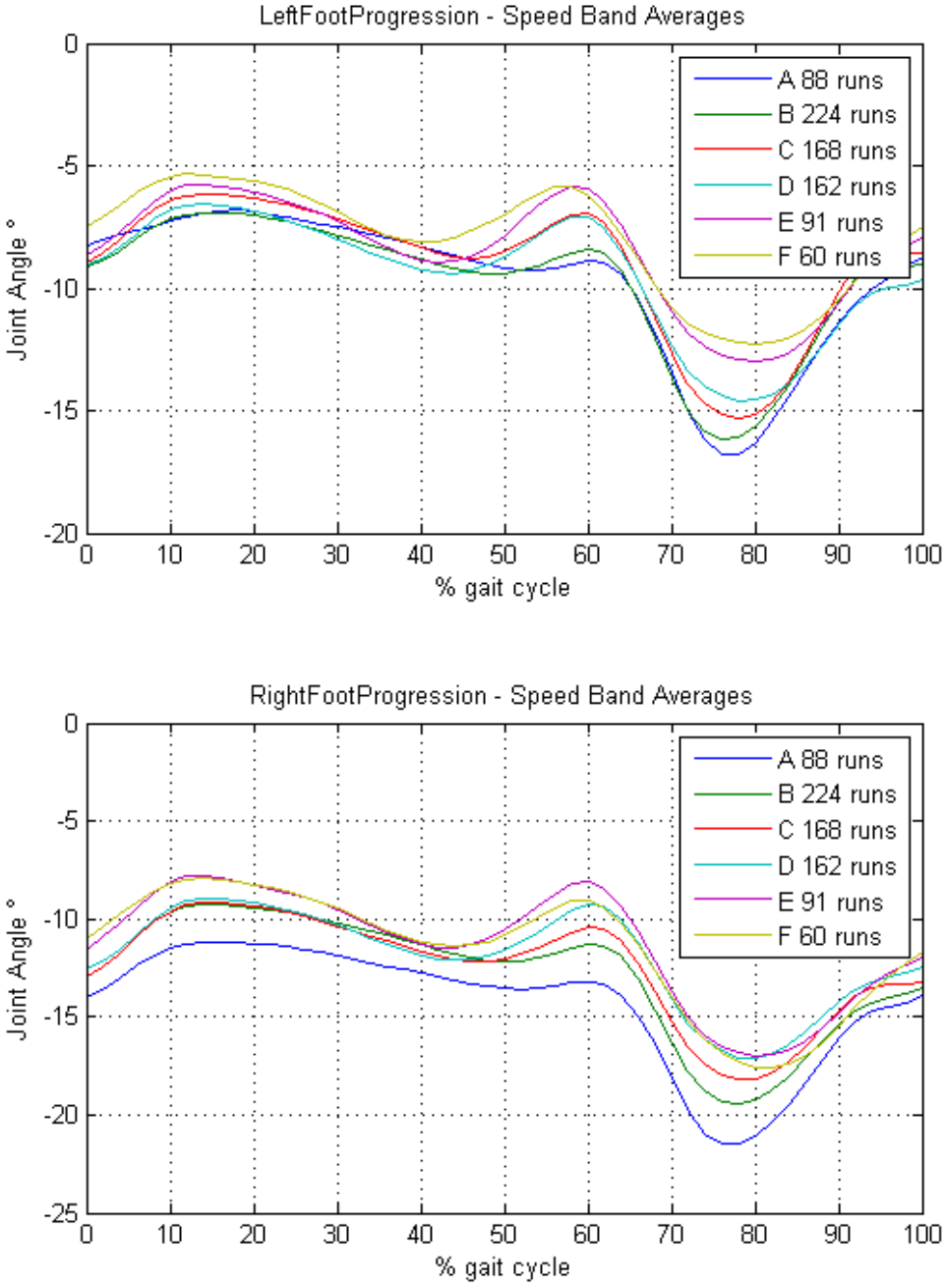

Figure C.8: Left and Right Foot Progression Angle

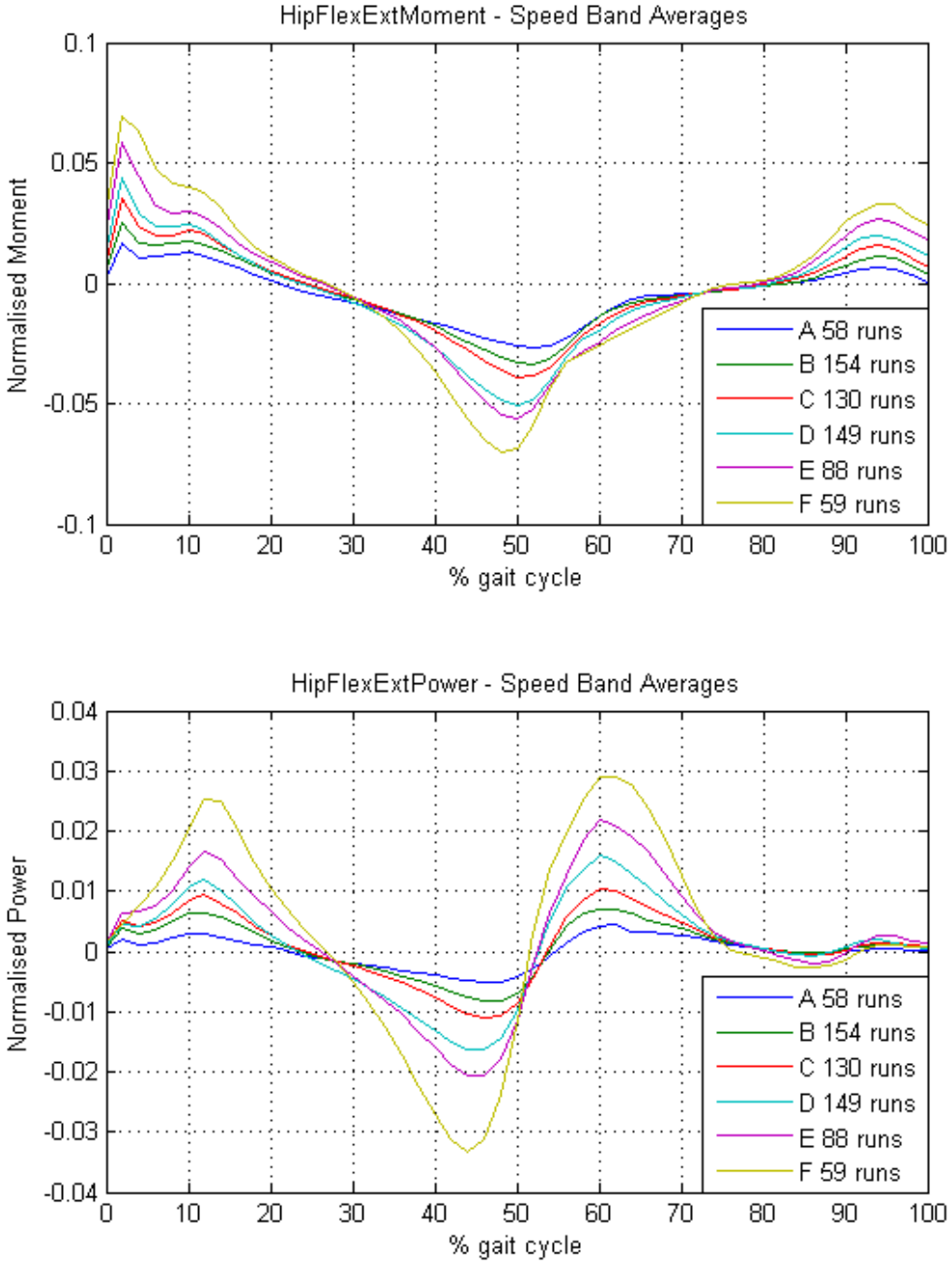

Figure C.9: Hip Flexion Moment and Power

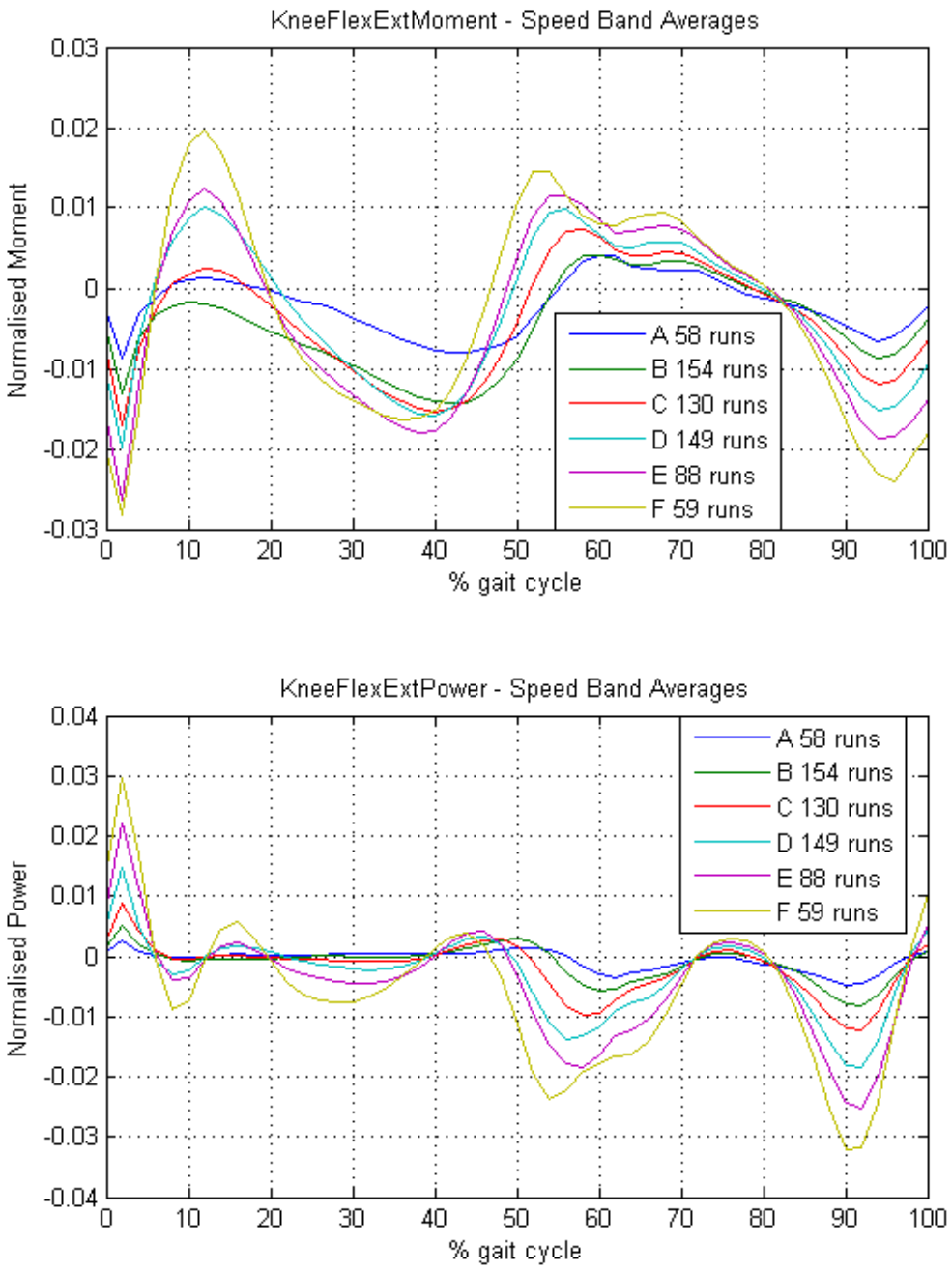

Figure C.10: Knee Flexion Moment and Power

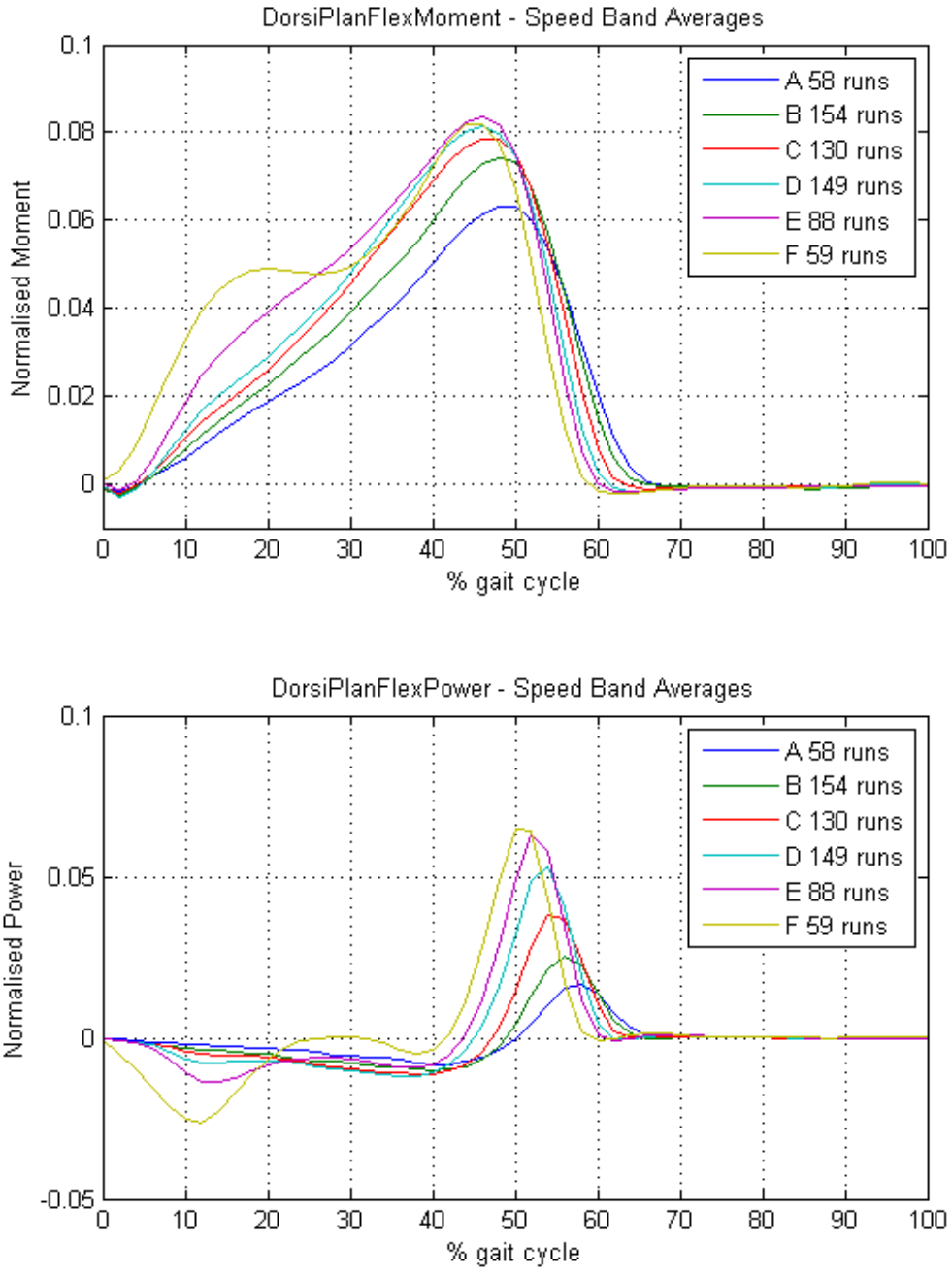

Figure C.11: Dorsi-Plantarflexion Moment and Power

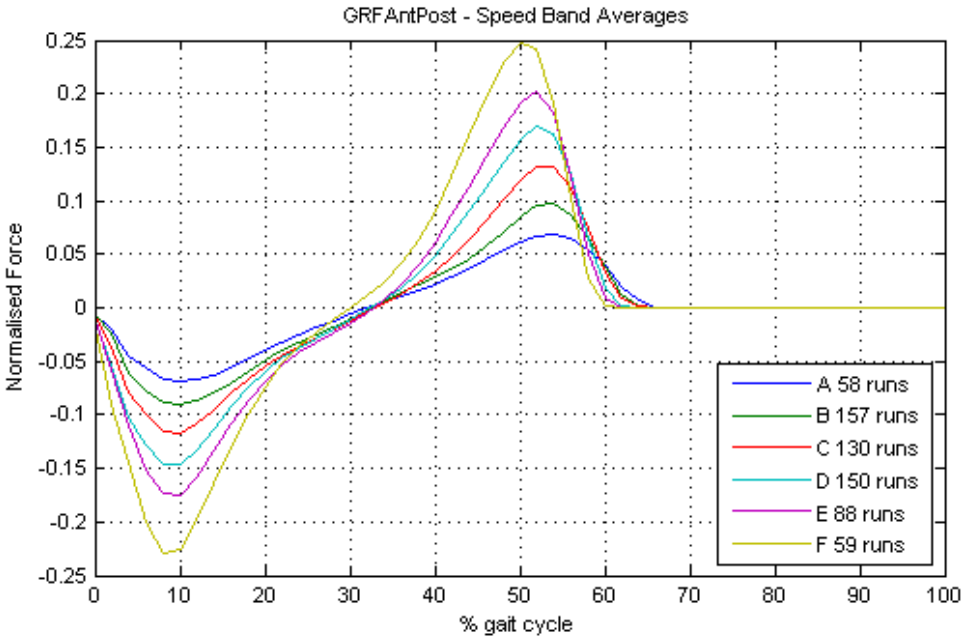

Figure C.12: Antero-Posterior Ground Reaction Force

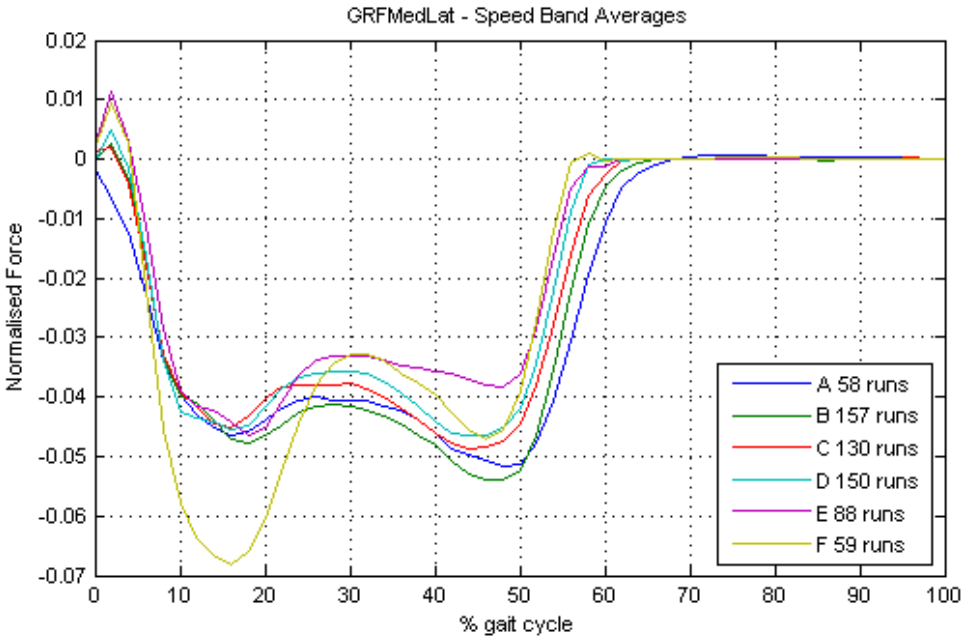

Figure C.13: Medio-Lateral Ground Reaction Force

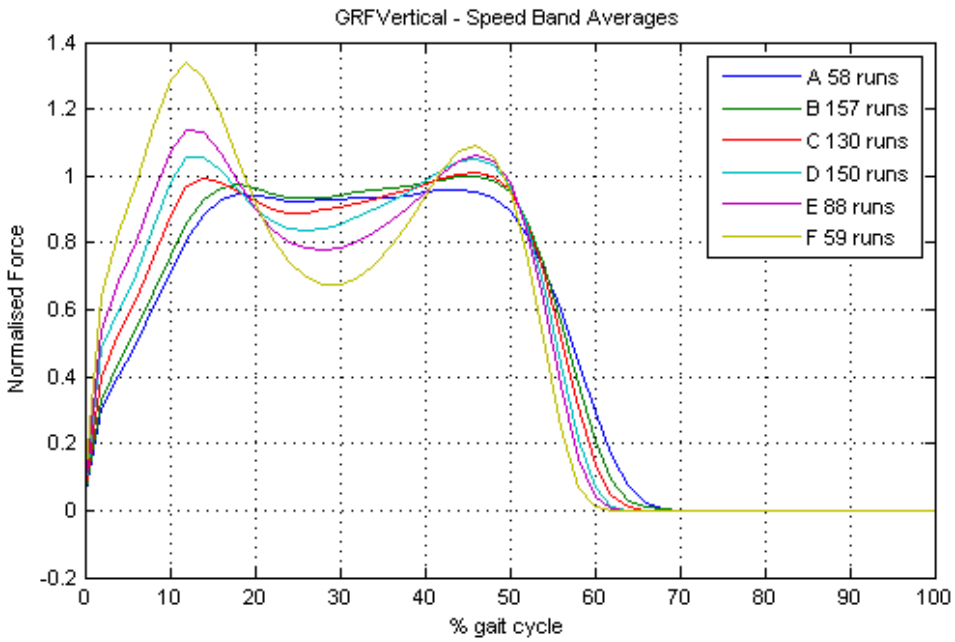

Figure C.14: Vertical Ground Reaction Force

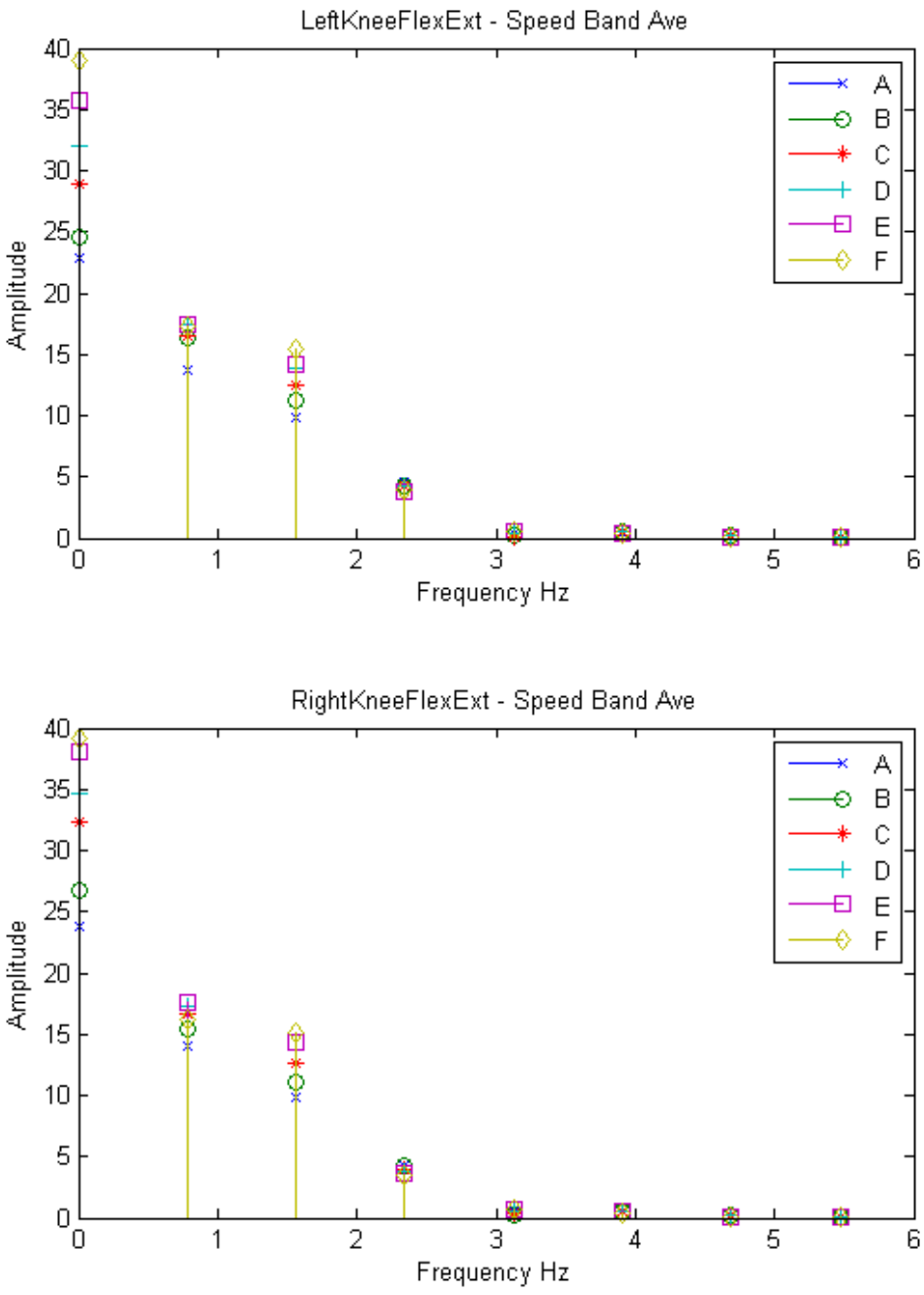

Figure C.15: Left and Right Knee Flexion in Frequency Domain

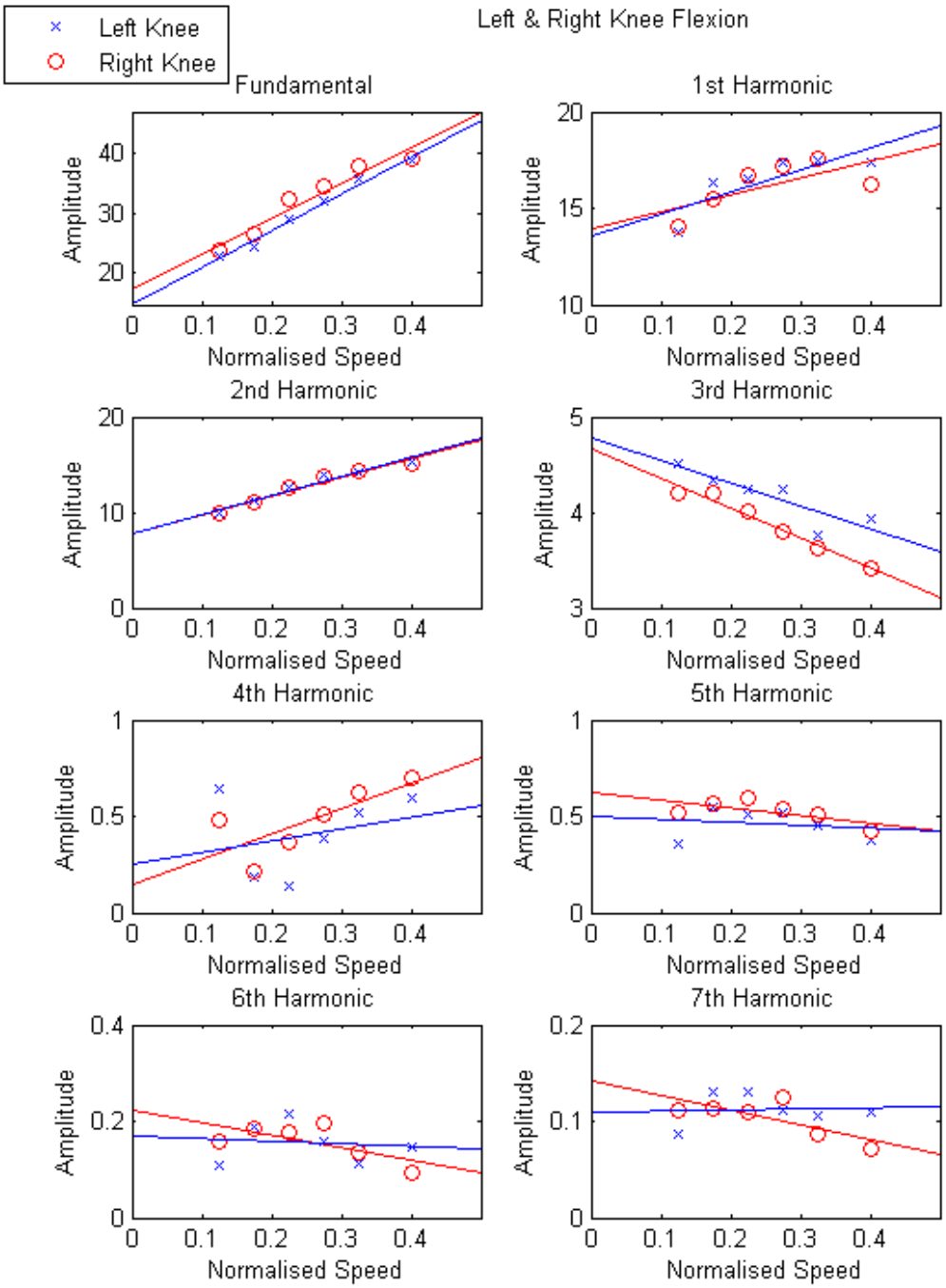

Figure C.16: Left and Right Knee Flexion Harmonic Amplitudes versus Normalised Speed

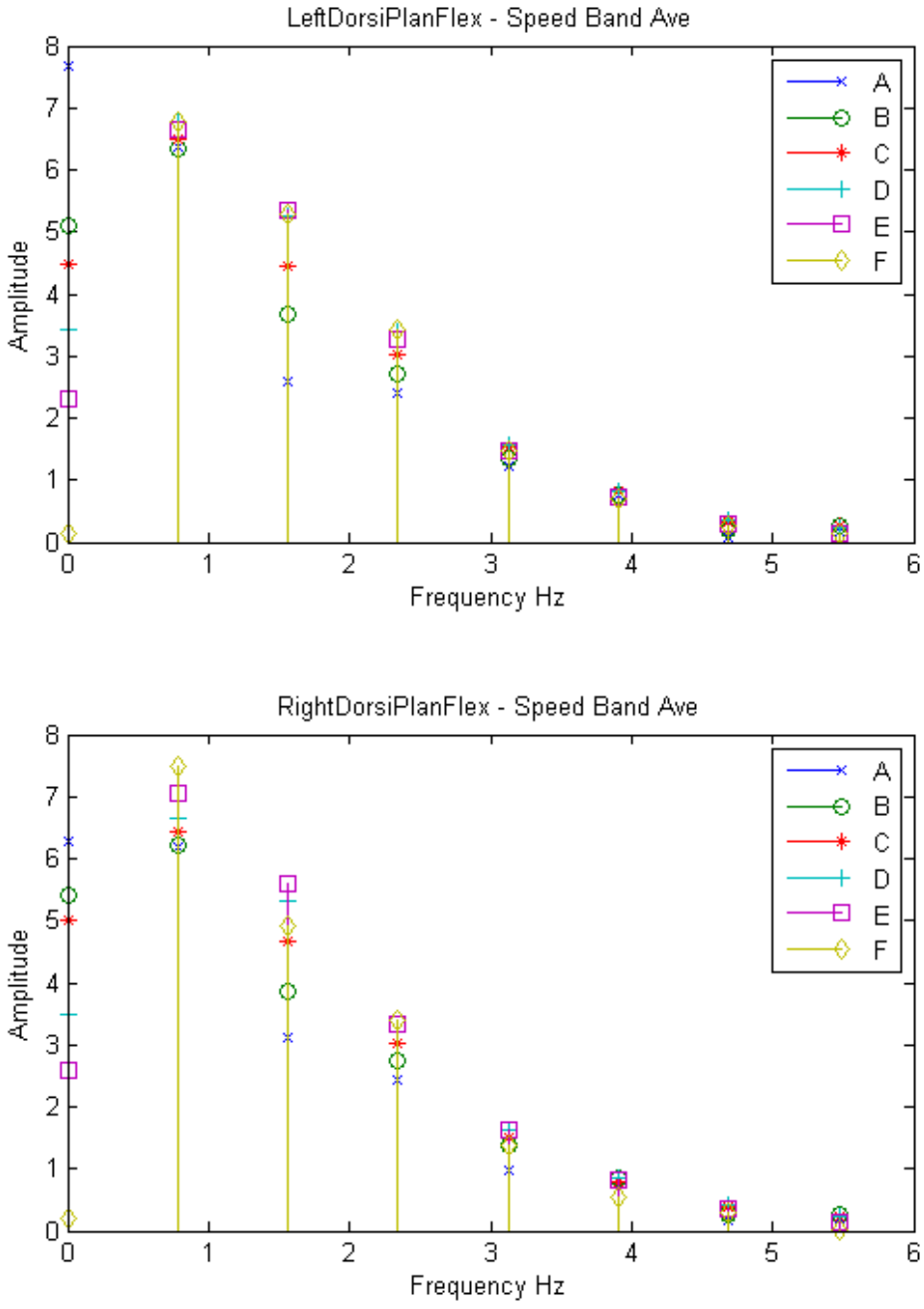

Figure C.17: Left and Right Dorsi-Plantarflexion in Frequency Domain

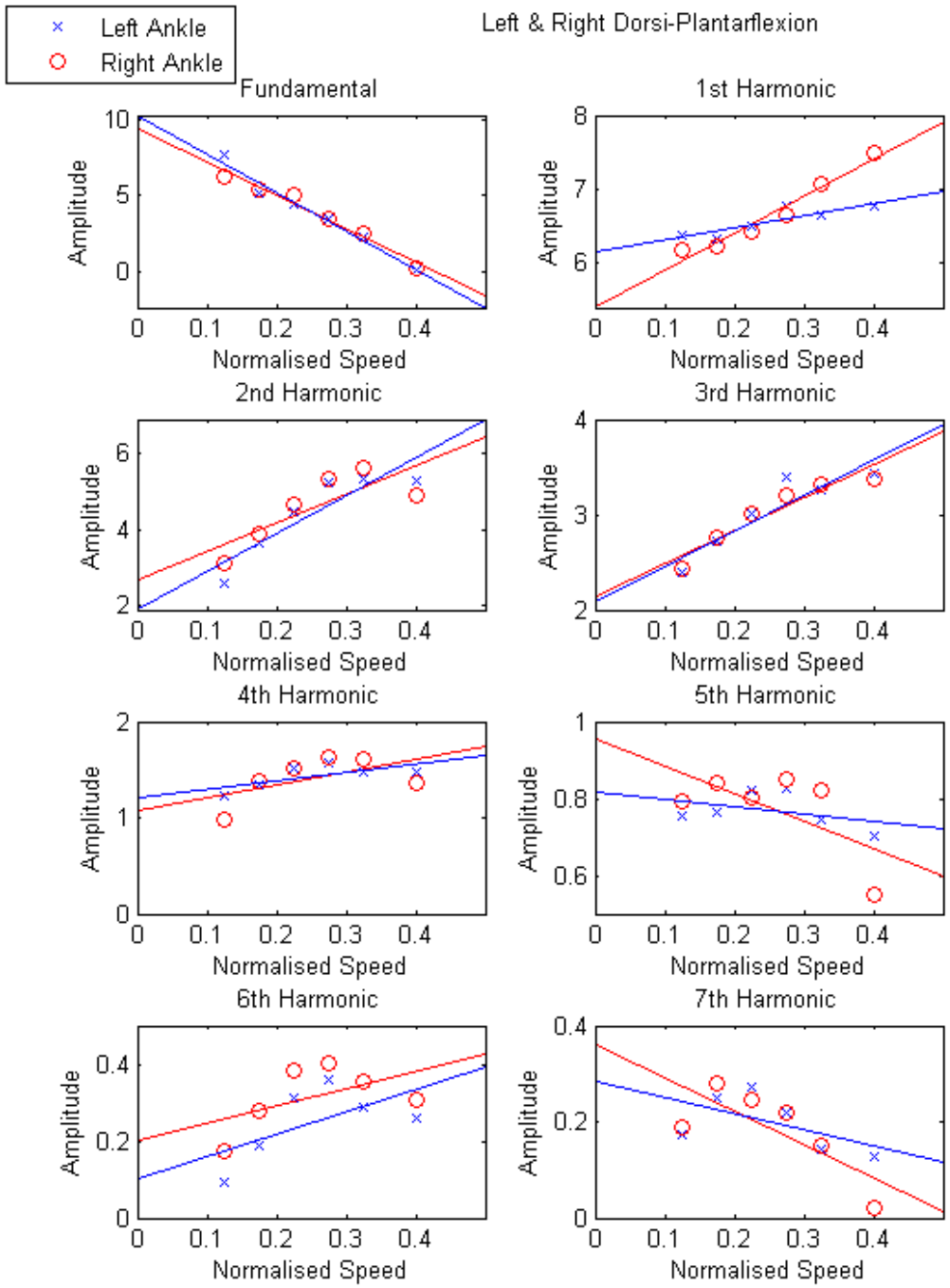

Figure C.18: Left and Right Dorsi-Plantarflexion Harmonic Amplitudes versus Normalised Speed

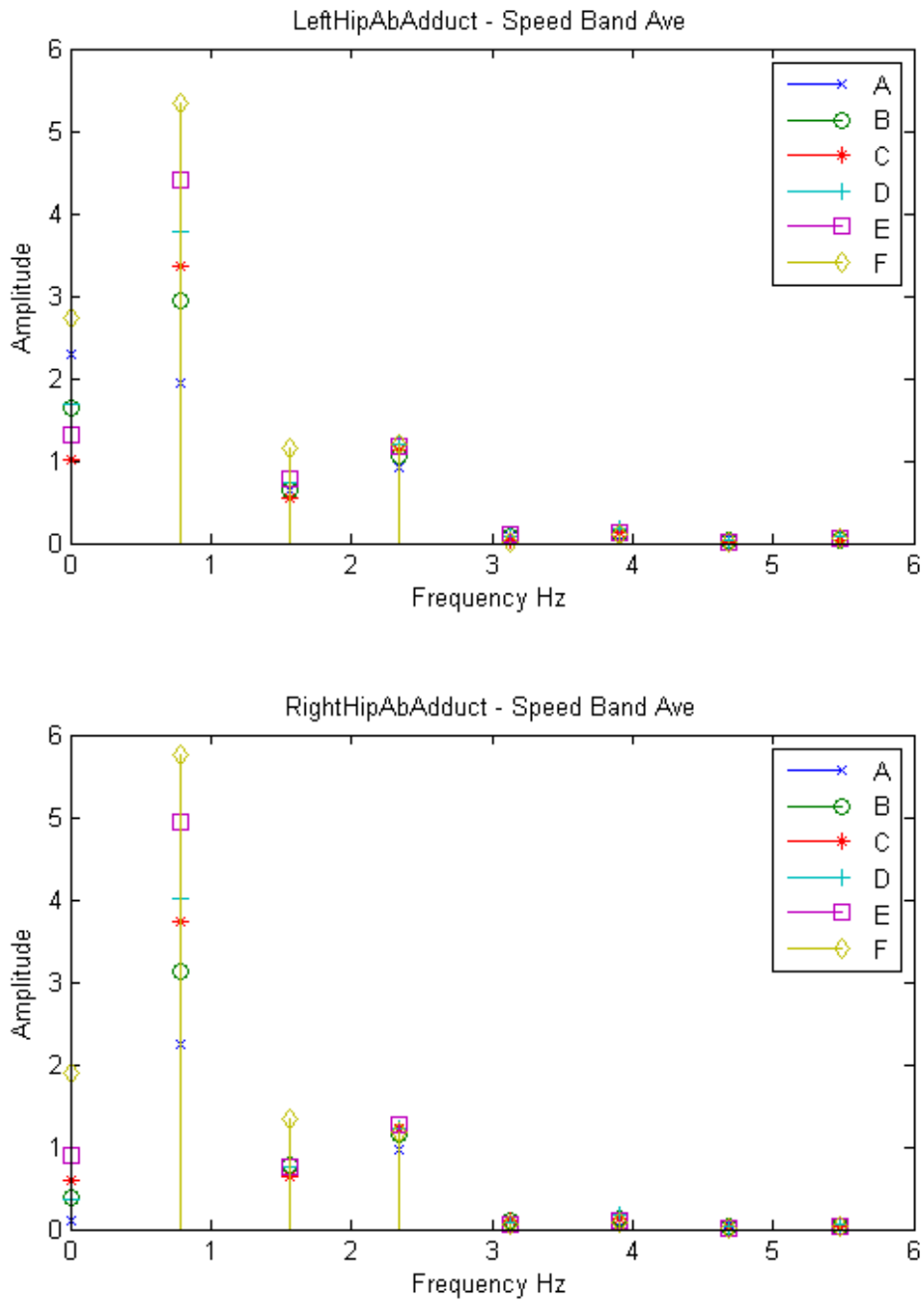

Figure C.19: Left and Right Hip Ab-Adduction in Frequency Domain

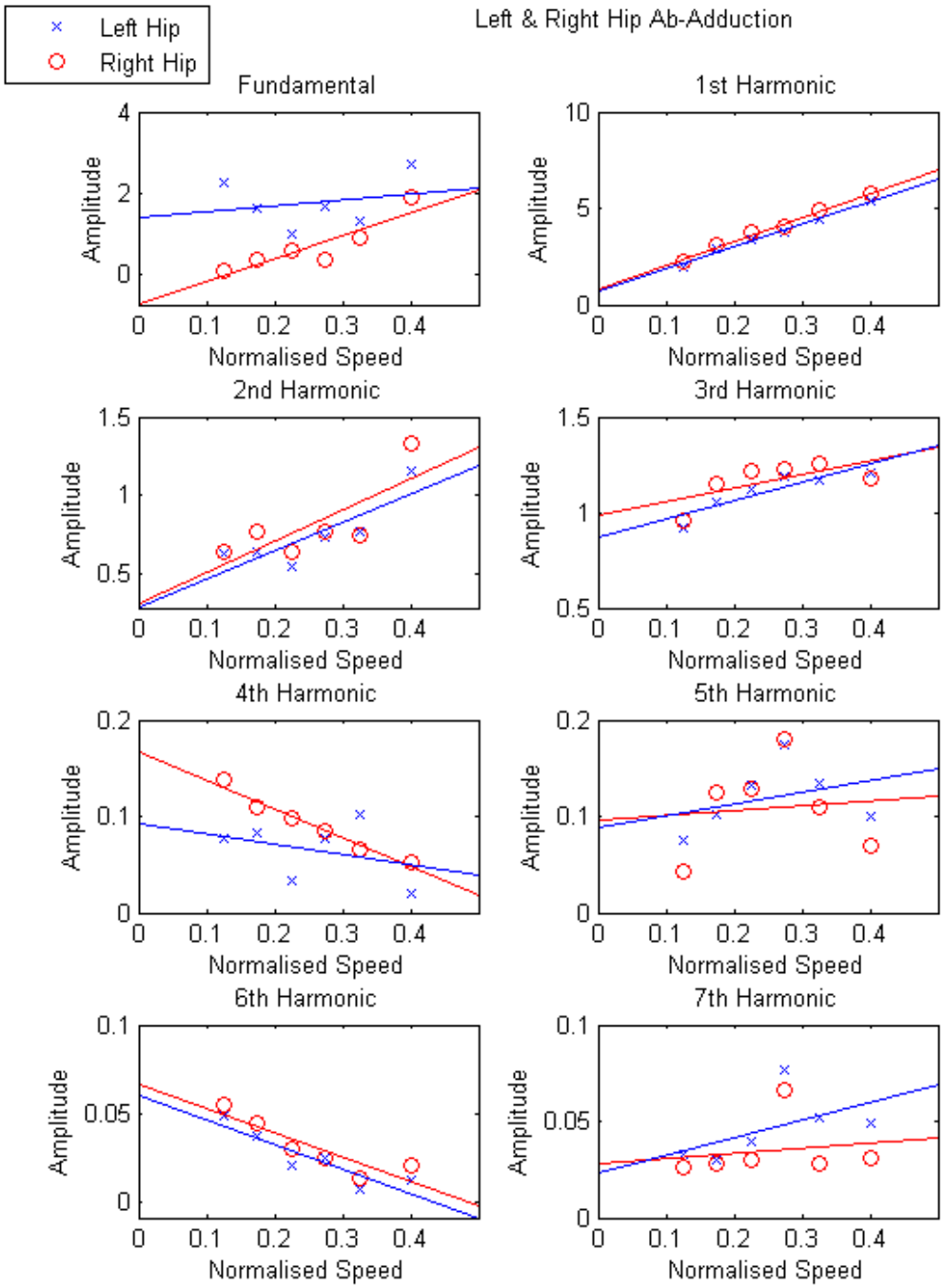

Figure C.20: Left and Right Hip Ab-Adduction Harmonic Amplitudes versus Normalised Speed

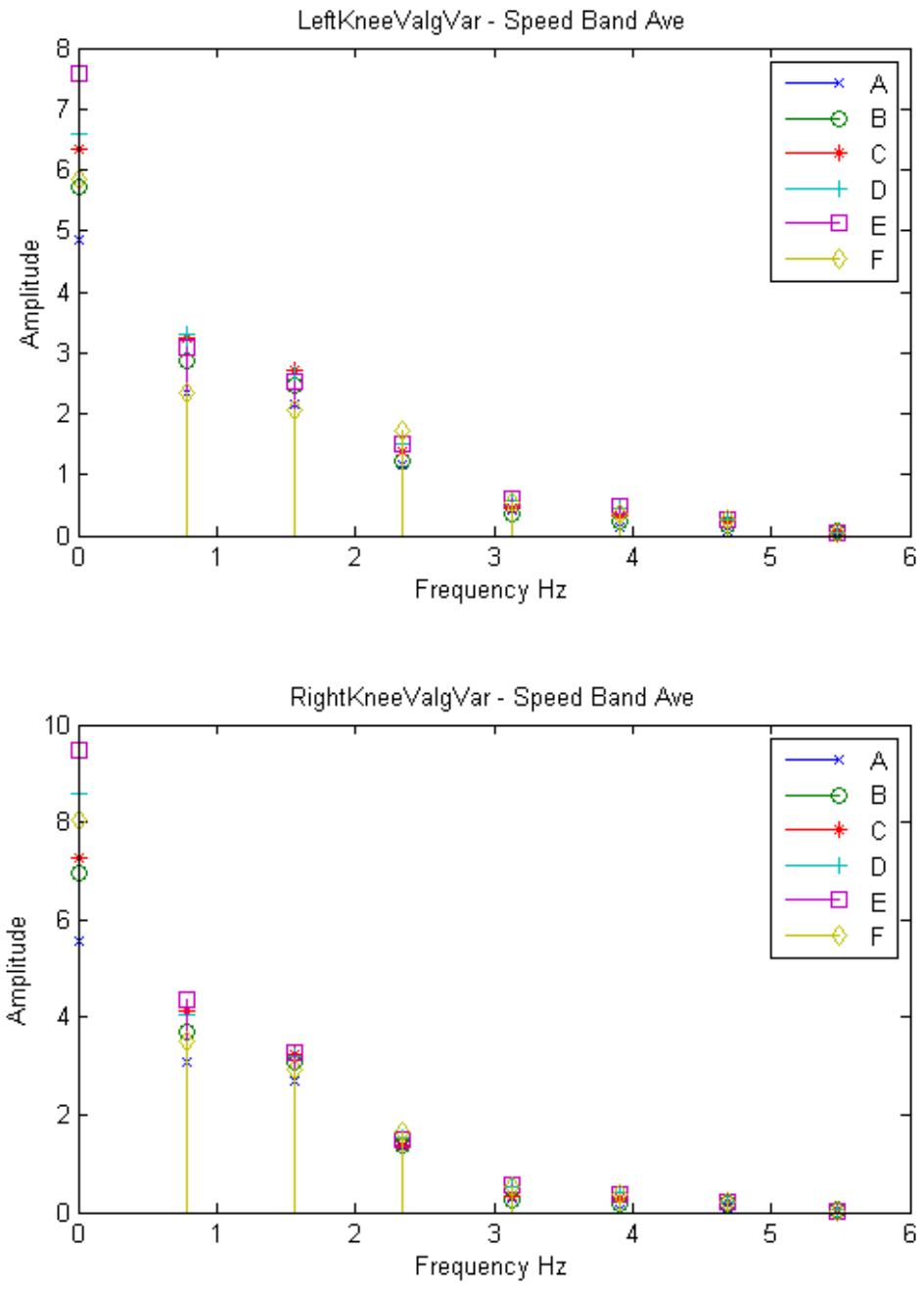

Figure C.21: Left and Right Knee Valgus-Varus in Frequency Domain

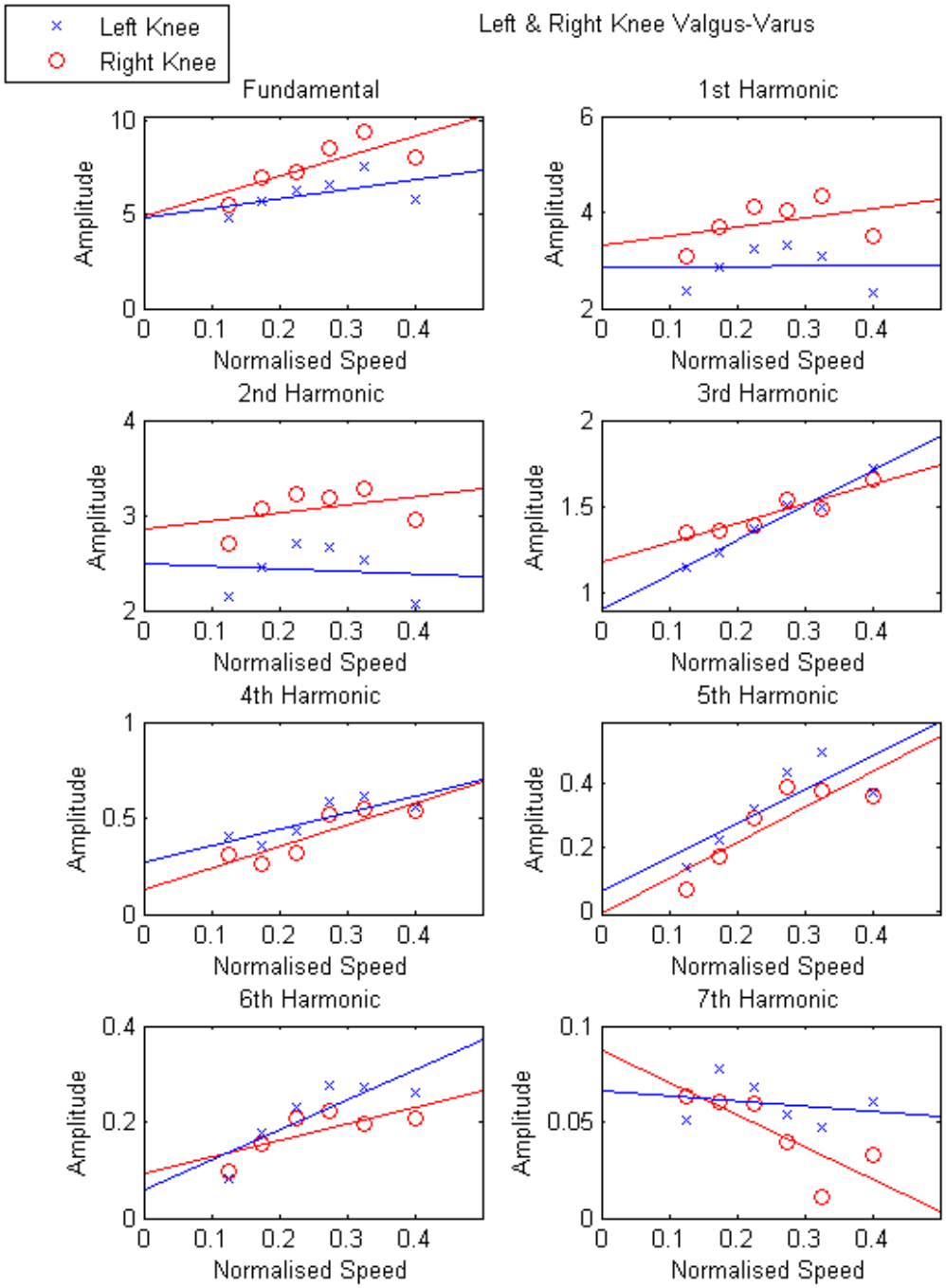

Figure C.22: Left and Right Knee Valgus-Varus Harmonic Amplitudes versus Normalised Speed

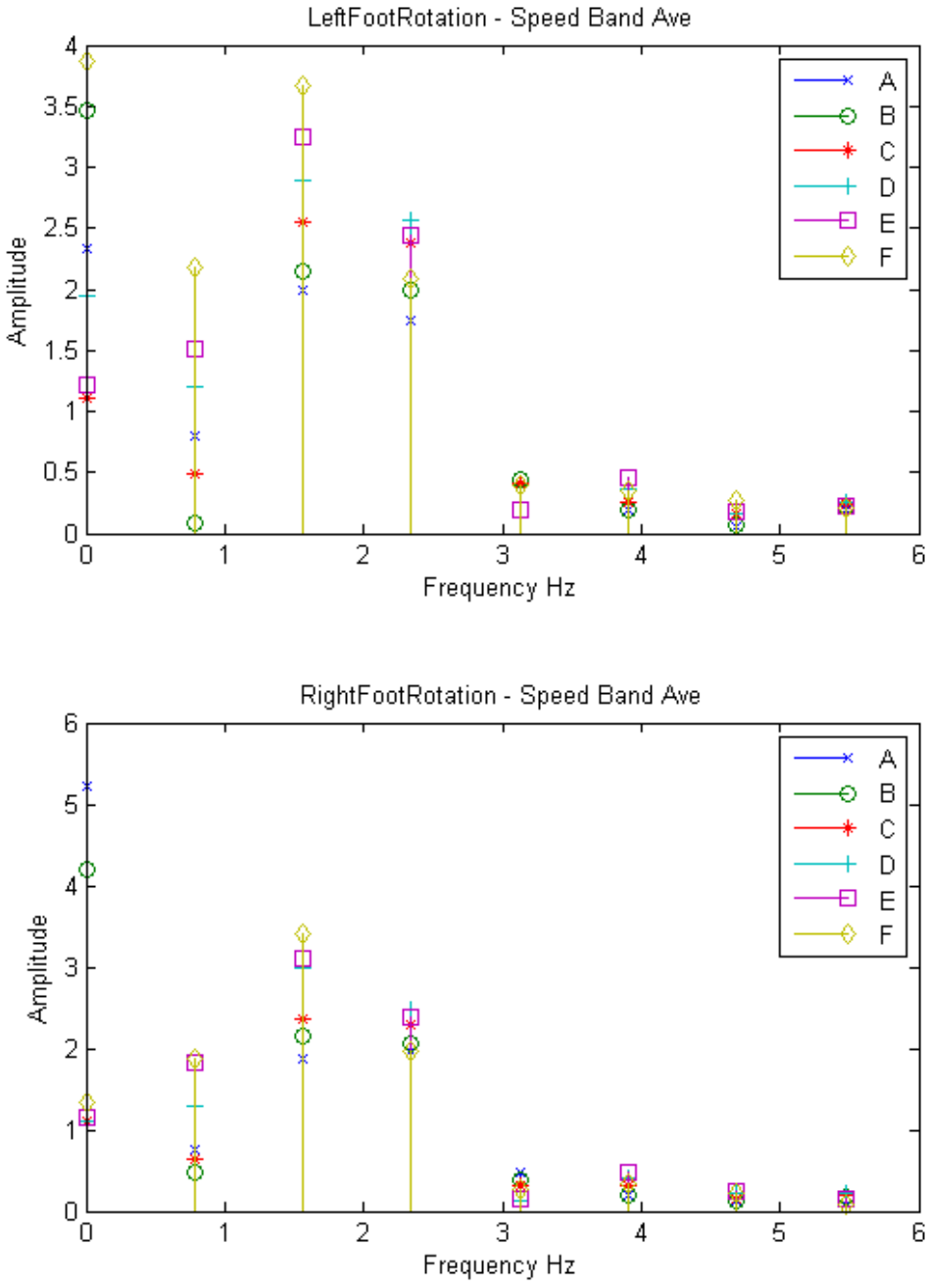

Figure C.23: Left and Right Foot Rotation in Frequency Domain

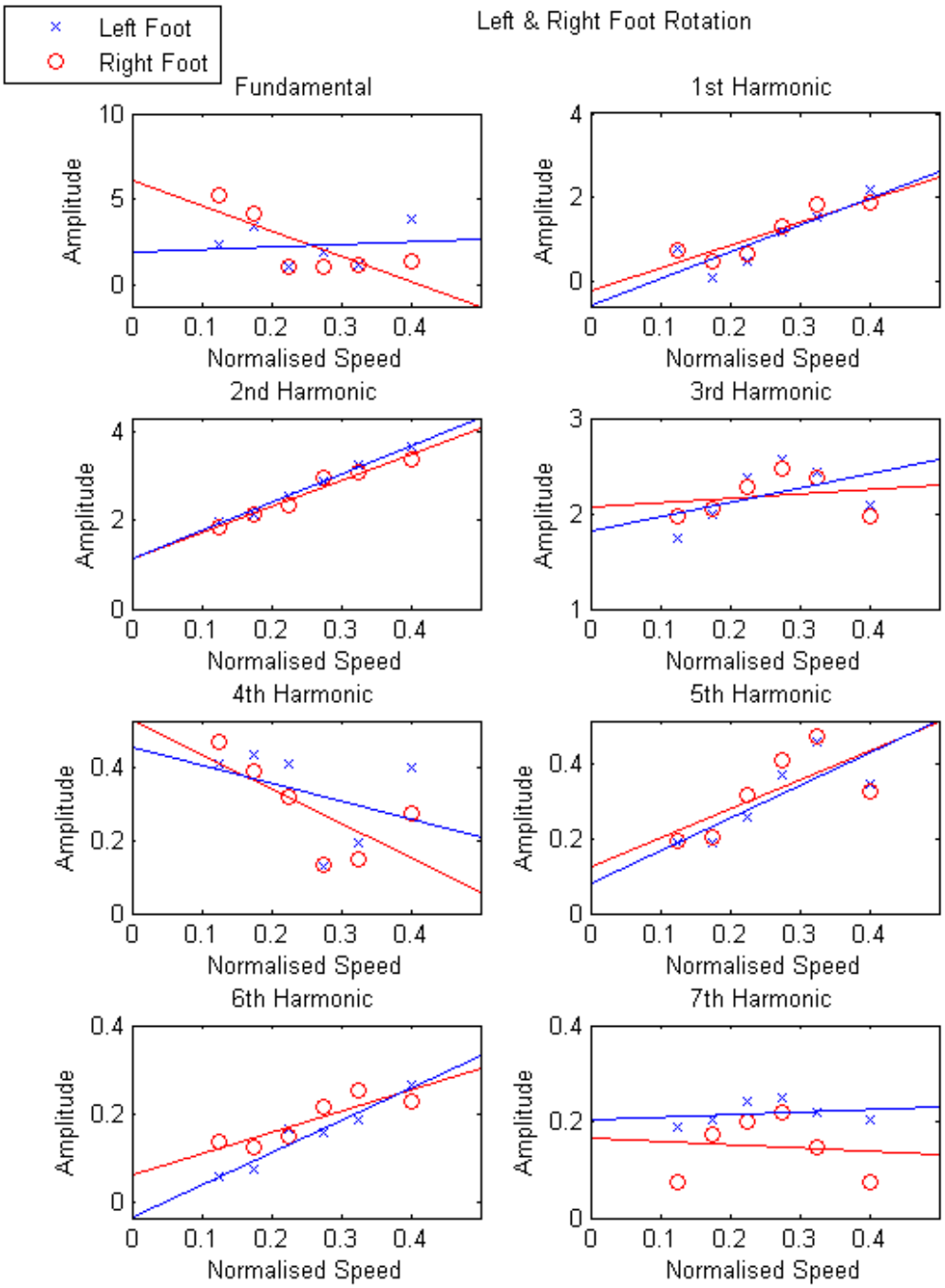

Figure C.24: Left and Right Foot Rotation Harmonic Amplitudes versus Normalised Speed

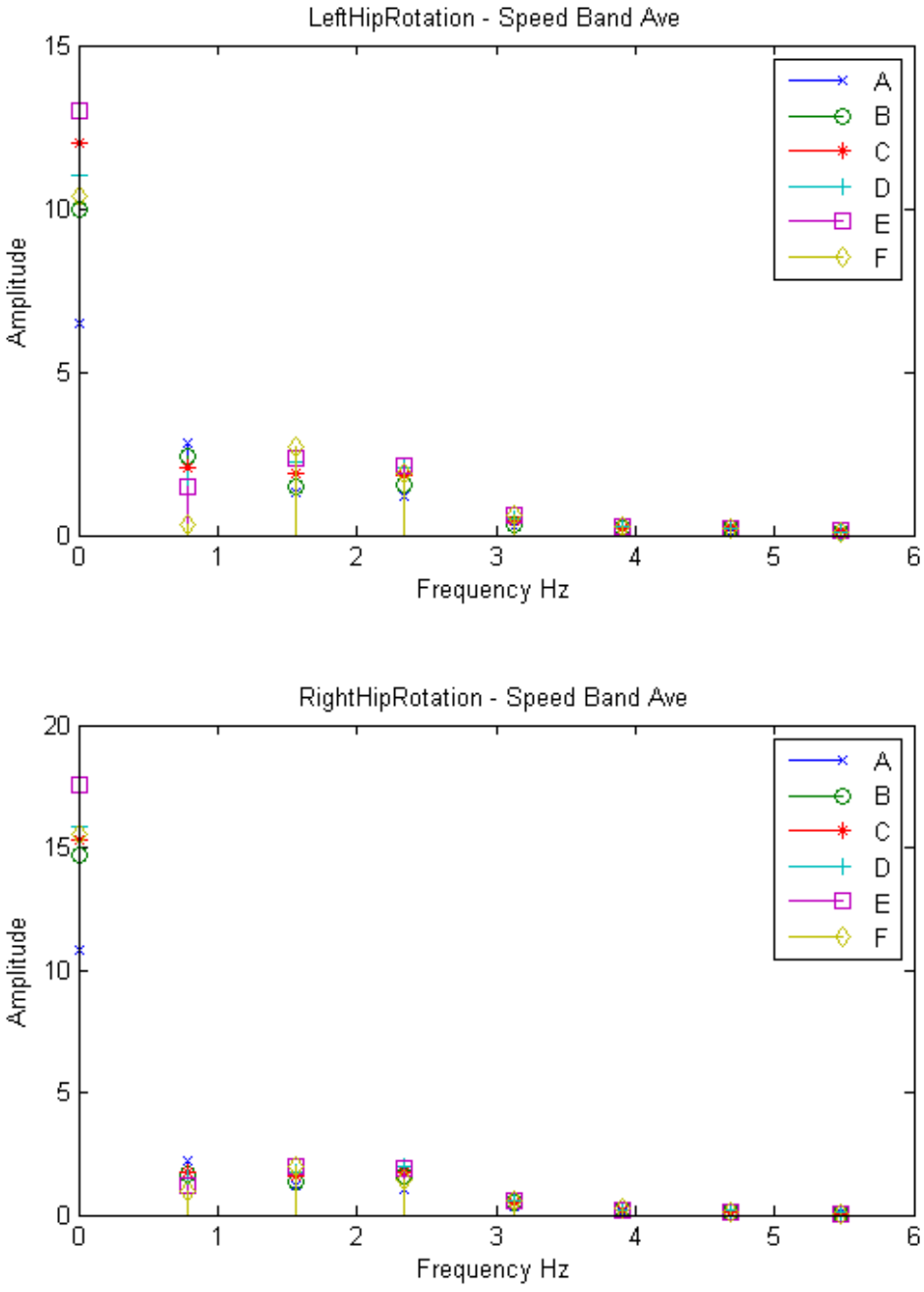

Figure C.25: Left and Right Hip Rotation in Frequency Domain

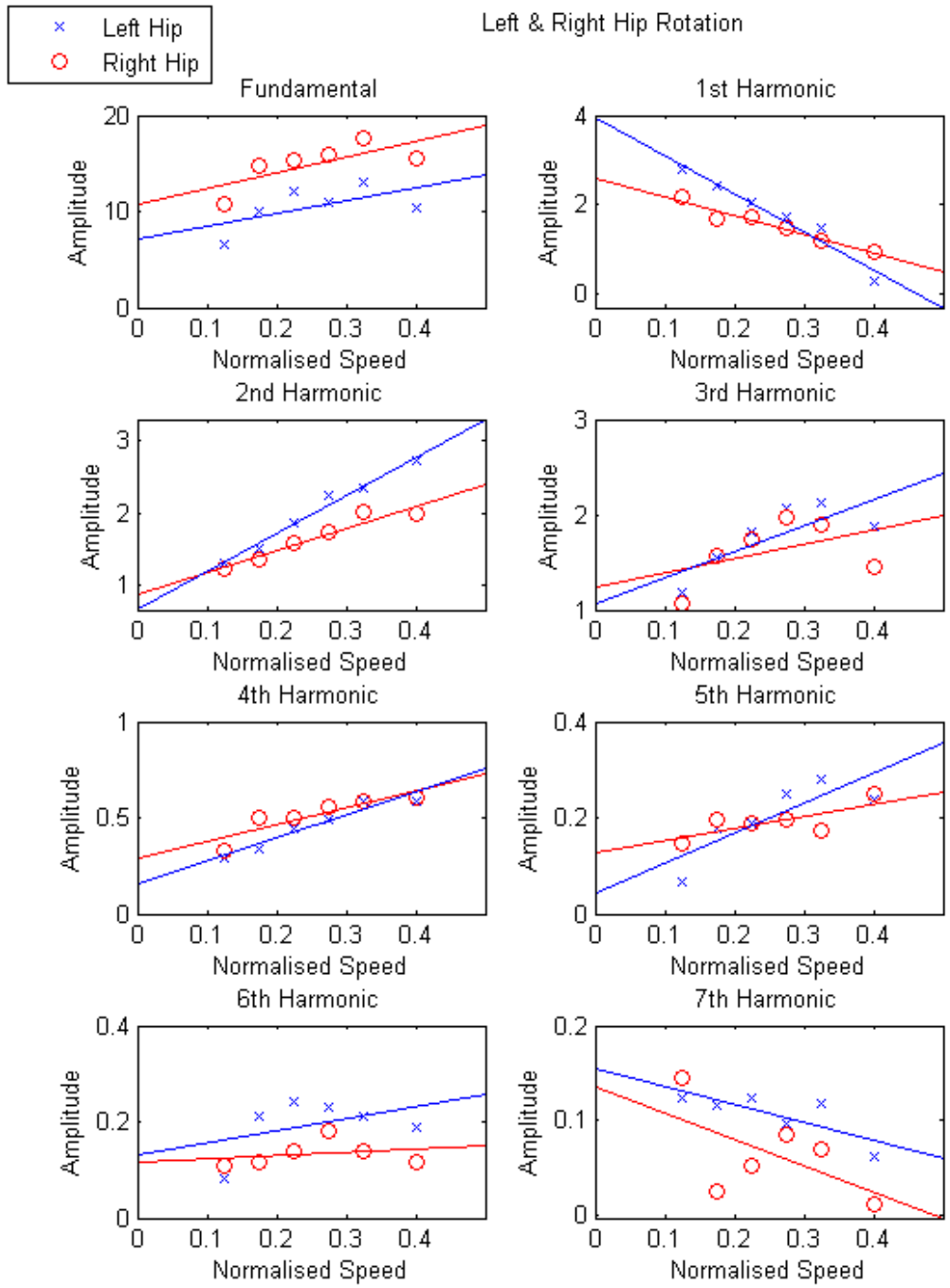

Figure C.26: Left and Right Hip Rotation Harmonic Amplitudes versus Normalised Speed

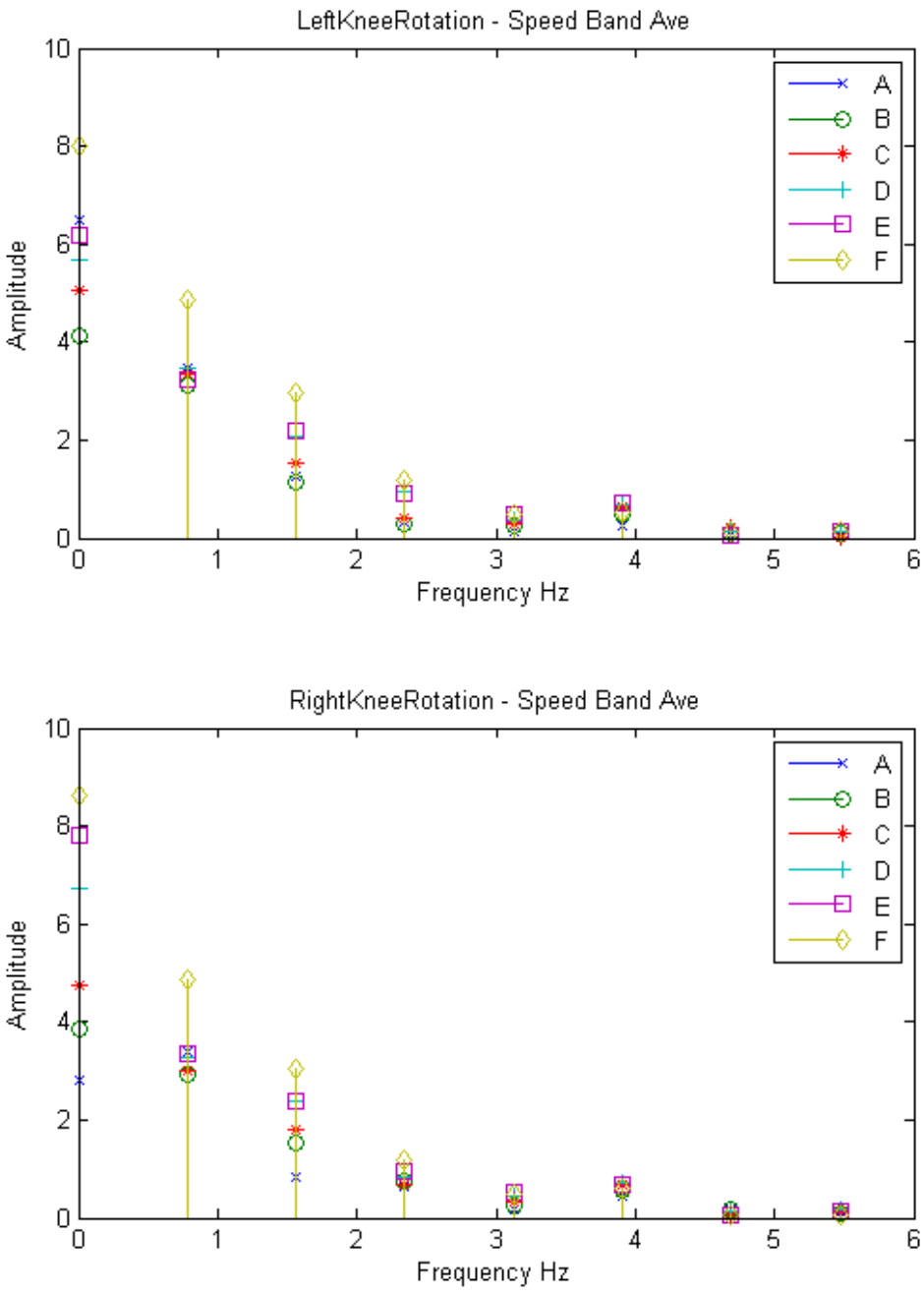

Figure C.27: Left and Right Knee Rotation in Frequency Domain

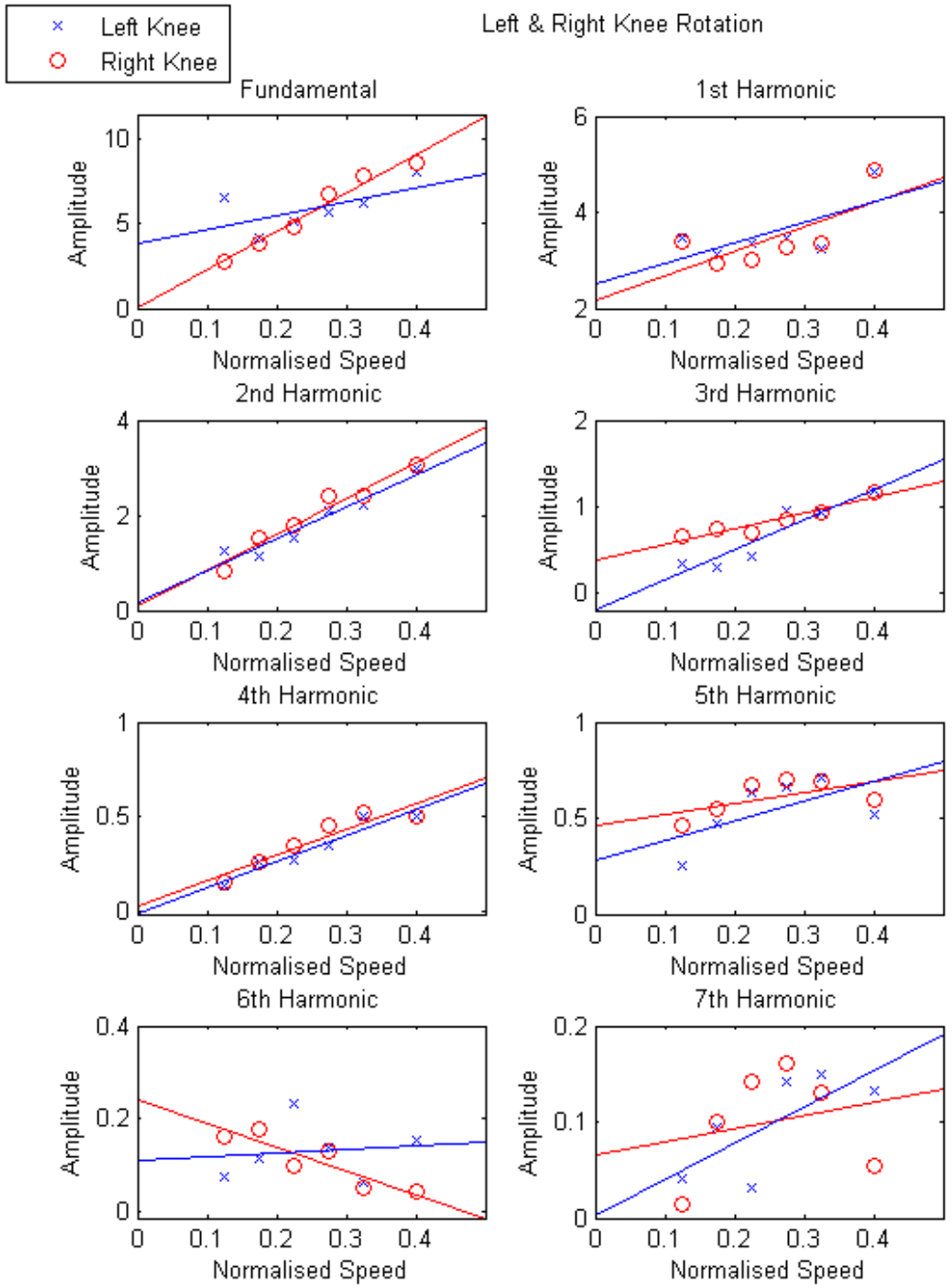

Figure C.28: Left and Right Knee Rotation Harmonic Amplitudes versus Normalised Speed

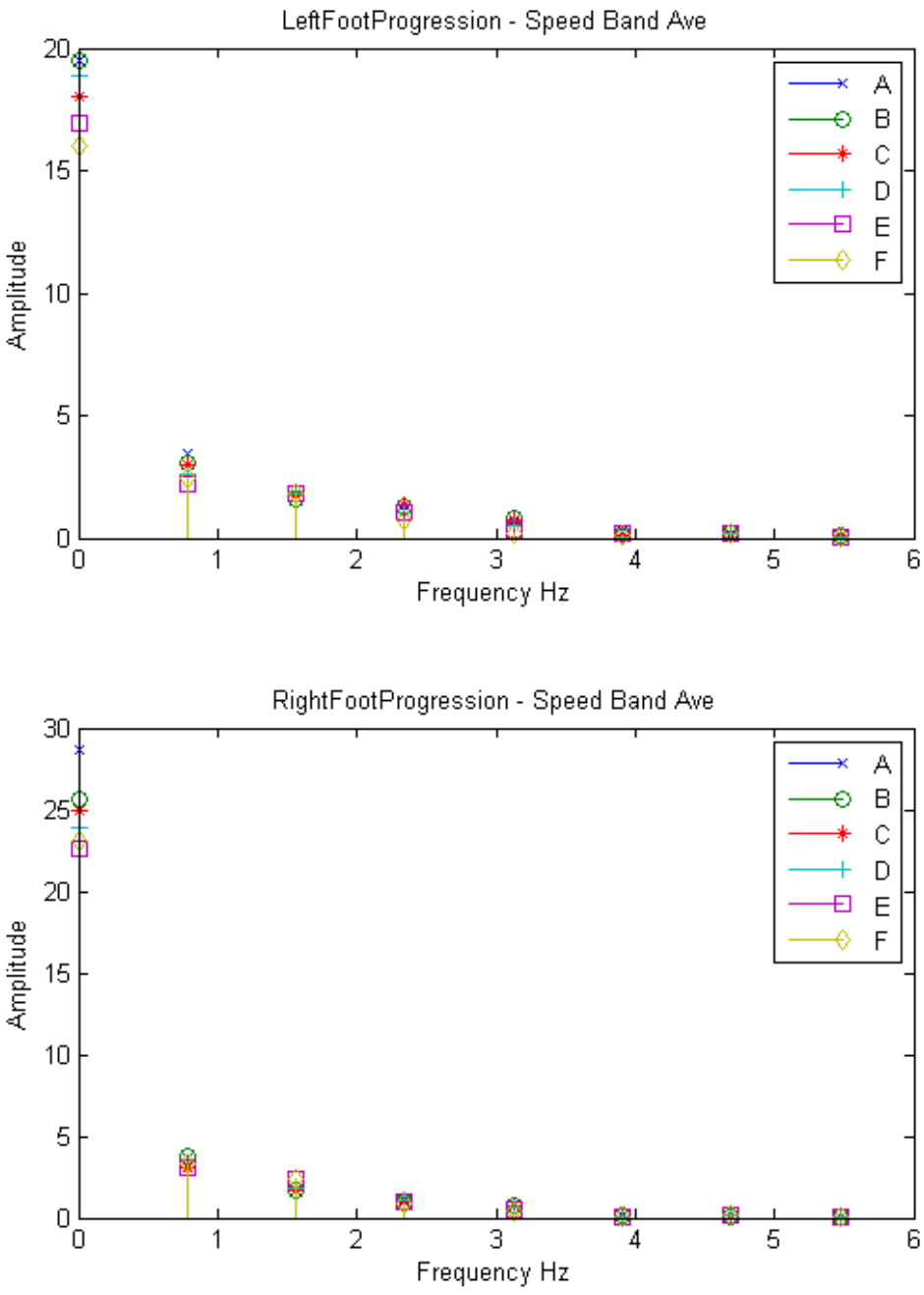

Figure C.29: Left and Right Foot Progression in Frequency Domain

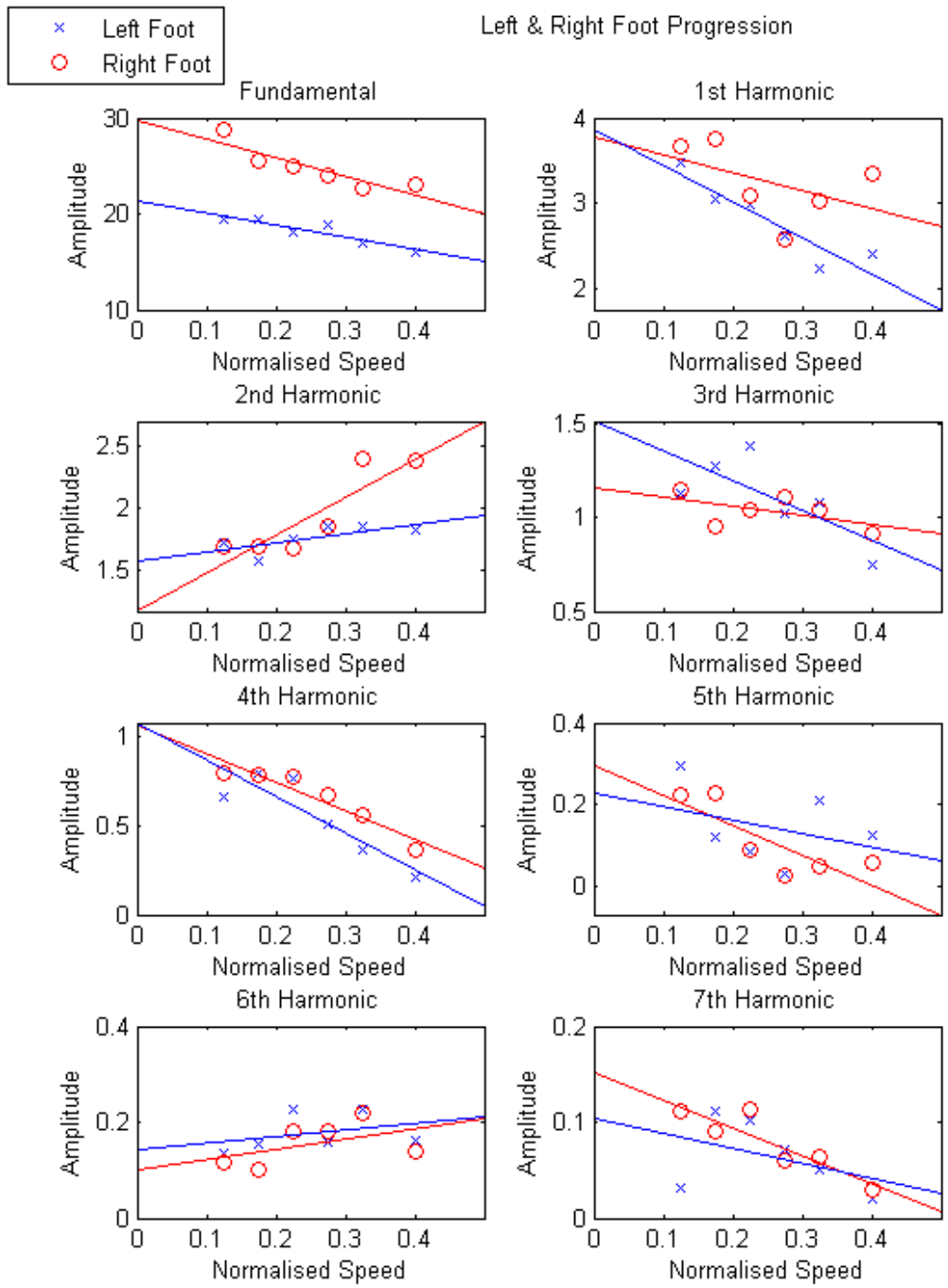

Figure C.30: Left and Right Foot Progression Harmonic Amplitudes versus Normalised Speed

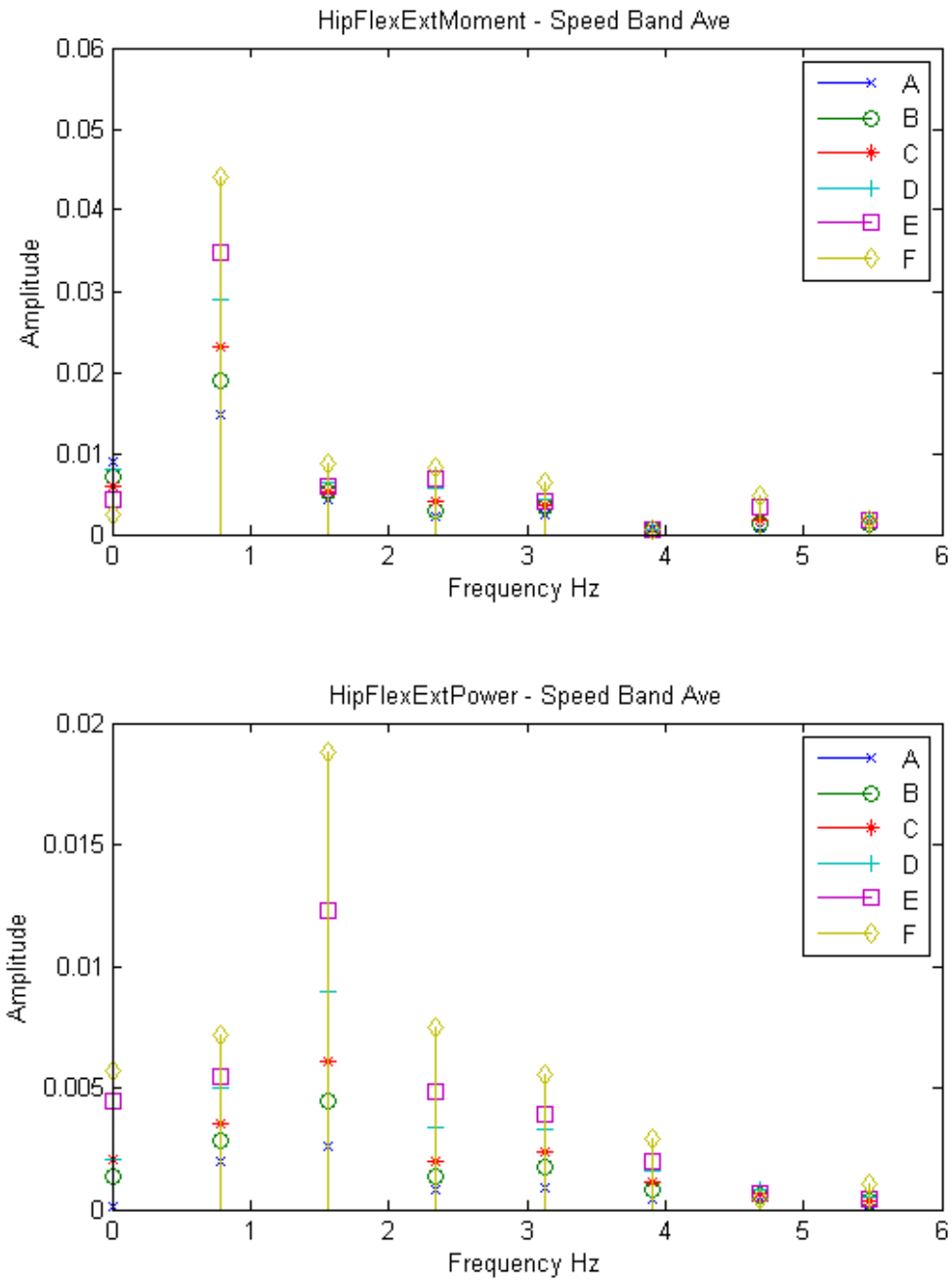

Figure C.31: Hip Flexion Moment and Power in Frequency Domain

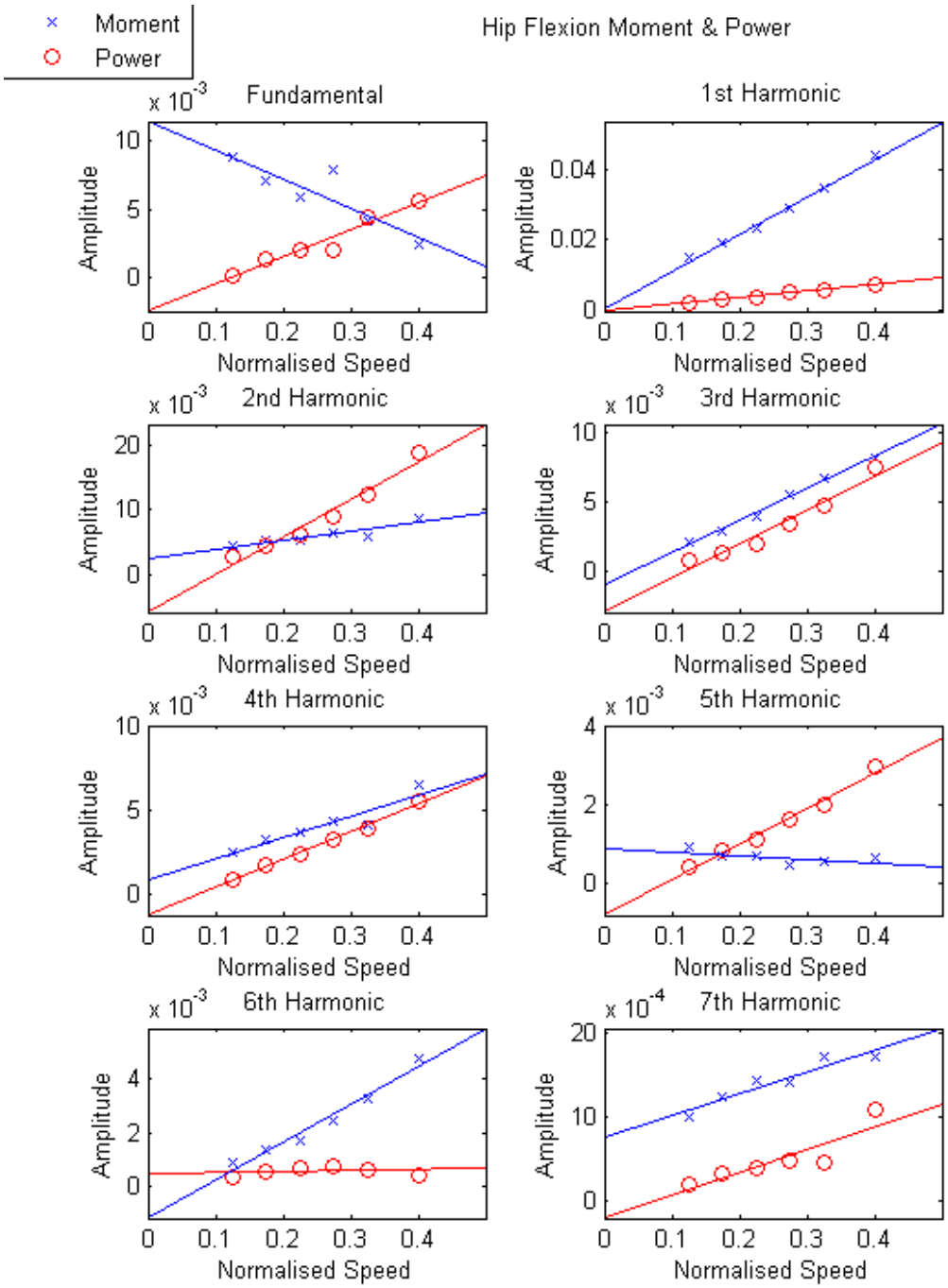

Figure C.32: Hip Flexion Moment and Power Harmonic Amplitudes versus Normalised Speed

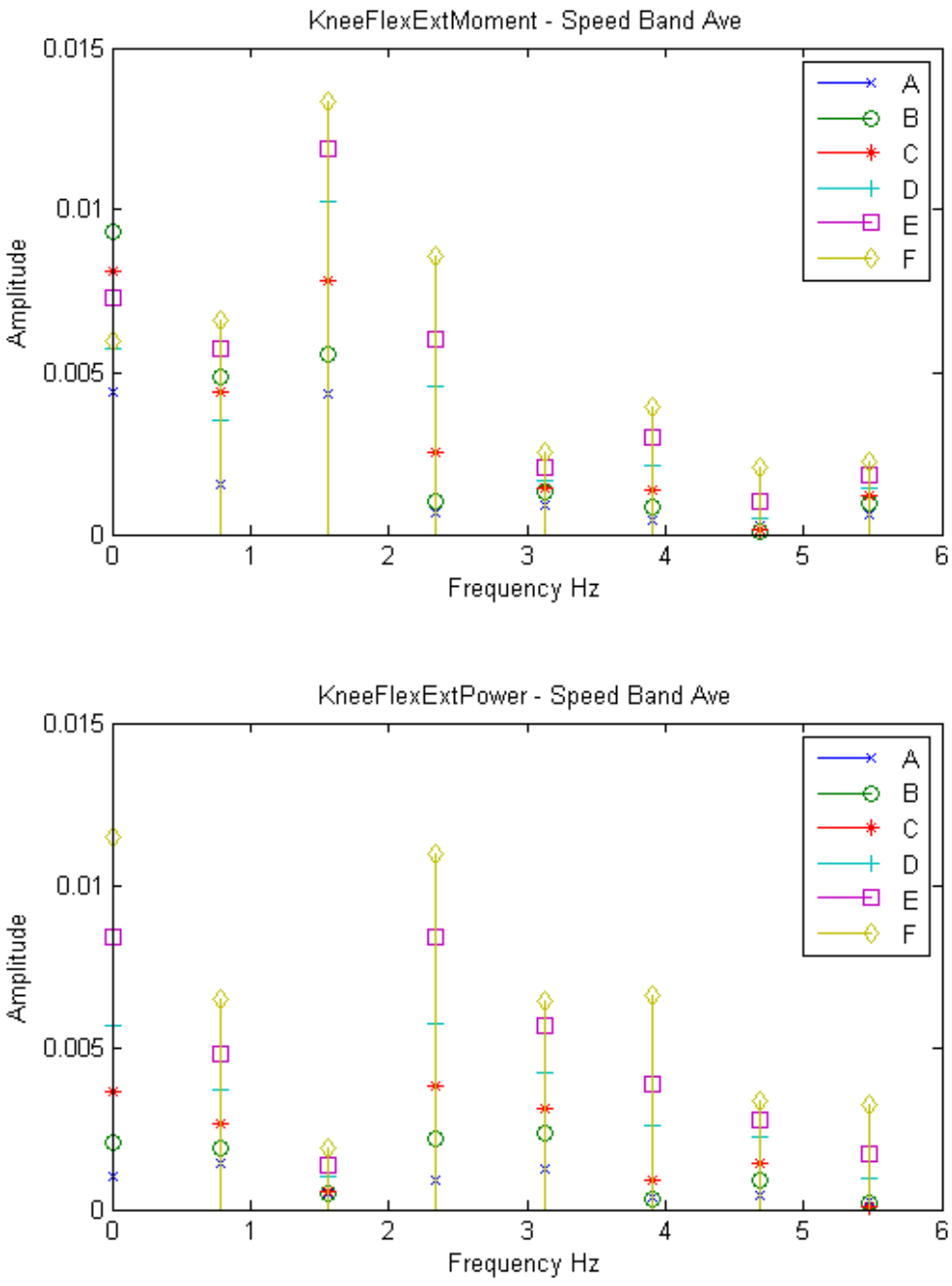

Figure C.33: Knee Flexion Moment and Power in Frequency Domain

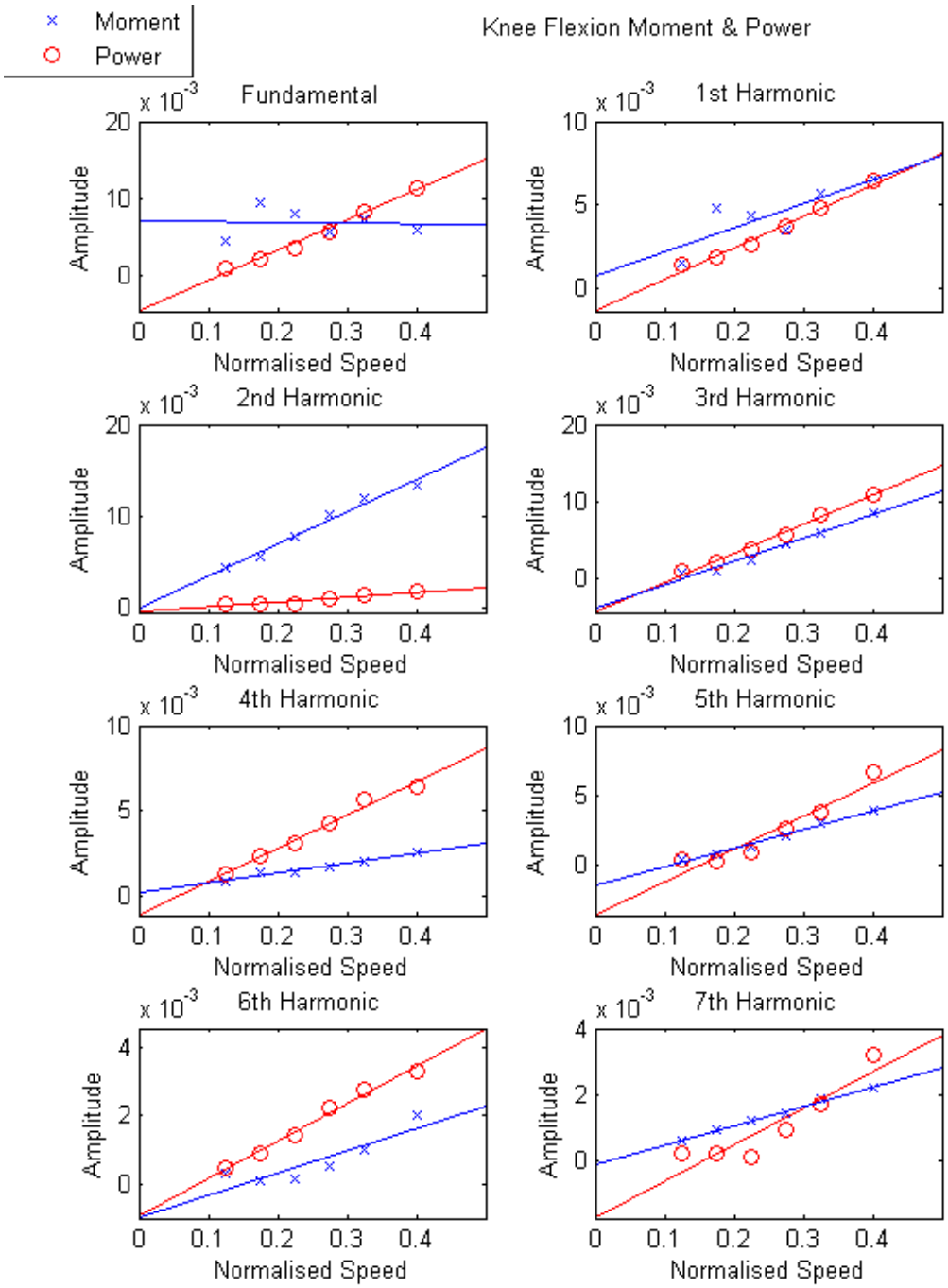

Figure C.34: Knee Flexion Moment and Power Harmonic Amplitudes versus Normalised Speed

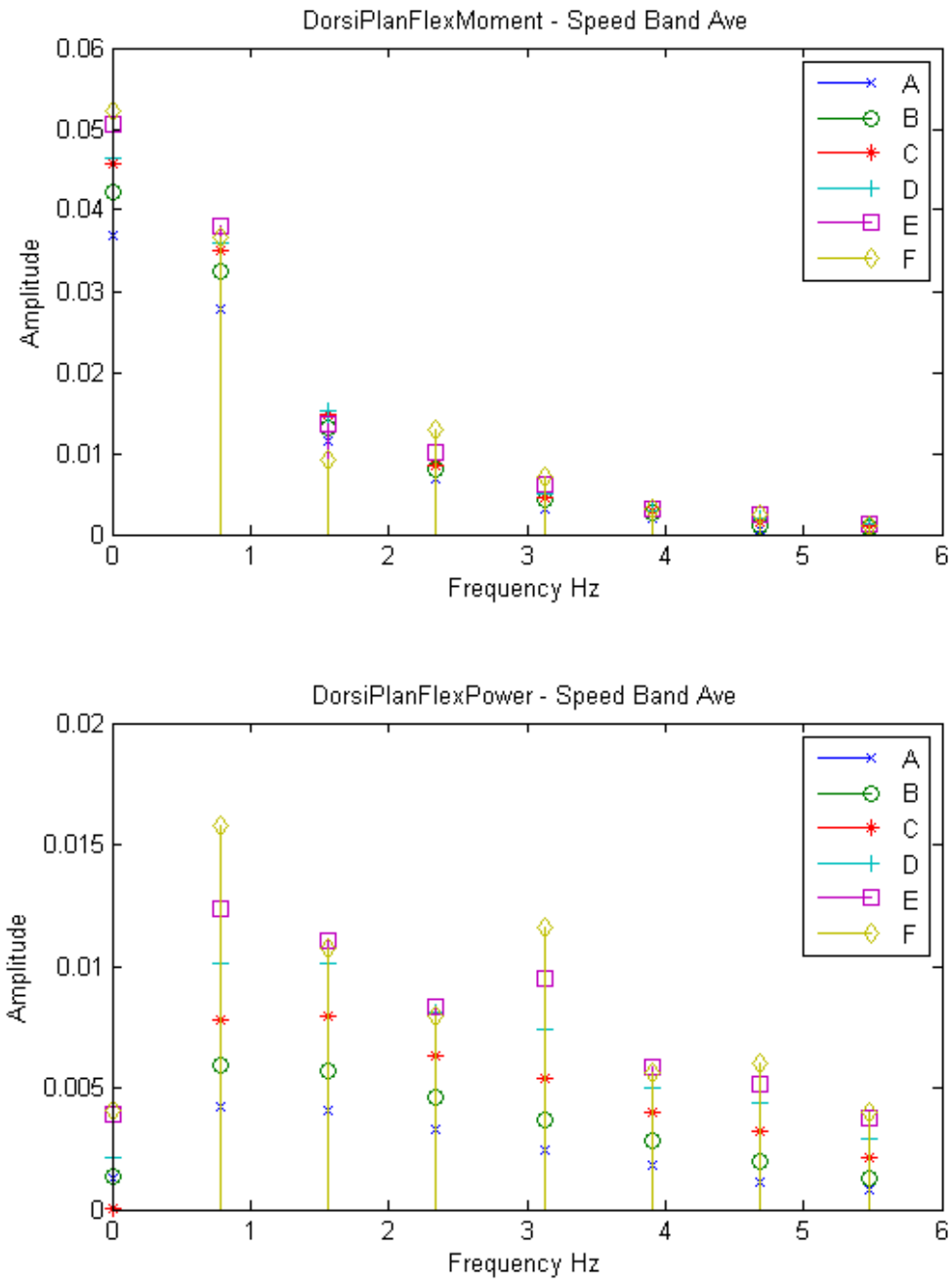

Figure C.35: Dorsi-Plantarflexion Moment and Power in Frequency Domain

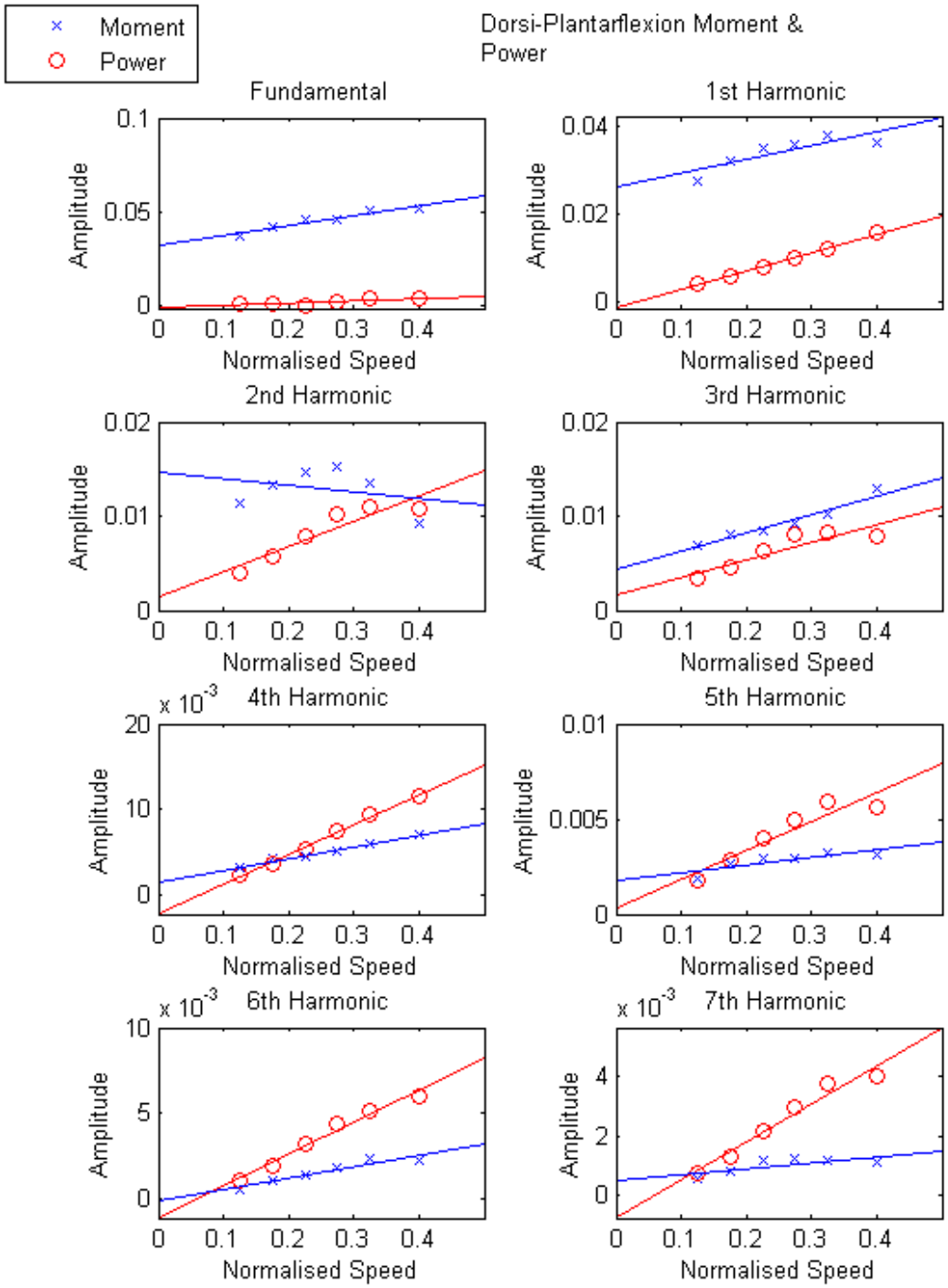

Figure C.36: Dorsi-Plantarflexion Moment and Power Harmonic Amplitudes versus Normalised Speed

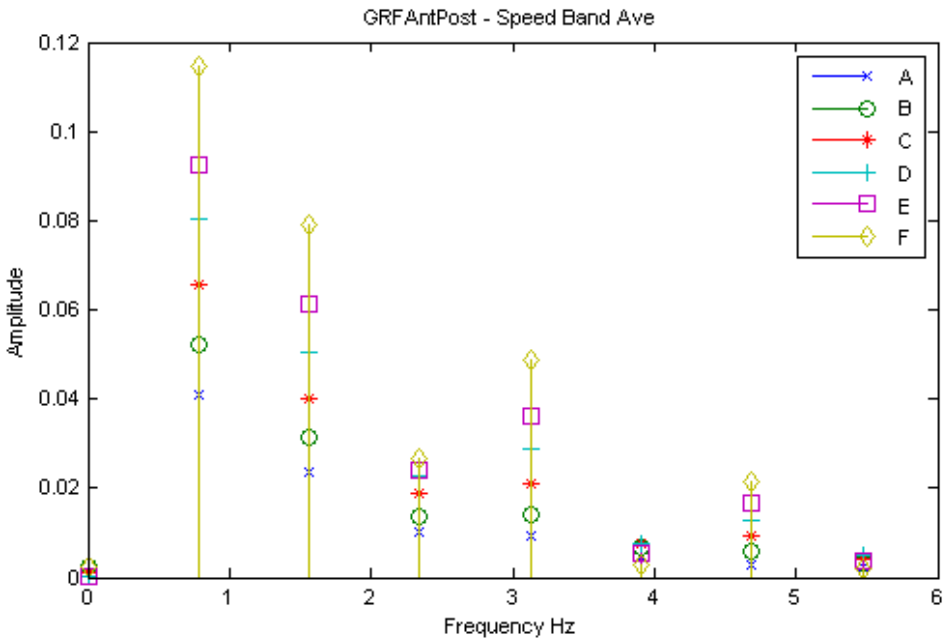

Figure C.37: Antero-Posterior Ground Reaction Force in Frequency Domain

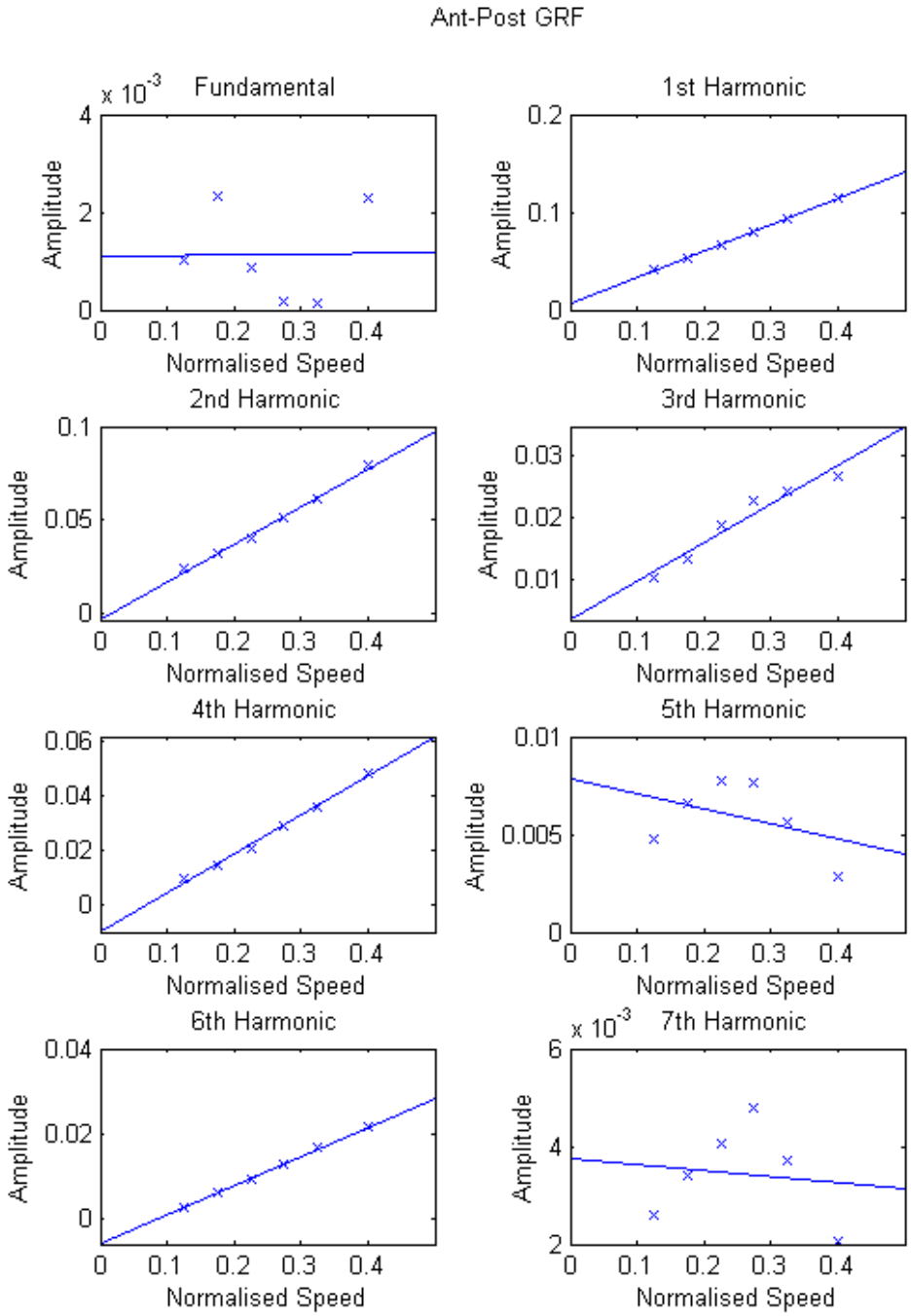

Figure C.38: Antero-Posterior Ground Reaction Force Harmonic Amplitudes versus Normalised Speed

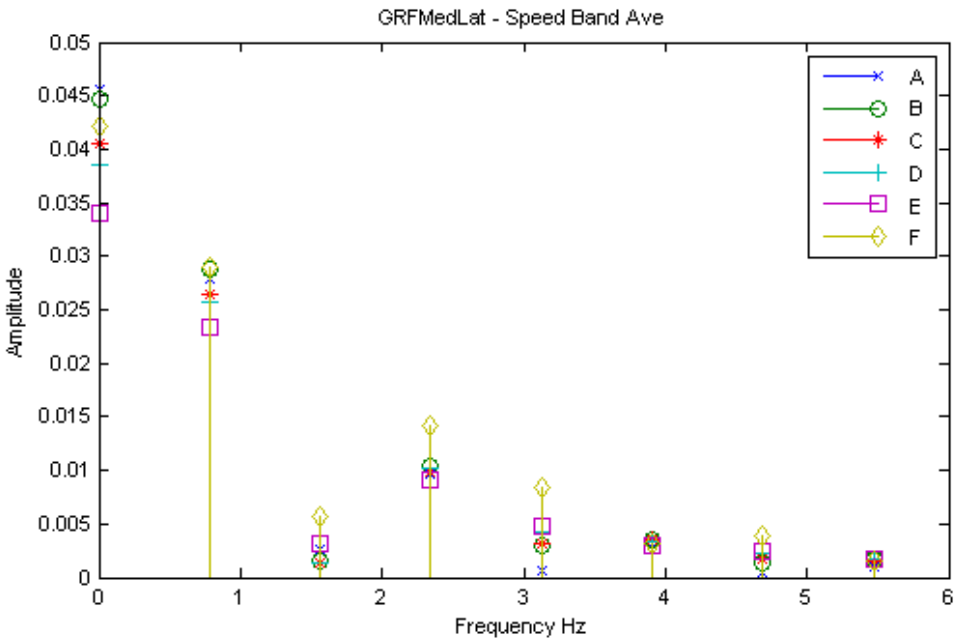

Figure C.39: Medio-Lateral Ground Reaction Force in Frequency Domain

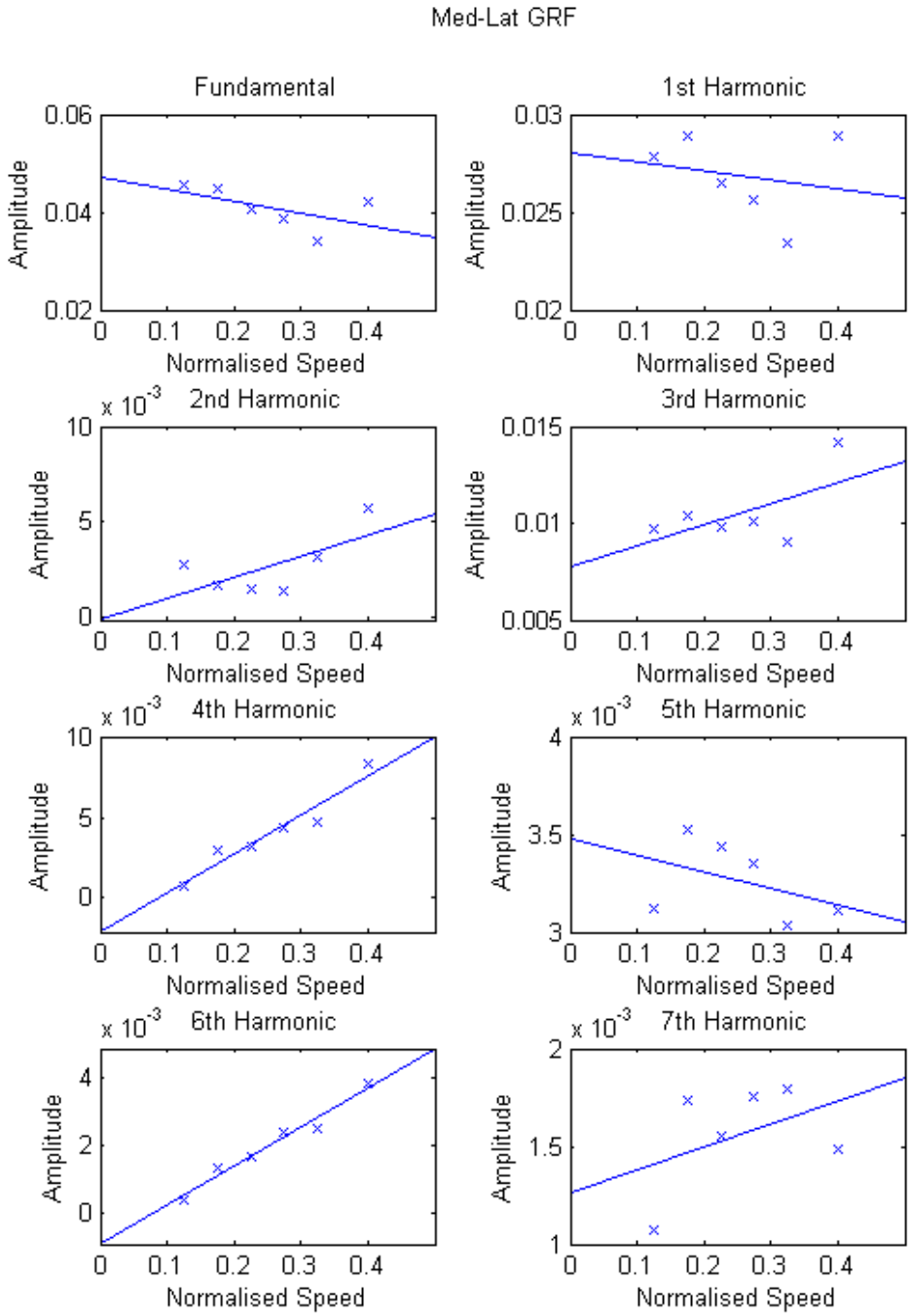

Figure C.40: Medio-Lateral Ground Reaction Force Harmonic Amplitudes versus Normalised Speed

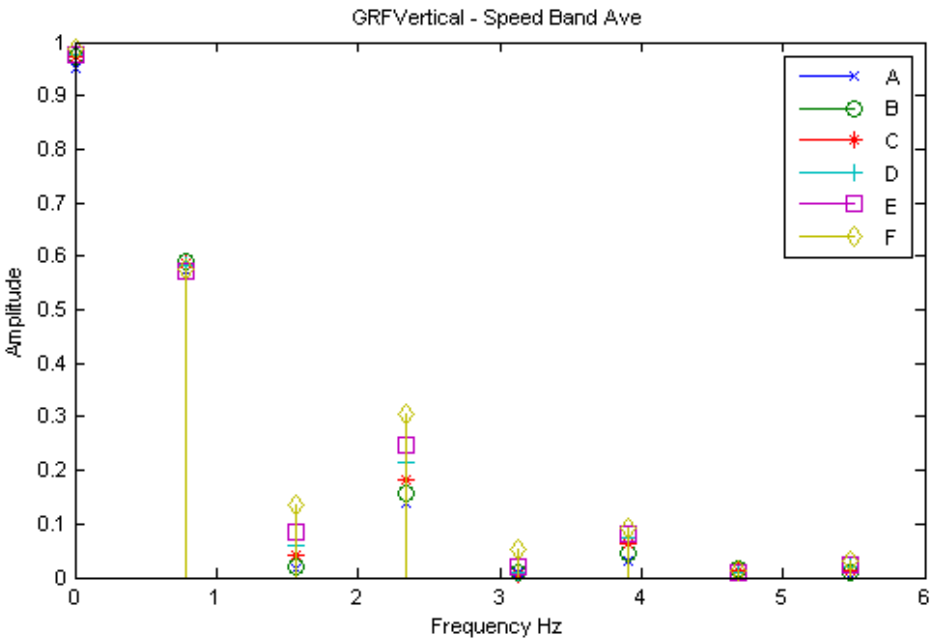

Figure C.41: Vertical Ground Reaction Force in Frequency Domain

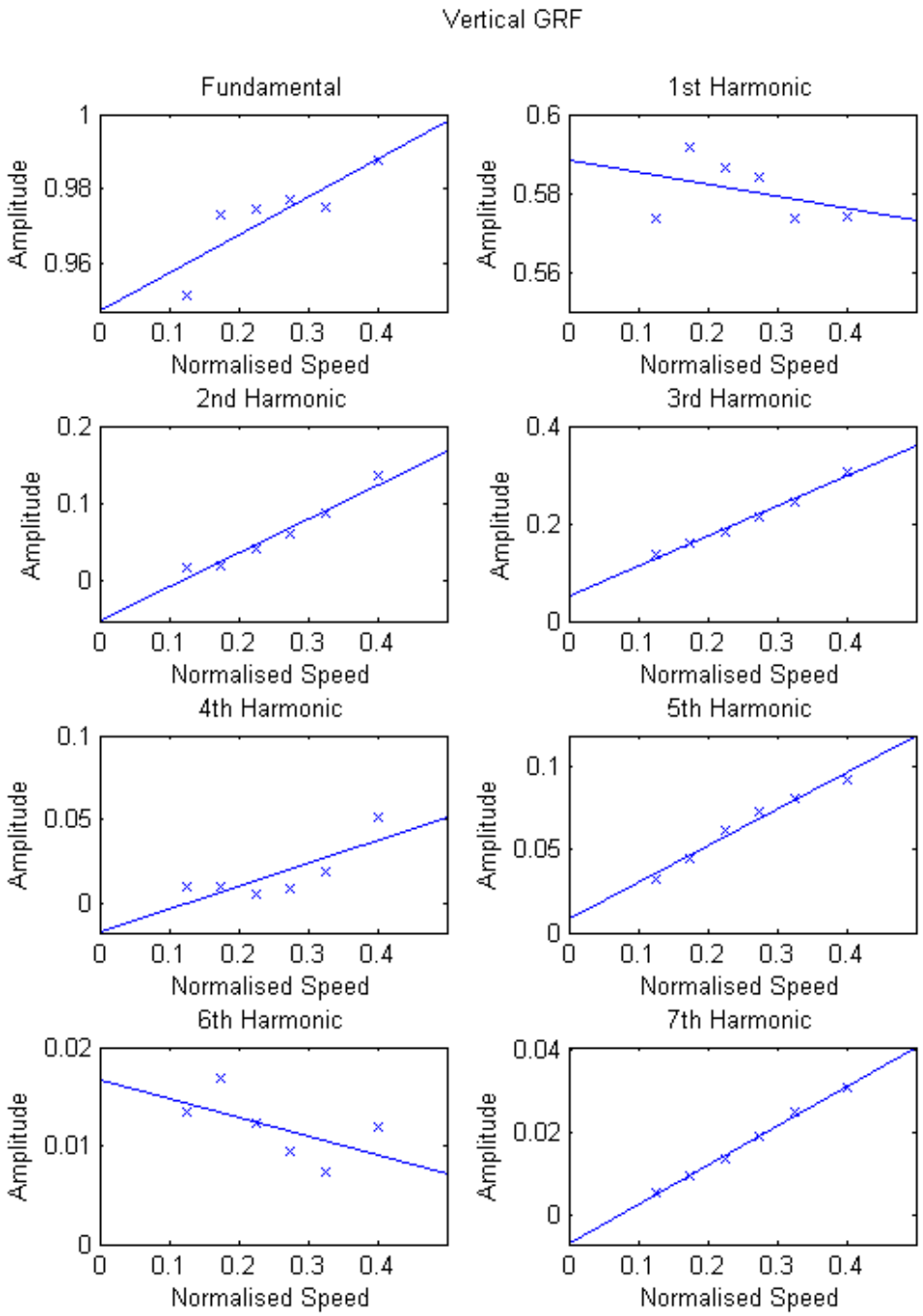

Figure C.42: Vertical Ground Reaction Force Harmonic Amplitudes versus Normalised Speed

Appendix D

Case Study - Further Plots

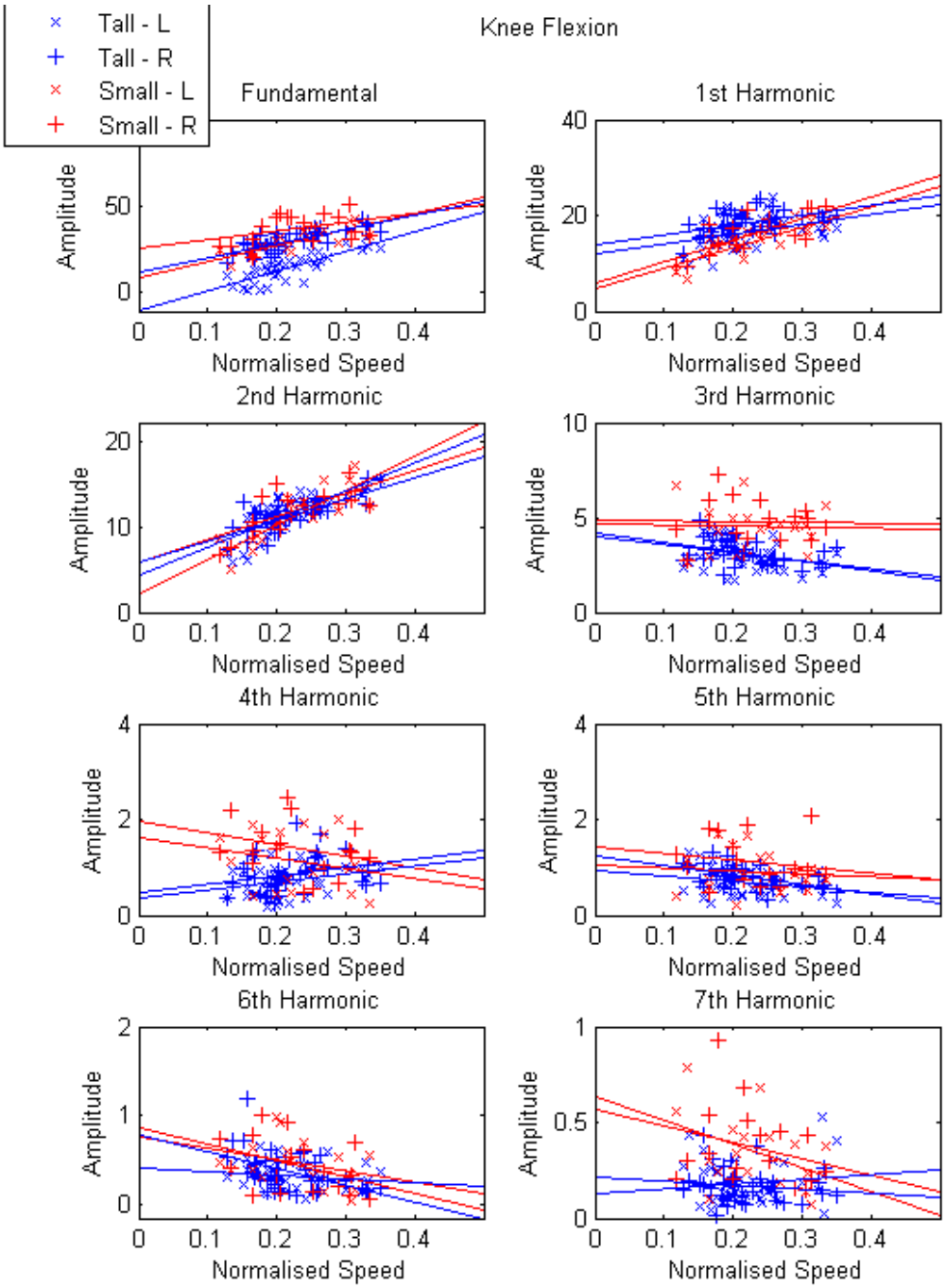

Figure D.1: Tallest and Smallest Knee Flexion Harmonic Amplitudes versus Normalised Speed

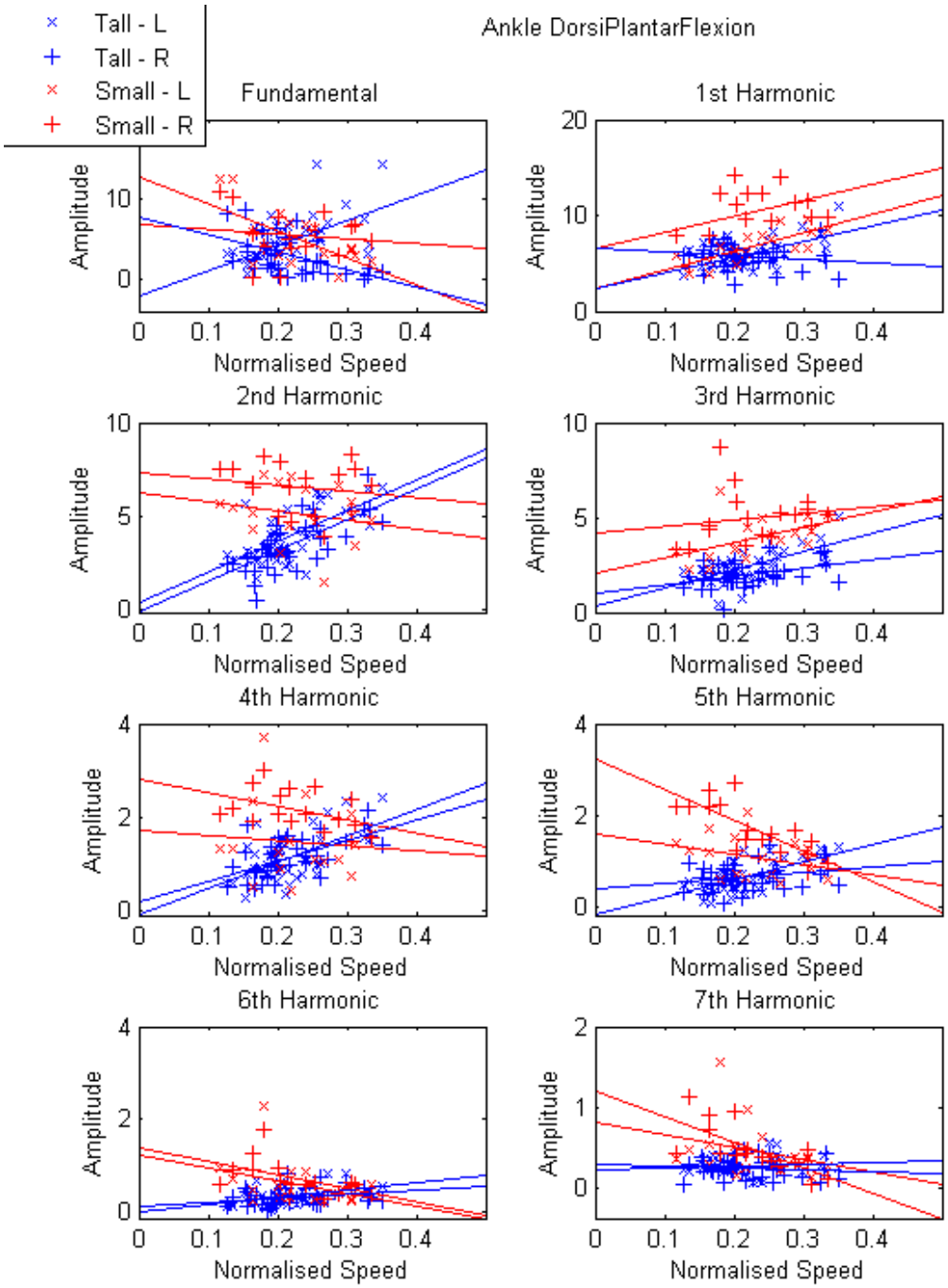

Figure D.2: Tallest and Smallest Dorsi-Plantarflexion Harmonic Amplitudes versus Normalised Speed

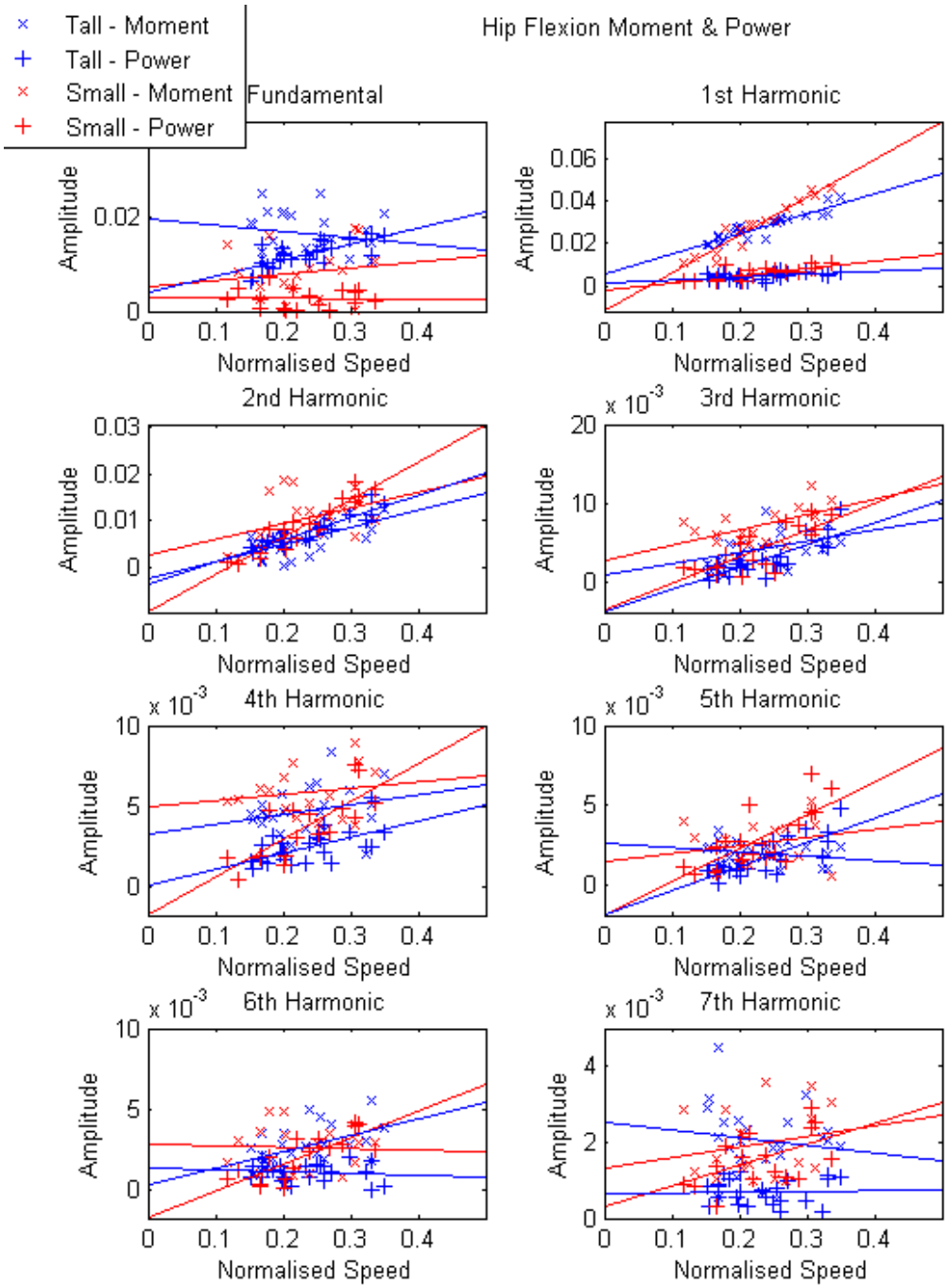

Figure D.3: Tallest and Smallest Hip Flexion Moment and Power Harmonic Amplitudes versus Normalised Speed

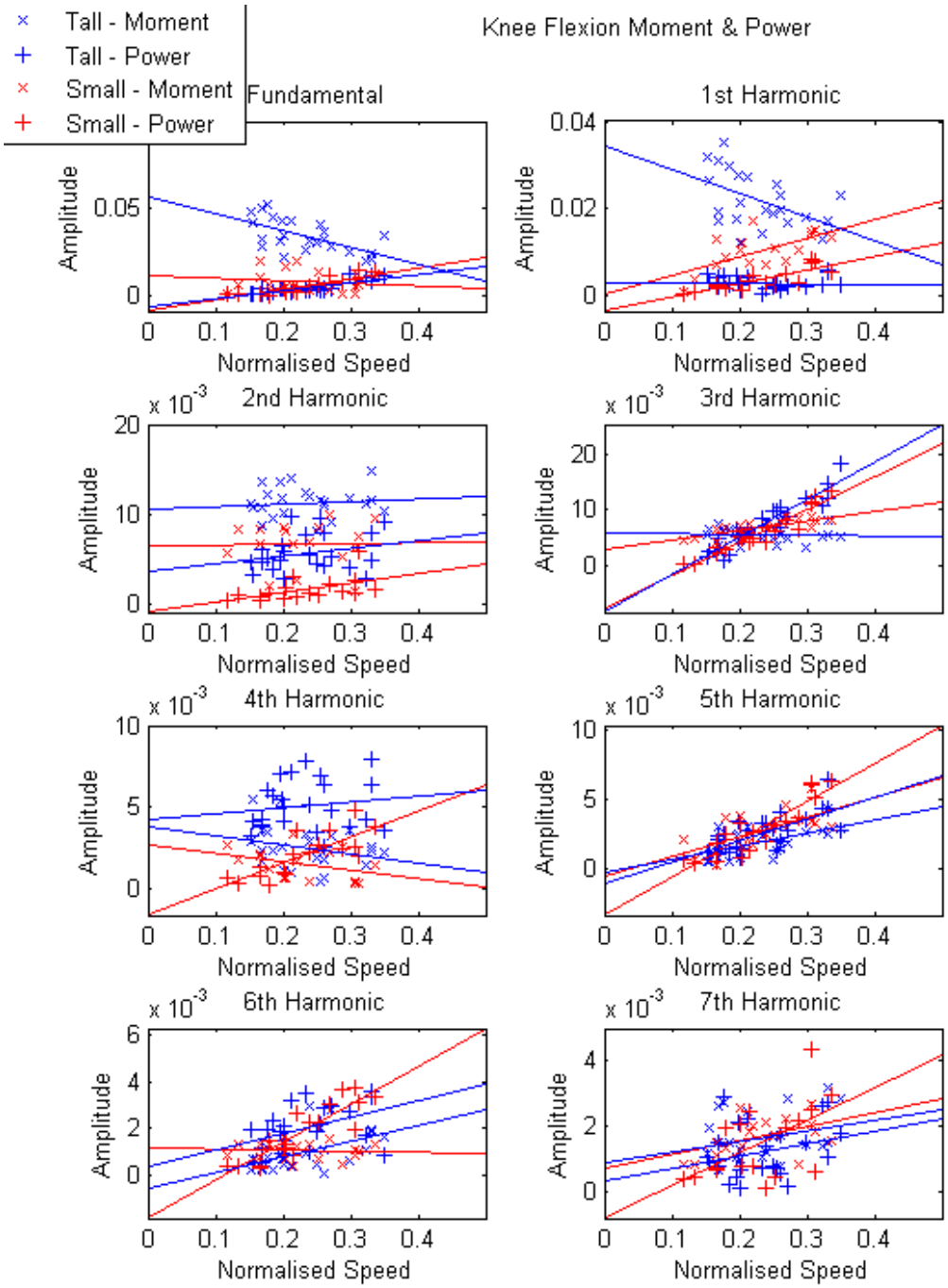

Figure D.4: Tallest and Smallest Knee Flexion Moment and Power Harmonic Amplitudes versus Normalised Speed

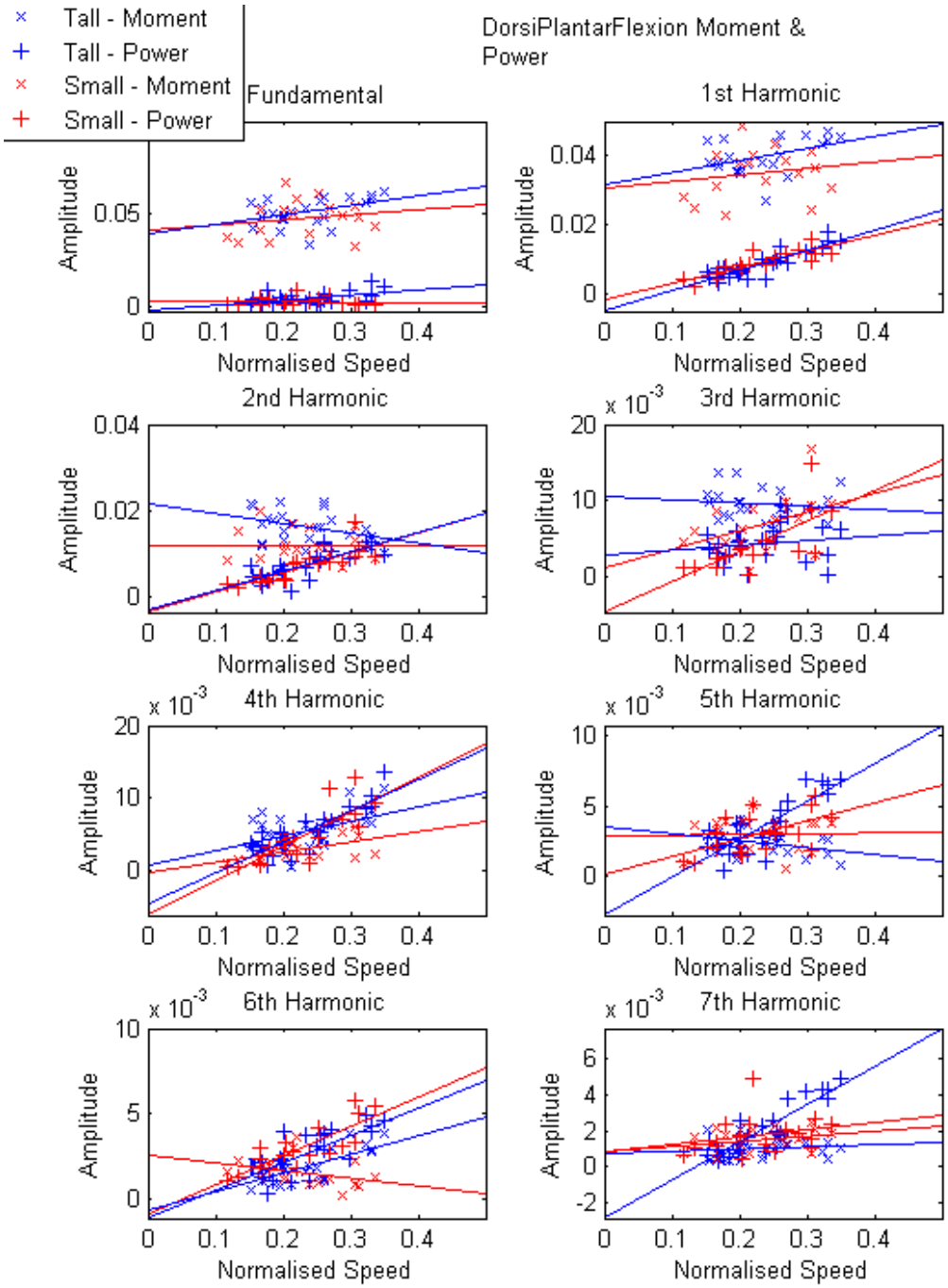

Figure D.5: Tallest and Smallest Dorsi-Plantarflexion Moment and Power Harmonic Amplitudes versus Normalised Speed

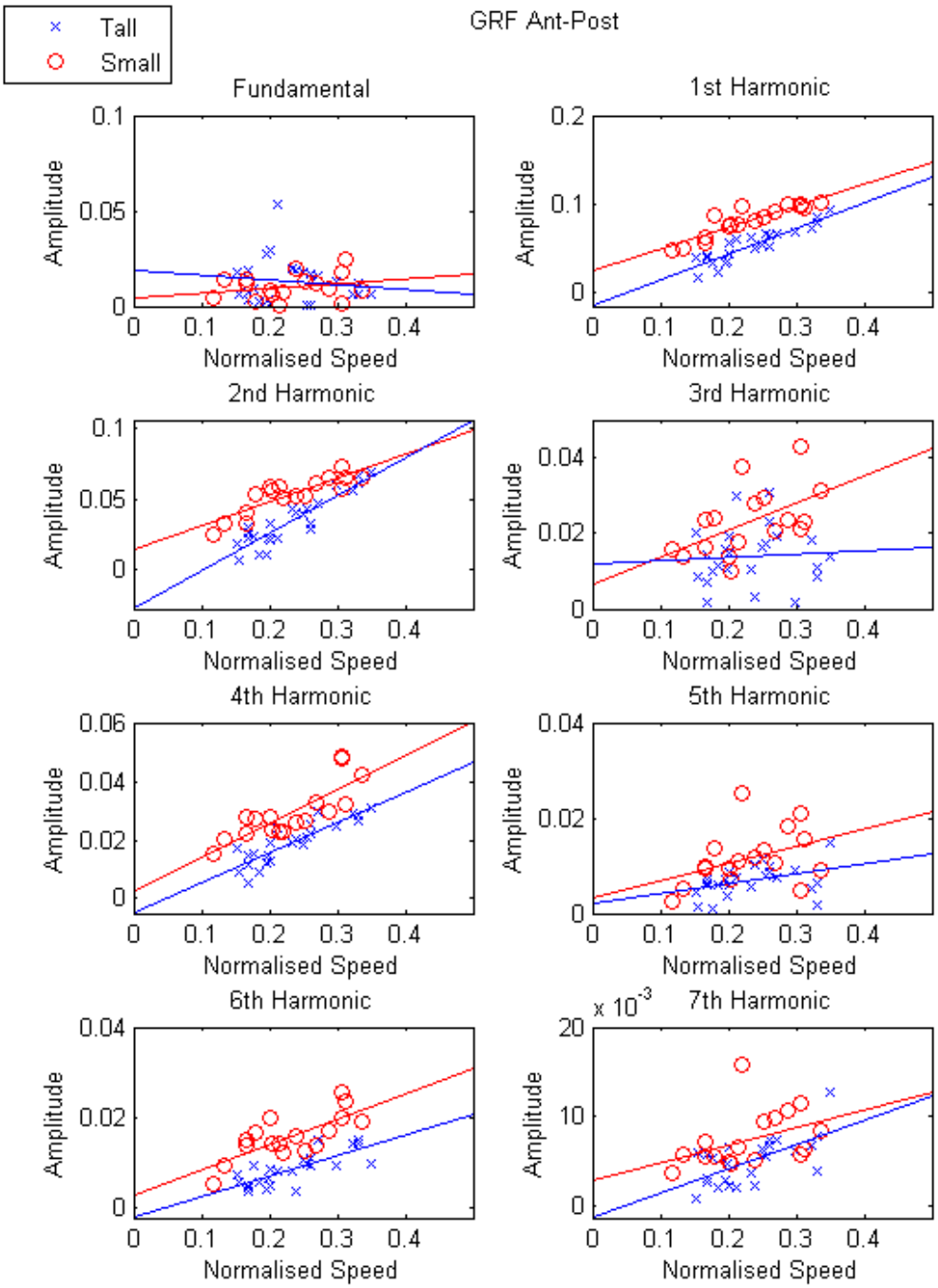

Figure D.6: Tallest and Smallest Antero-Posterior Ground Reaction Force Harmonic Amplitudes versus Normalised Speed

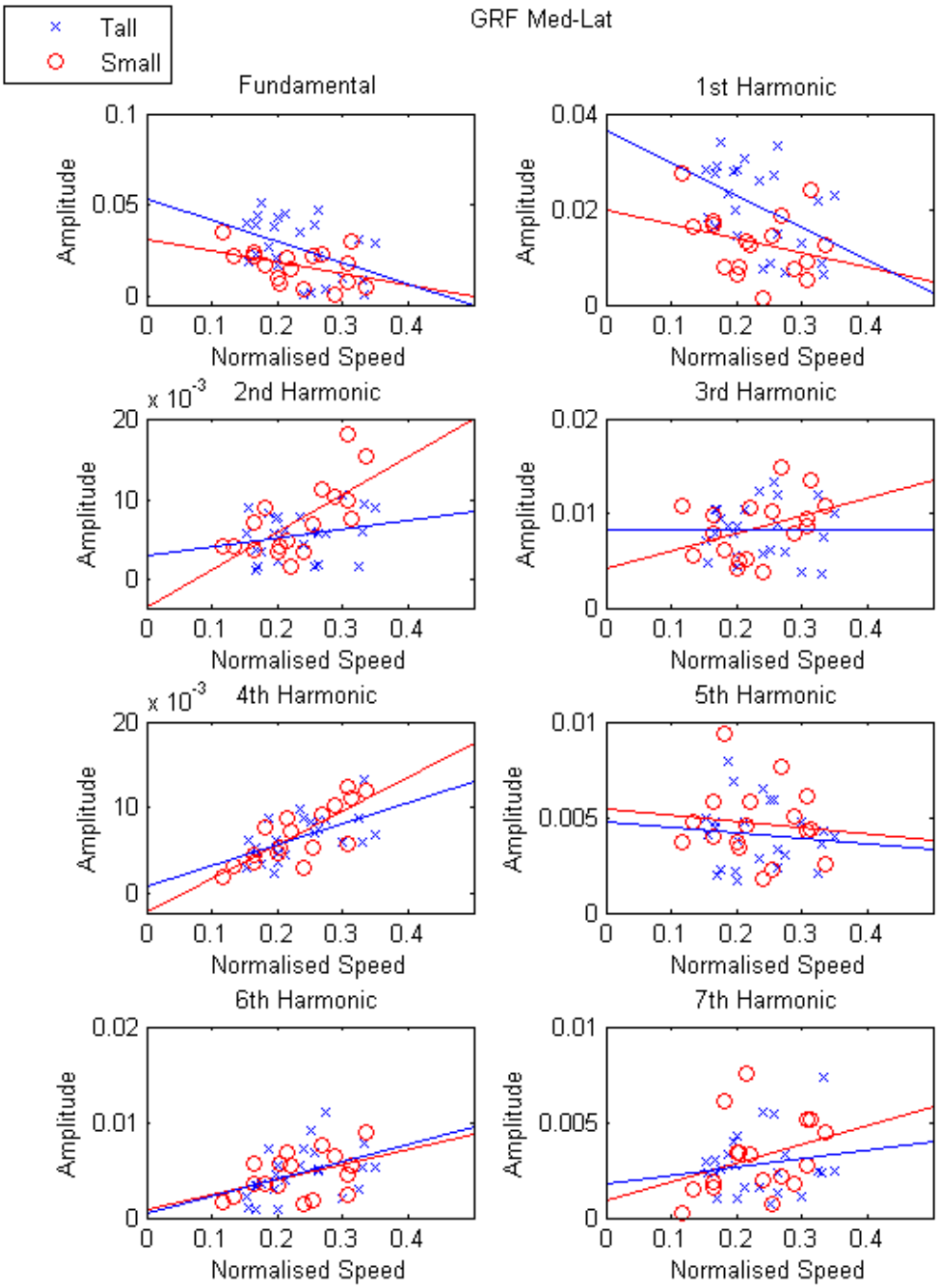

Figure D.7: Tallest and Smallest Medio-Lateral Ground Reaction Force Harmonic Amplitudes versus Normalised Speed

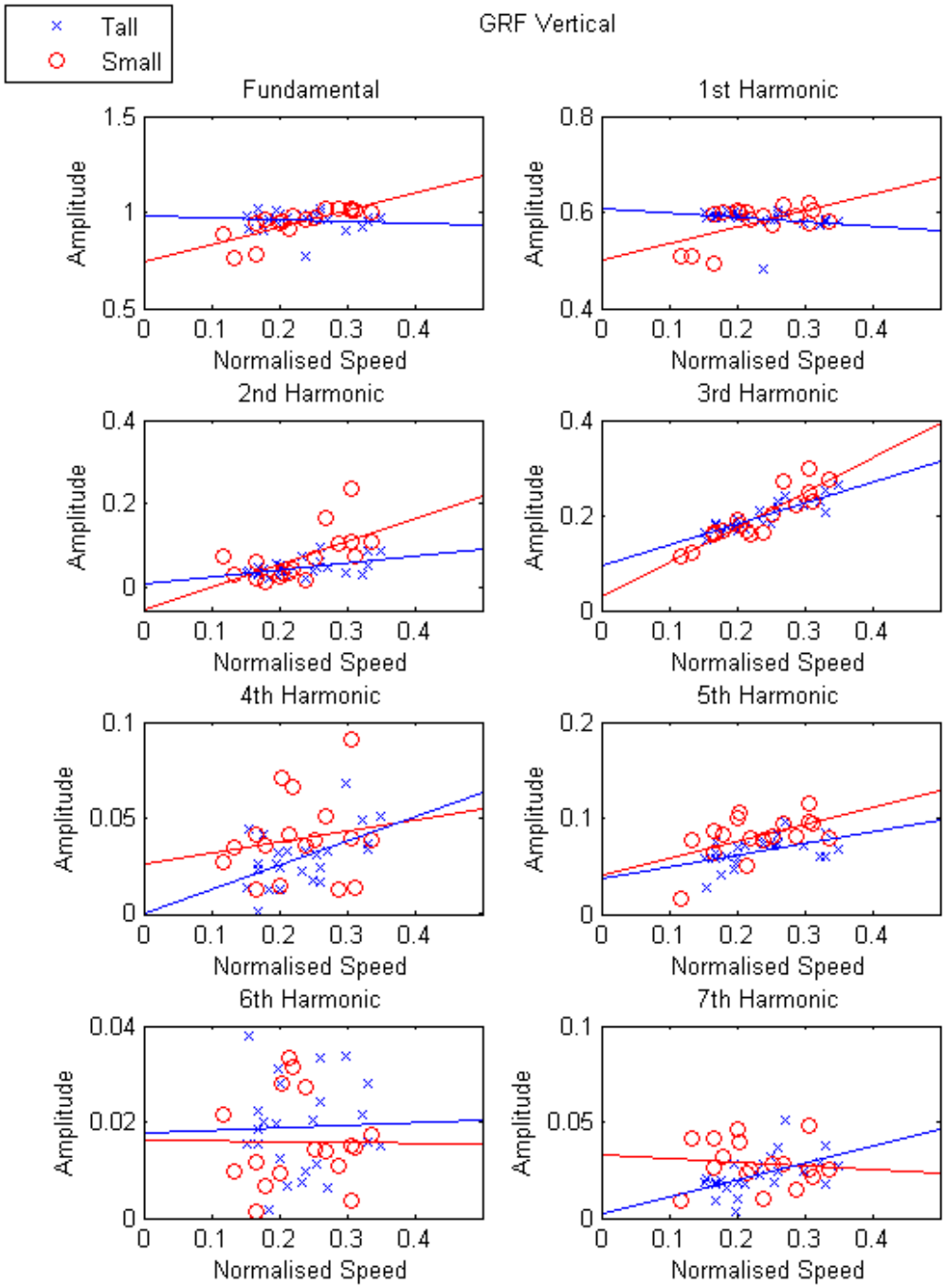

Figure D.8: Tallest and Smallest Vertical Ground Reaction Force Harmonic Amplitudes versus Normalised Speed